

Characterization of PAR-3 in early *Xenopus*
laevis development

by

Kallie Shires

A thesis
presented to the University of Waterloo
in fulfillment of the
thesis requirement for the degree of
Master of Science
in
Biology

Waterloo, Ontario, Canada, 2013

©Kallie Shires 2013

Author's Declaration

I hereby declare that I am the sole author of this thesis. This is a true copy of the thesis, including any required final revisions, as accepted by my examiners.

I understand that my thesis may be made electronically available to the public.

Abstract

Polarized cell movements are essential to the cell rearrangements that occur during morphogenesis. In *Xenopus*, cell polarity is reflected in the directional cell intercalations that drive the morphogenetic movements characterizing gastrulation. While these cell behaviours are well described, the molecular mechanism underlying this cell polarity is unknown. PAR-3 is a multi-domain scaffolding protein and a key regulator of cell polarity. I have isolated a cDNA encoding *Xenopus* PAR-3 and generated several mutant constructs, each lacking a conserved domain. Initial characterization of GFP-tagged PAR-3 in A6 cells demonstrates localization to points of cell-cell contact in epithelial sheets, as well as at the leading edge of migrating cells. PAR-3 constructs lacking the CR1 or PDZ1 domain fail to compartmentalize properly and are found in the cytoplasm. Eliminating the PDZ3 domain resulted in a loss of contact inhibition. Mutation of the aPKC phosphorylation site created a membrane hyper-accumulation phenotype. Together these data suggest that the CR1 and PDZ1 domains mediate membrane compartmentalization that is modulated through aPKC phosphorylation, while the PDZ3 domain is required for contact inhibition. In embryos, PAR-3 is expressed throughout gastrulation and over-expression of PAR-3 inhibits blastopore closure indicating a requirement during gastrulation. Inhibition is relieved when the construct lacking the CR1 domain is over-expressed. PAR-3 was localized to the cell periphery in axial mesoderm. Localization was abolished with deletion of the CR1 domain indicating that membrane targeting of PAR-3 is required for gastrulation and this targeting is dependent on oligomerization of PAR-3. This investigation also suggests PAR-3 functions independent of the PAR complex in *Xenopus* embryos indicating involvement of a different PAR-3 signaling pathway.

Acknowledgements

I am sincerely grateful to my supervisor Dr. Mungo Marsden for all his encouragement and guidance as well as the knowledge he has shared with me throughout my studies. I am also appreciative of the input my committee members Dr. Matt Vijayan and Dr. Michael Beazely have provided into my project.

I would also like to extend my gratitude to my lab-mates, both past and present. With a special thanks to Catherine Studholme for helping me learn new lab techniques and to Kate Stock and Victoria Banderob for their unfailing optimism through times of stress.

Thank you to my friends for always being there for me, and to my parents Roger and Margaret for their constant support.

Last but most certainly not least, I cannot express how thankful I am for the support provided by my sister Raelyn. I could not have done this without her to lean on and rant to, and most importantly without her amazing cooking.

Table of Contents

Author's Declaration	ii
Abstract	iii
Acknowledgements	iv
Table of Contents	v
List of Figures	vii
List of Tables	ix
List of Abbreviations	x
Chapter 1 Introduction	1
1.1 Polarized cell movements in <i>Xenopus laevis</i> Gastrulation	1
1.2 Cell Polarity	5
1.3 PAR Mediated Cell Polarity	6
1.3.1 Polarization of the <i>C. elegans</i> Zygote	6
1.3.2 The PAR Complex	8
1.3.3 Epithelial Polarity	10
1.3.4 Polarized Cell Migration	13
1.4 PARs in <i>Xenopus</i>	14
1.5 Experimental Objectives	15
Chapter 2	17
Materials and Methods	17
2.1 Cloning and Mutagenesis	17
2.1.1 Initial Cloning of PAR-3	17
2.1.2 Mutagenesis of PAR-3	18
2.1.3 Subcloning	21
2.2 Generation of <i>in vitro</i> transcripts	22
2.3 Temporal Expression of PAR-3	23
2.4 Tissue Culture	24
2.4.1 Scratch Assay	24
2.4.2 Calcium Switch Assay	25
2.5 <i>Xenopus</i> embryos, microinjections and explants	26
2.5.1 Raising embryos	26
2.5.2 Microinjections	26

2.5.3 Keller Explants.....	27
2.6 Western Blot	28
Chapter 3 Results	30
3.1 Cloning and Mutation of <i>Xenopus laevis</i> PAR-3.....	30
3.2 PAR-3 is expressed throughout <i>Xenopus</i> gastrulation.....	36
3.3 Mutation of PAR-3	37
3.4 PAR-3 in <i>Xenopus</i> A6 cells	38
3.4.1 Polarized localization of PAR-3 in epithelial cells	38
3.4.2 Polarized localization of PAR-3 in migrating cells.....	41
3.5 PAR-3 localization in A6 cells requires multiple functional domains.....	43
3.5.1 The CR1 and PDZ1 domains of PAR-3 are required for membrane localization.....	43
3.5.2 The PDZ2 domain of PAR-3 is not required for membrane localization	49
3.5.3 The PDZ3 domain of PAR-3 is required for contact inhibition.....	52
3.5.4 Removal of the aPKC phosphorylation results in hyper-accumulation	55
3.6 PAR-3 is required for convergent extension.....	58
3.7 The CR1 domain of PAR-3 is required for convergent extension	60
3.8 PAR-3 localizes to the cell membrane in <i>Xenopus</i> mesoderm cells	67
3.9 The CR1 domain is required for localization of PAR-3 in mesoderm cells	67
Chapter 4 Discussion	70
4.1 <i>Xenopus</i> PAR-3.....	70
4.2 PAR-3 is expressed throughout <i>Xenopus</i> development	71
4.3 PAR-3 in A6 cells	71
4.3.1 PAR-3 localization in epithelial cells.....	71
4.3.2 PAR-3 localization in migrating cells	73
4.3.3 Role of conserved domains in PAR-3 localization in <i>Xenopus</i> A6 cells	74
4.3.4 The PDZ3 domain is required for the generation of polarity in A6 cells.....	78
4.4 Localization of PAR-3 is required for convergent extension.....	79
4.5 Conclusions.....	81
4.6 Future Directions	82
Appendix A.....	83
References.....	84

List of Figures

Figure 1. <i>Xenopus</i> Gastrulation Movements.....	2
Figure 2. Mediolateral Cell Intercalation.....	4
Figure 3. PAR localization in the <i>C. elegans</i> zygote	7
Figure 4. The PAR Complex	9
Figure 5. Epithelial Polarization	12
Figure 6. The PAR complex in cell migration.....	14
Figure 7. PAR-3 Constructs.....	20
Figure 8. CS2GFP-N1 Plasmid.....	22
Figure 9. Keller Explants	28
Figure 10. Comparison of <i>Xenopus</i> PAR-3 with known PAR-3 homologs.....	31
Figure 11. Alignment of <i>Xenopus</i> PAR-3 with known PAR-3 homologs	35
Figure 12. Temporal expression of PAR-3	37
Figure 13. PAR-3 Localizes to cell-cell contacts in <i>Xenopus</i> A6 cells.....	40
Figure 14. PAR-3 localizes to the leading edge of migrating A6 cells.....	42
Figure 15. The CR1 domain is required for localization of PAR-3	45
Figure 16. The CR1 domain is required for localization of PAR-3 in migrating cells	46
Figure 17. The PDZ1 domain is required for PAR-3 recruitment to cell-cell contacts	47
Figure 18. The PDZ1 domain is required for recruitment of PAR-3 to the leading edge.....	48
Figure 19. The PDZ2 domain is not necessary for PAR-3 localization in A6 cells.....	50
Figure 20. The PDZ2 domain is not necessary for localization of PAR-3 in wounded A6 cells.....	51
Figure 21. The PDZ3 domain of PAR-3 is required for epithelial polarity	53
Figure 22. The PDZ3 domain of PAR-3 is required for wound healing.....	54
Figure 23. S777A in strongly localized to cell-cell contacts in <i>Xenopus</i> A6 Cells.....	56
Figure 24. S777A localizes to the leading edge of wounded A6 cells.....	57
Figure 25a. PAR-3 is required for convergent extension.....	59
Figure 25b. The CR1 domain is required for convergent extension	63
Figure 26. The CR1 domain of PAR-3 is required for <i>Xenopus</i> gastrulation	64
Figure 27. The CR1 domain of PAR-3 is required for <i>Xenopus</i> convergent extension (CE)	65
Figure 28. Δ PDZ2 and Δ PDZ3 phenotypes were inconsistent	66
Figure 29. PAR-3 localizes to the cell membrane mesoderm cells.....	68

Figure 30. The CR1 domain is required for PAR-3 localization	69
Figure A1. Sequencing of deletions and point mutation constructs.....	83

List of Tables

Table 1. PCR Primers.....	21
---------------------------	----

List of Abbreviations

APC	Adenomatous polyposis coli	TAE	Tris/Acetic acid/EDTA
aPKC	Atypical protein kinase C	TBS	Tris buffered saline
BCR	Blastocoel roof	Vang	Vang-gogh
BS	Bluescript	ZO-1	Zona Occludens 1
BSA	Bovine serum albumin		
CE	Convergent extension		
CR	Conserved region		
Crb	Crumbs		
CRIB	CDC42/Rac-interactive binding		
DFA	Danilchik's for Amy		
Dgl	Discs large		
Dgo	Diego		
Dsh	Dishevelled		
ESB	Embryo solubilization buffer		
EST	Expressed sequence tag		
FBS	Fetal bovine serum		
FN	Fibronectin		
Fz	Frizzled		
GFP	Green fluorescent protein		
GSK-3 β	Glycogen synthase kinase 3		
HRP	Horseradish peroxidase		
JAM	Junctional adhesion molecule		
LB	Luria Broth		
Lgl	Lethal giant larvae		
MBS	Modified Barth's saline		
MT	Microtubules		
MTOC	Microtubule organizing centre		
NSB	Notochordal somitic boundary		
PAR	Partitioning defective		
PBS	Phosphate buffered saline		
PCP	Planar cell polarity		
PDGF	Platlet-derived growth factor		
PDZ	PSD-95/Dlg/ZO-1		
Pk	Prickle		
PNK	Polynucleotide kinase		
PTEN	Phosphatase and tensin homolog		
Scrib	Scribble		

Chapter 1

Introduction

1.1 Polarized cell movements in *Xenopus laevis* Gastrulation

Establishing polarity is fundamental to the function of all eukaryotic cells. Cell polarity is required for oriented cell divisions, functional specialization of cells, and tissue organization (1, 2). Polarity is also essential to the directed cell movements which drive embryogenesis (3). In *Xenopus laevis*, an animal/vegetal polarity is first noticeable in the mature oocyte through asymmetric accumulation of yolk granules, pigment, mRNA and proteins (4). Following fertilization, cleavage results in the subdivision of the domains established during oogenesis (4, 5). As cleavage proceeds a fluid filled cavity, the blastocoel, is formed at the animal pole. During cleavage the three primary germ layers are established through inductive interactions between the animal and vegetal tissues (6). This results in presumptive ectoderm at the animal pole, an equatorial band of presumptive mesoderm and the vegetal hemisphere is occupied by the large yolk-filled endoderm.

Gastrulation is the process in which the three primary germ layers are rearranged to generate the triploblastic embryo (6, 7). Gastrulation is driven through localized domains of oriented cell movements (8). The global rearrangements that are seen during gastrulation are the summation of the individual cell movements that occur within the segregated domains (6, 7). *Xenopus* gastrulation is characterized by spatially and temporally controlled morphogenetic movements; involution, vegetal rotation, epiboly and convergent extension (Figure 1) (6, 9, 10).

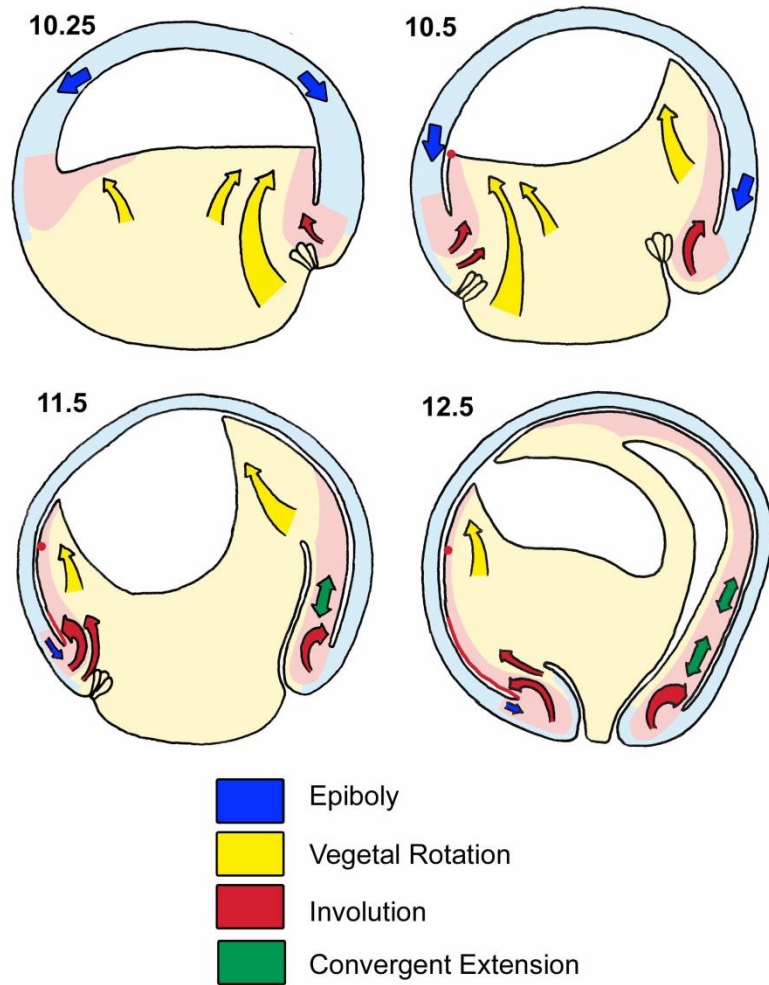


Figure 1. *Xenopus* Gastrulation Movements. Gastrulation generates the architecture of the early triploblastic embryo by positioning the ectoderm (blue) on the outside, endoderm (yellow), on the inside and mesoderm (red) in between. Gastrulation is initiated at Stage 10 with formation of the blastopore lip and is distinguished by several morphogenetic movements, vegetal rotation (yellow), epiboly (blue), involution (red) and convergent extension (green). *Adapted from Sevan, 2010(11).*

Gastrulation is first observed on the dorsal side of the embryo when a group of superficial epithelial bottle cells constrict apically creating an invagination on the dorsal side of the embryo known as the blastopore lip (12). Vegetal rotation, the inward surge of deep vegetal endoderm cells (Figure 1, yellow arrows) drives involution of the dorsal bottle cells as well as the superficial equatorial mesoderm (Figure 1, red arrows) (10). At the onset of gastrulation a fibronectin (FN) matrix is assembled across the blastocoel roof (BCR) (13). The leading edge of the involuted mesoderm (mesendoderm) migrates directionally along the FN matrix towards the animal pole (14). The directionality of mesendoderm migration stems from a planar polarity signal emanating from the vegetal endoderm cells (15).

Subsequent to involution, the axial mesoderm converges towards the midline and extends towards the anterior of the embryo (Figure 1, green). Convergent extension (CE) is driven by the mediolateral intercalation of cells resulting in axial extension (9). The cell movements of CE are directional, and cells acquire polarity cues before the initiation of intercalation (16). Prior to CE, axial mesoderm cells are irregular in shape and exhibit random protrusive activity (Figure 2a) (16). At the onset of CE cells become bipolar, displaying medial and lateral lamellar protrusions (Figure 2b). The mesoderm cells then use these lamellar protrusions to crawl past each other using the surface of neighboring cells for traction (16, 17). The tension created by the cells pulling on their neighbors results in further cell elongation along the mediolateral axis (17). At the mid-gastrula stage, Stage 11.5, the FN rich notochord-somite boundary (NSB) forms (Figure 2c) (18).

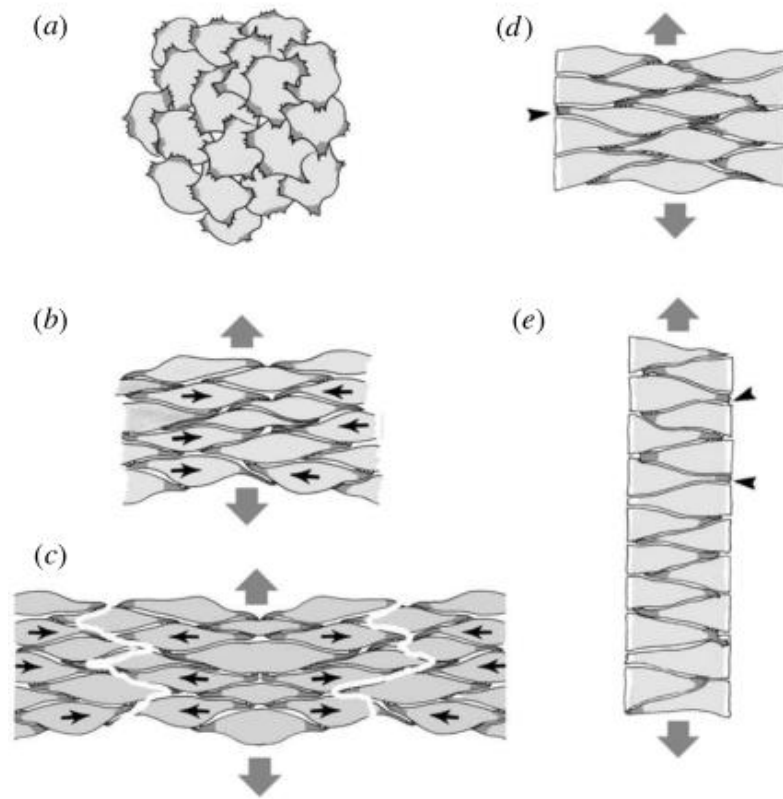


Figure 2. Mediolateral Cell Intercalation. Before convergent extension (CE) begins mesoderm cells are unpolarized and randomly protrusive (a). Lamellar protrusions become isolated to the mediolateral ends at the onset of CE and exert traction on adjacent cells. As a result the cells pull past one another intercalating toward the midline with the resulting tension causing an elongate cell shape (b). The notochordal somatic boundary (NSB) begins to form at the late midgastrula stage (c). The NSB matures as lamellopodial protrusion ceases and cells flatten at the NSB (d). The axial mesoderm continues to intercalate eventually bringing all cells into contact with the NSB and causing elongation of the anterior/posterior axis (e). *Adapted from Keller et al., 2000.*

Cells in the notochord and pre-somitic mesoderm continue to undergo mediolateral intercalation between the tissue boundaries resulting in thinning of the tissue mediolaterally and extension of the anterior/posterior axis (Figure 2e) (16, 19).

In the animal hemisphere, the ectoderm spreads through epiboly to encompass the embryo surface (Figure 1, blue). Epiboly occurs as deep cells intercalate normal to the embryo surface thinning to a single layer. In this way the BCR is thinned resulting in a circumferential vegetal spreading of the ectoderm (16). The molecular mechanisms behind radial intercalation remain uncharacterized however, they require both cell polarization and contact of the deep cells with the FN matrix on the BCR (20).

The directional cell movements that ultimately drive gastrulation require the establishment and manifestation of cell polarity. *Xenopus laevis* embryos are a preferred model for the study of the morphogenetic movements which drive gastrulation because of their large size and rapid development. Furthermore, explanted tissues from *Xenopus* embryos will reiterate the complex morphogenetic movements, allowing both external and deep cell movements to be observed (21). While the individual cell movements and the consequent tissue rearrangements have been extensively characterized in *Xenopus* the molecular mechanism regulating polarity remains unknown.

1.2 Cell Polarity

Cell polarity can be described in reference to the orientation of the organelles and cytoskeleton of an individual cell, or as the orientation of a cell with respect to its neighbors. Molecular analysis of these two forms of polarity identified two distinct signaling cassettes.

Coordination of polarity with respect to neighboring cells is regulated by planar cell polarity (PCP) signaling and is essential to embryogenesis. First characterized in *Drosophila* the PCP cassette includes Dishevelled (Dsh), Frizzled (Fz), Vang-gogh (Vang), Prickle (Pk) and Diego (Dgo) proteins (3). PCP signaling has been extensively studied in *Drosophila* and is responsible for orientation of wing hairs, ommatidia in the eye, as well as sensory bristles (22). In mammals a similar system was identified (often referred to as the non-canonical Wnt pathway) and regulates orientation of auditory stereocilia and epithelial hairs (3). PCP signaling has also been identified in *Xenopus* and plays unidentified roles in conditioning of the FN matrix as well as CE (8, 23, 24). Coordination of polarity across tissues was initially considered separate from individual cell polarization. However, recent investigations have found that the PCP cassette demonstrates convergent signaling with individual cell polarity. Individual cell polarity is mediated through a family of proteins known as the PAR proteins (see section 1.3 below). PAR-1 has been shown to regulate Dsh and aPKC function and interacts with Vang2 (25, 26). These interactions may indicate that polarity whether in sheets of cells or in isolated cells stems from the same basic signaling cassettes.

1.3 PAR Mediated Cell Polarity

1.3.1 Polarization of the *C. elegans* Zygote

The partitioning defective (*par*) genes were initially identified in *Caenorhabditis elegans* through maternal-effect mutations disrupting polarization of the first zygotic cleavage. The *par* genes encode the six PAR proteins which make up a set of cortically enriched signaling and scaffolding proteins. PAR-1 and PAR-4 are serine-threonine kinases, PAR-5 is a member of the 14-3-3 protein family which binds phosphoserine residues, PAR-3 and PAR-6 are scaffolding

proteins, and PAR-2 is a RING finger protein involved in protein ubiquitination (1, 27, 28)

Mutation of the *pkc-3* gene, which encodes an atypical protein kinase C (aPKC), also resulted in a loss of polarized division and as a consequence aPKC is included in the *par* cassette (29).

The PAR proteins generate asymmetry in the *C. elegans* oocyte through the formation of polarized domains at the anterior and posterior cortex of the oocyte (Figure 3) (1, 30). Prior to fertilization the *C. elegans* oocyte is unpolarized and the PARs are expressed throughout the oocyte. PAR-3, PAR6, and aPKC are enriched at the cell cortex, while the remaining PARs are present mostly in the cytoplasm. Oocyte symmetry is broken upon fertilization through a cue given by the male centrosome defining the prospective posterior of the zygote (31). The polarity cue results in down-regulation of cortical contraction at the posterior of the zygote creating an anterior cortical flow (31). The cortically enriched PAR-3/PAR-6/aPKC clears from the non-contractile posterior cortex, moving with the anterior flow, and is replaced by PAR-1 and PAR-2 (31).

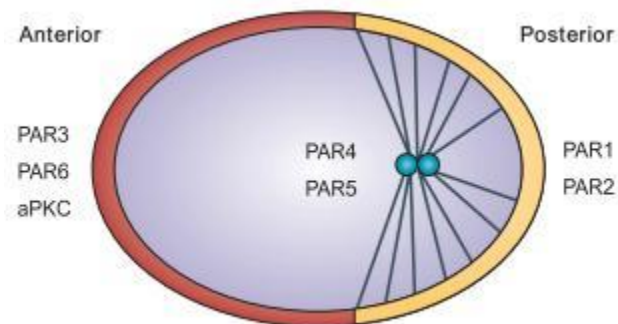


Figure 3. PAR localization in the *C. elegans* zygote. Distinct domains are formed through the segregation of PAR3/PAR6/aPKC to the anterior cortex (red) and PAR-1/PAR-2 to the posterior cortex (yellow). These domains are then maintained through mutual antagonism between the anterior and posterior PARs. PAR-4 and PAR-5 remain uniformly distributed and aid in maintenance of the two domains. Adapted from Macara, 2004.

PAR-3, PAR-6 and aPKC define the anterior domain while PAR-1 and PAR-2 define the posterior domain. The separate domains are stabilized and maintained through antagonistic kinase activity between the anterior and posterior PARs. In the posterior PAR-1 phosphorylates PAR-3 while aPKC phosphorylates PAR-1 at the anterior (1, 29). PAR-5, which remains distributed symmetrically, is responsible for the binding and removal of phosphorylated proteins (1). The antagonism between the opposing PARs is essential to the maintenance of the anterior and posterior domains and removal of either set of PARs results in the loss of polarity. In the *C. elegans* embryo the manifestation of cell polarity is the segregation of determinants as well as displacement of the mitotic spindle towards the posterior. The subsequent cleavage is asymmetric creating two unique daughter cells with distinct fates.

1.3.2 The PAR Complex

The anterior PARs (PAR-3, PAR-6, and aPKC, hereafter referred to as the PAR complex) co-localize and form a signaling complex with each member having a clearly defined role (Figure 4). PAR-3 and PAR-6 are scaffolding proteins and aPKC is the catalytic member of the complex phosphorylating target molecules (27). Atypical PKC possesses a PB1 scaffolding domain which constitutively binds PAR-6 through binding of the PB1 domain in PAR-6 (27, 30). PAR-6 then functions as an adapter scaffold linking aPKC to other members of the complex. PAR-6 also contains a PDZ domain responsible for recruitment of targets for aPKC phosphorylation including Crumbs (Crb) and the Lethal giant larvae (Lgl) which are downstream

regulators of cell polarity (32, 33). Furthermore, PAR-6 recruits PAR-3 to the PAR complex through interaction of the PDZ of PAR-6 with the PDZ1 domain of PAR-3 (34).

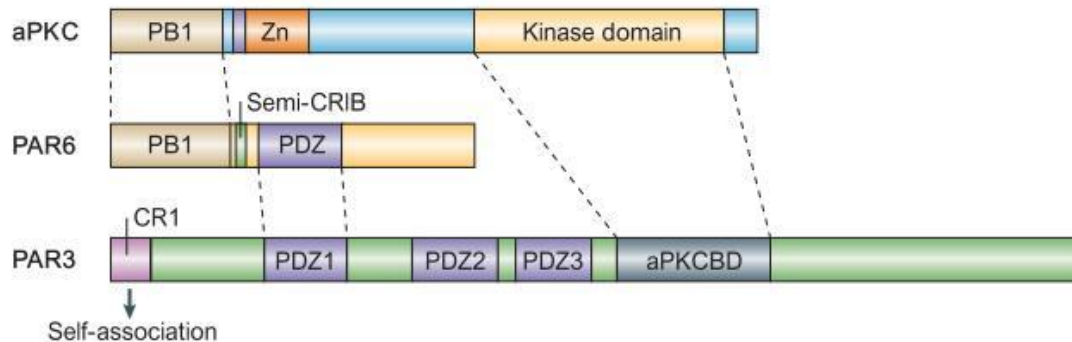


Figure 4. The PAR Complex. PAR-3, PAR-6, and aPKC associate to form a polarity complex. PAR-6 and aPKC interact through their PB1 domains, while PAR-3 and PAR-6 associate through PDZ domains. PAR-3 recruits aPKC phosphorylation targets through the PDZ domains, and is a target itself for aPKC phosphorylation at its aPKC binding domain (aPKCBD). *Adapted from Macara, 2004.*

PAR-3 is a multi-PDZ scaffolding protein responsible for targeting the PAR-complex to the cell cortex. This targeting is mediated by the second PDZ domain of PAR-3 which has a high affinity for membrane phospholipids (35). Oligomerization of PAR-3, mediated through the N-terminal CR1 domain, results in higher-order scaffolds and enhanced recruitment of the PAR complex to the membrane (35, 36). The PAR-3 scaffold then recruits downstream effector molecules such as the lipid phosphatase PTEN (phosphatase and tensin homolog), which associates with the third PDZ domain of PAR-3 (35, 37), as well as further phosphorylation targets for aPKC including the Rac-specific nucleotide exchange factor (Rac-GEF) Tiam1 and the endocytic adapter protein Numb (37–40). PAR-3 itself is a target for aPKC and when phosphorylated PAR-3 dissociates from the PAR complex. This release frees the first PDZ

domain of PAR-3 from PAR-6, allowing this domain to mediate interaction with the adhesion molecules JAM (junctional adhesion molecule) and nectin, as well as the cytoskeletal motor protein dynein (41–44).

Regulation of aPKC is mediated in part by its zinc finger motif as well as through activation by CDC42 (30, 42). PAR-6 contains a semi-CRIB (CDC42/Rac-interactive binding) motif which binds CDC42 allowing for CDC42 activation of aPKC (42). The PAR complex is highly conserved and the scaffolding properties of PAR-3 and PAR-6 combined with the catalytic activity of aPKC allow the PAR complex to regulate multiple effector pathways including spindle orientation, epithelial junction formation, endocytosis, and the actin cytoskeleton (45).

1.3.3 Epithelial Polarity

Cell polarization is essential to the structure and function of epithelia. Epithelial cells are bound together through tight junctions and adherens junctions to form epithelial sheets that act as physical and molecular barriers. The tight junctions are formed at the apical/lateral surface and define the boundary between the apical and basolateral membrane domains. The PAR proteins play essential roles in establishing and maintaining epithelial cell membrane domains.

In mammalian cells epithelial polarization is initiated by cell-cell contact. Adhesion molecules of the nectin family along with junctional adhesion molecules (JAM) accumulate at the cell-cell contact region and form intercellular adhesions (31, 46). PAR-3 is then recruited to adhesion sites through interactions mediated via its first PDZ domain and nectins or JAM (29, 31, 46). PAR-3 in turn recruits E-cadherins through the third PDZ domain to the forming

nascent adherens junctions (47). This results in CDC42 activation by E-cadherin and subsequent recruitment of activated aPKC and PAR-6 (1, 27). The activated PAR-6/aPKC complex recruits the Crumbs complex, consisting of Crumbs (Crb), and the scaffolding proteins PALS1 and PATJ and together they define the apical membrane (1, 31). Subsequently, PAR-1 and the Scribble complex consisting of Discs large (Dgl), Scribble (Scrib) and Lethal giant larvae (Lgl), are localized to the basolateral membrane (31, 48).

Once the apical/basolateral membrane domains are established the PAR-6/aPKC/Crb and PAR-1/Scrib complexes maintain the integrity of these domains through mutual antagonism (Figure 5). In the apical domain PAR-1 is phosphorylated by aPKC. This creates a binding site for PAR-5 which binds PAR-1 and removes it from the apical membrane (1). Lgl is similarly phosphorylated by active aPKC preventing Lgl association with the apical cortex (49). Conversely, in the basolateral domain Lgl binds aPKC/PAR-6 resulting in its inactivation and removal from the membrane (50). PAR-1 also phosphorylates PAR-3 creating a PAR-5 binding site and inhibiting basal PAR-3 localization (1, 51). Activated aPKC phosphorylates PAR-3 resulting in its dissociation from the PAR complex and exclusion from the apical domain (27). The antagonism of both aPKC and PAR-1 against PAR-3 segregates PAR-3 into a band at the boundary between the apical and basolateral domains. Here PAR-3 stabilizes tight junction formation through sequestering the Rac-GEF Tiam1 (37). The sequestering of Tiam1 prevents its activation by aPKC resulting in lowered Rac activity and stabilization of cortical actin fibers (37).

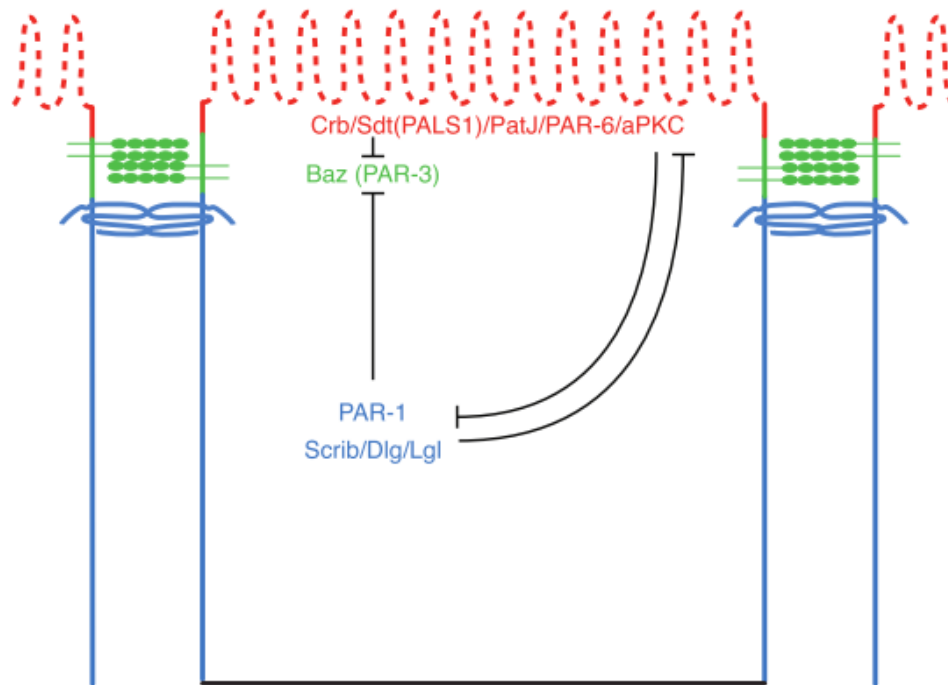


Figure 5. Epithelial Polarization. The PARs work together with the Crumbs (Crb) and Scribble (Scrib) complexes to generate the three unique epithelial domains: apical (red), junctional (green), and basolateral (blue). The apical domain is defined by the Crb complex along with PAR-6 and aPKC, while the basolateral domain is defined by PAR-1 and the Scrib complex. PAR-3 is responsible for the recruitment of junctional molecules and defines the junctional membrane domain at the apical/lateral boundary. The separate domains are maintained through antagonism between the polarity complexes. *Adapted from St Johnston and Sanson, 2011.*

1.3.4 Polarized Cell Migration

Cell migration is an essential behaviour in most cells types. Migrating cells are polarized with a protrusive front end and retracting rear. This polarized phenotype is regulated through the cytoskeleton. Migrating cells display two defining morphologies: orientation of the centrosome in the direction of migration and the formation of membrane protrusive activity at the front end.

In astrocytes, after initiation of migration PAR-6 and aPKC are recruited to the leading edge by activated CDC42. CDC42 subsequently activates aPKC which in turn phosphorylates and inactivates GSK-3 β . The result of this phosphorylation is a clustering of APC at microtubule plus ends orienting the centrosome and promoting microtubule (MT) outgrowth towards the leading edge (33). In astrocytes cell polarization appears to be mediated primarily through the MT cytoskeleton and PAR-3 does not localize to the leading edge and instead remains at cell-cell contacts where it maintains centrosome positioning (44). PAR-3 binds the motor protein dynein, which generates tension through the MTs that orient the centrosome (44).

In migrating fibroblasts polarized protrusive activity is mediated by PAR complex regulation of the Rac/Rho pathway GTPases. In these cells the PAR complex is localized to the protrusive front end of migrating cells. PAR-3 then recruits Tiam1 to the leading edge where it is activated by aPKC, resulting in accumulation of active Rac at the leading edge (52). Rac activity stimulates lamellopodial formation at the front end (53). The PAR complex also recruitments Smurf1, a ubiquitin ligase, to the leading edge where it promotes degradation of RhoA preventing actin contraction at the front end (52, 54). This results in accumulation of RhoA at the rear end of the cell where it promotes retraction of the trailing end of the migrating cell.

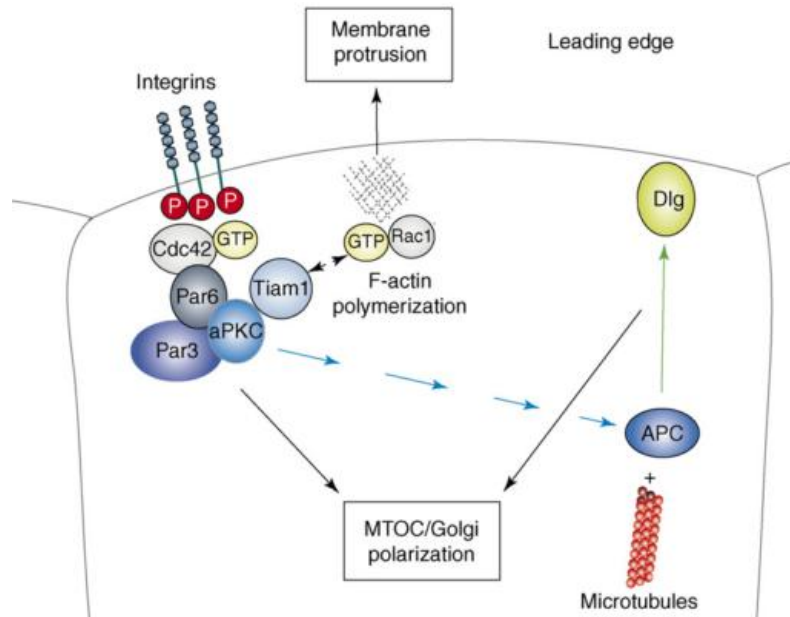


Figure 6. The PAR complex in cell migration. The PAR complex orients the microtubule organizing centre (MTOC) and regulates protrusive activity during cell migration. MTOC orientation is regulated through aPKC phosphorylation and subsequent inactivation of GSK-3 β . APC then associates with Dlg at the leading edge where it stabilizes microtubules. The PAR complex also recruits and activates Tiam1 at the leading edge resulting in Rac activation and up regulation of protrusive activity. *Adapted from Humbert et al., 2006.*

1.4 PARs in *Xenopus*

The highly conserved nature of the PAR proteins and their ubiquitous role in cell polarization makes them key candidates for the molecular mechanism underlying convergent extension in *Xenopus laevis*. PAR-1 and PAR-6 are expressed throughout *Xenopus* development, and PAR-3 and aPKC have only been described in the mature oocyte (55–57).

Roles for the PAR proteins have been described in functional assays that evaluate the cell movements of CE. Explants isolated from the animal pole of the blastula stage embryo (Animal cap) will elongate by CE when treated with activin. Animal caps taken from embryos over-expressing PAR-1, PAR-6, rat PAR-3, aPKC or a dominant negative aPKC failed to extend when treated with activin. Similar results were obtained in animal caps when PAR-1 or PAR-6 were knocked down with morpholinos (58). The similar effects observed with either over-expression or knockdown indicates balanced expression of PAR-1, PAR-6 and aPKC is required for control of CE movements. This indicates critical roles for PAR proteins in regulating convergent extension during *Xenopus* gastrulation.

1.5 Experimental Objectives

The tissue rearrangements that occur during *Xenopus* development require polarized cell movements. With evidence that the PAR proteins are likely involved in this polarization, the cell movements during *Xenopus* gastrulation provide a good *in vivo* model for describing the functional role of PAR-3. The aim of this study is to provide an initial characterization of the role PAR-3 plays in early *Xenopus* development. Previous studies of PARs in *Xenopus* have focused on PAR-1, PAR-6 as well as aPKC and little is known about *Xenopus* PAR-3. The approach I used to address the function of *Xenopus* PAR-3 was to isolate a species-specific cDNA, and generate constructs that lack the conserved functional domains described in mammalian PAR-3 (see Section 2.1). The deletion constructs were then tagged with GFP and localization was observed in *Xenopus* A6 cells. Domain function was correlated with sub-cellular localization using functional assays (Scratch and Calcium switch assays) in A6 cells. The

GFP tagged constructs were then over-expressed in embryos and sub-cellular localization was correlated with developmental defects in polarized cell movements. This approach allows me to form an initial functional characterization of *Xenopus* PAR-3.

Chapter 2

Materials and Methods

2.1 Cloning and Mutagenesis

2.1.1 Initial Cloning of PAR-3

A full length *Xenopus laevis* PAR-3 cDNA EST was obtained as an Image Consortium clone from Open Biosystems (Waltham MA, Accession# NM_001092545, Clone ID:5084932). The protein coding sequence was isolated using hot-start PCR and Pfu polymerase (Fermentas, Burlington, ON). Briefly, a 50µL reaction was prepared containing 20ng of the PAR-3 EST, 100ng Forward Primer, 100ng Reverse primer (Table 1), 0.2mM dNTPs (Fermentas, Burlington, ON), and 1xPfu buffer with MgSO₄ (supplied by the manufacturer). The forward and reverse primers were designed to include EcoRI and XbaI restriction enzyme consensus sites. The PCR was conducted with a two minute hot start at 95°C after which 2.5u Pfu polymerase (Fermentas, Burlington, ON) was added then 28 cycles of: 30 sec at 95°C, 30 sec at 50°C, 7 min at 68°C. An additional five minutes at 68°C was included at the end of the last cycle. The PCR product was digested with EcoRI and XbaI restriction enzymes (Fermentas, Burlington, ON). The restriction digest was separated on a 1% TAE agarose gel (59) containing 0.2µg/mL ethidium bromide and the band representing the PAR-3 cDNA isolated using an illustra GFX PCR DNA and Gel Band Purification kit (GE Healthcare, Baie d'Urfe, QC).

The PAR-3 coding sequence was ligated for two hours at room temperature into Bluescript SK II (+) (Agilent Technologies Canada Inc., Mississauga, ON), previously digested with EcoRI and XbaI, using 200u T4 DNA ligase (Fermentas, Burlington, ON). The ligated product was then transformed into competent XL-1 Blue E. coli (60). Briefly, XL-1 Blue were

thawed on ice and 250ng of the ligated plasmid was added. The samples were mixed gently and incubated on ice for 10 minutes. The samples were then heat shocked for 45 sec at 42°C and replaced on ice for two minutes. Luria broth (LB: 5g Tryptone, 2.5g Yeast extract, 5g NaCl in 500mL H₂O) was added to the samples (300µL) and they were placed on a shaker at 37°C for 30 minutes. The bacterial mixture was spread onto two LB agar plates containing 50µg/mL ampicillin one with a low cell density (50µL) and one with a high cell density (250µL). Cultures were incubated overnight at 37°C. Two positive colonies were then selected and inoculated in LB containing 50µg/mL of ampicillin and placed on a shaker at 37°C overnight. The plasmid was isolated from the bacterial culture using a High-Speed Plasmid Mini Kit (FroggaBio, Toronto, ON) according to the instructions provided. The isolated plasmid was run on a 1% TAE agarose gel, as previously described, to determine DNA concentration. The PAR-3 Bluescript plasmid (XPAR-3 BS) was digested with EcoRI and XbaI and the digest separated on a 1% TAE agarose gel to confirm the presence of insert.

2.1.2 Mutagenesis of PAR-3

The XPAR-3 BS construct was then used to create the deletion constructs described below (Figure 7). To create the Δ CR1 construct, the sequence that encodes the N-terminal 50 amino acids was removed from PAR-3 coding sequence using the Δ CR1 forward primer and PAR-3 reverse primer (Table 1). The mutagenesis was carried out using standard techniques (59) and the PCR was conducted with a combination of 0.25u Pfu and 5.0u Taq polymerase (Fermentas, Burlington, ON). The PCR was conducted as described in Section 2.1.1 using the

following cycles: 30 sec at 95°C, 30 sec at 45°C, 3 min at 72°C. An additional five minutes at 72°C was included at the end of the last cycle.

The Δ PDZ1-3 constructs were created through inverse PCR according to standard protocols (61) using the corresponding primers described in Table 1. The Δ PDZ1 construct contains a deletion of bp 634-915 of the PAR-3 coding sequence, encoding aa 212-305. The Δ PDZ2 construct contains a deletion of bp 1216-1458 of the PAR-3 coding sequence resulting in deletion of aa 406-486. Lastly, Δ PDZ3 contains a deletion of bp 1621-1881 of the PAR-3 coding sequence, deleting aa 541-627. Following the PCR reaction the template was removed from the reaction using DpnI (Fermentas, Burlington, ON). The digested samples were separated on a 1% TAE agarose gel and the band representing the deletion construct was purified as outlined in Section 2.1.1. One hundred and fifty nanograms of the purified deletion constructs was phosphorylated using 10u T4 Polynucleotide Kinase (PNK) (Fermentas, Burlington, ON), with 1mM ATP, and 1xPNK Reaction Buffer A (10x stock provided by manufacturer). The samples were incubated at 37°C for 30 minutes then heated to 70°C for 10 minutes before being purified using a Gel/PCR DNA Fragments Extraction Kit (FroggaBio, Toronto, ON). The purification was conducted according to the instructions provided and the DNA eluted from the column using 22 μ L of sterile water. The samples were then run on a 1% agarose gel to determine the concentration and 100ng of each sample was ligated overnight at 14°C then transformed into XL-1 Blue described previously (Section 2.1.1).

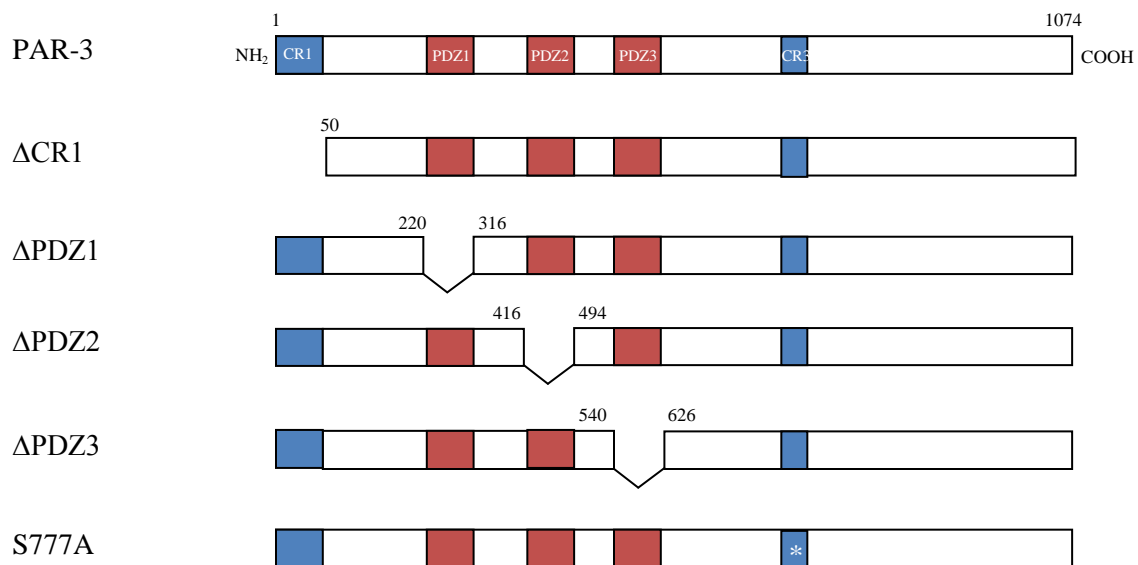


Figure 7. PAR-3 Constructs. Illustration of full length PAR-3 and PAR-3 deletion and point mutation constructs. PDZ domains are shown in red and conserved regions (CR) are shown in blue. Point mutations are represented by *. For the CR1 construct an ATG start codon was included in the forward primer.

Site directed mutagenesis (62) was used to alter the aPKC phosphorylation site by replacing the adenine and guanine residues of the AGC codon (bp 2329-2331) with guanine and cytosine residues respectively. This point mutation changes the encoded amino acid, serine 777, to an alanine. The PCR reaction was carried out as described for the Δ PDZ mutations using the S777A primers described in Table 1. The PCR product was digested with DpnI to remove template, purified, and then transformed as previously described (Section 2.1.2).

Table 1. PCR Primers

Construct	DNA Primer Sequence	Location (bp)
PAR-3	For 5' GCGGAATTC ATG AAGGTGACG 3'	1-12 (5'EcoRI site)
	Rev 5' GGGTCTAGACTACCTGTCACAGGTGAAGG 3'	3202-3222(5'XbaI site)
Δ CR1	For 5' GCGGAATTC ATG CGTTTTGGAACATGGTGACGG 3'	148-167 (5'EcoRI site)
	Rev 5' GGGTCTAGACTACCTGTCACAGGTGAAGG 3'	3202-3222(5'XbaI site)
Δ PDZ1	For 5' CCCGTGATCTGGTTCCACGTGGTCCC 3'	916-941
	Rev 5' AGCATGGCCGACAGGTTCCACTCGGCT 3'	607-633
Δ PDZ2	For 5' CGAAGCACCAAGATGGACGGAGCAG 3'	1459-1483
	Rev 5' ACTGTTGGTGGGGGAGTTGACTGCACGC 3'	1189-1215
Δ PDZ3	For 5' AGAGGGATGATCCAGCTAATTGTGGC 3'	1882-1907
	Rev 5' CTCCCGTGTTCATCTGGAGTCAATAC 3'	1594-1620
S777A	For 5' GGGTTTGCCCGCCAA GCC ATGTCCGAAAAACGC 3'	2314-2346
	Rev 5' GCGTTTTTCGGACAT GGC TTGGCGGGCAAACCC 3'	

*Start codons are shown in yellow and the point mutation is indicated in red.

2.1.3 Subcloning

The PAR-3 coding sequence and Δ CR1 construct were isolated by PCR and digested using EcoRI and XbaI restriction enzymes as outlined in Sections 2.1.1 and 2.1.2. The Δ PDZ1-3 and S777A coding sequences were digested from corresponding BS plasmids with EcoRI and XbaI restriction enzymes as described. The plasmid was then further digested using ScaI before the sample was run on a 1% TAE agarose gel. The bands corresponding to coding sequences of the mutated constructs were purified from the gel. The digested PCR products were ligated (Section 2.1.1) into the CS2GFP-N1 vector (Figure 8, gift from J. Miller, University of Minnesota) that had been previously digested with EcoRI and XbaI. The ligated samples were

then transformed into XL-1 Blue and the plasmids isolated from bacterial culture as described (Section 2.1.1).

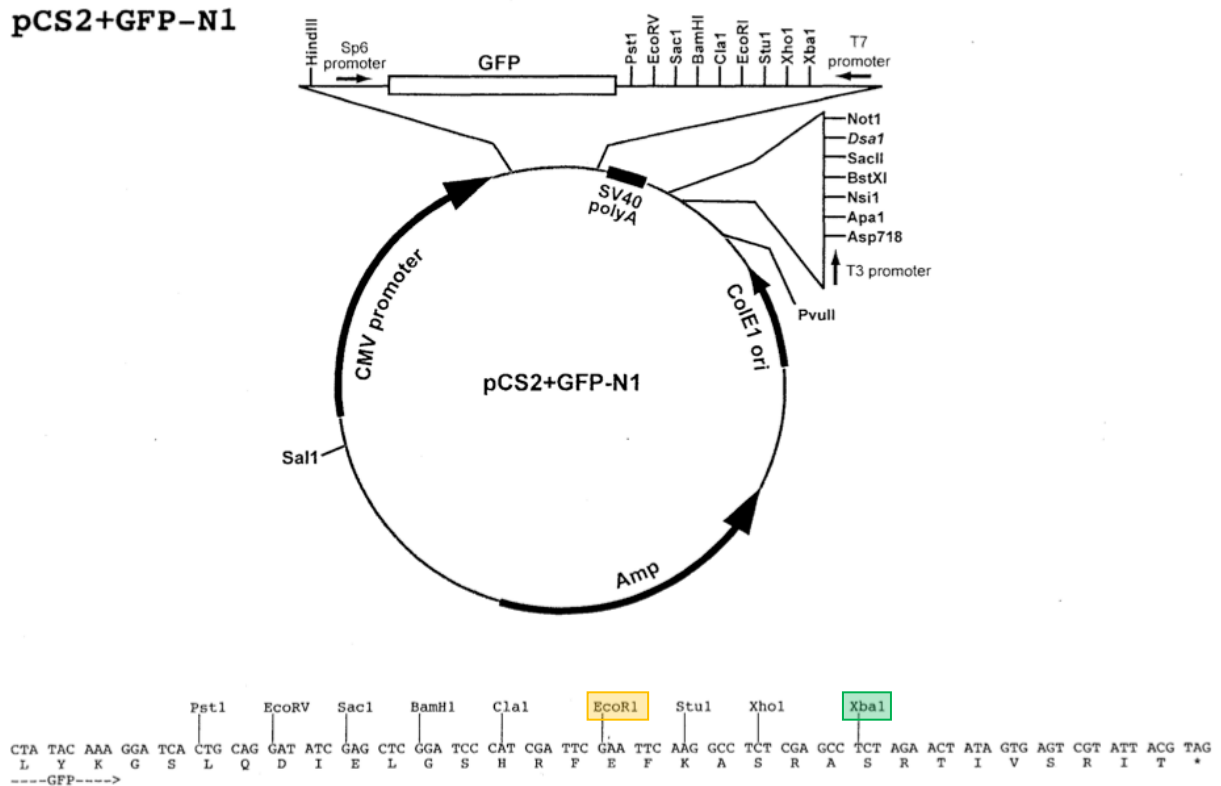


Figure 8. CS2GFP-N1 Plasmid. The CS2GFP-N1 plasmid was used to generate N-terminal GFP-tagged constructs. The coding sequences of the PAR-3 constructs were directionally cloned into the EcoRI (yellow) and XbaI (green) sites. Plasmid was a gift from Jeff Miller, University of Minnesota.

2.2 Generation of *in vitro* transcripts

The PAR-3 constructs in pCS2GFP-N1 were used as templates for *in vitro* transcription. Briefly, the plasmids were linearized with NotI (Fermentas, Burlington, ON) and purified using a Gel/PCR DNA Fragments Extraction Kit (Section 2.1.2). A 50 μ L transcription reaction was then

prepared containing 2.5 μ g of plasmid template, 1mM ATP, 1mM CTP, 1mM UTP, 0.1mMGTP, 1mM G(5')ppp(5')G RNA Cap Structure Analog (New England Biolabs Inc., Pickering, ON), 500u Sp6 RNA polymerase and 1xSP6 Buffer (New England Biolabs Inc., Pickering, ON). The reaction was incubated at 40°C for 30 minutes then 2.5 μ L of 10mM GTP added and incubation continued for an additional hour. The template was removed by addition of 1.5u of RNase free DNase I (Fermentas, Burlington, ON). The capped mRNA was purified using a MEGAclean Kit (Life Technologies Inc., Burlington, ON) according to the manufacturers recommendations. The purified RNA was precipitated with 5M ammonium acetate as described in the MEGAclean Kit procedure and the pellet was washed with 70% ethanol and resuspended in 25 μ L of sterile water. The mRNA was run on a 1% TAE agarose gel to estimate RNA integrity. The mRNA purity and yield was measured using an Ultraspec 2100 pro spectrophotometer (GE Healthcare, Baie d'Urfe, QC) by measuring the absorbance at 260nm and 280nm. Stocks of mRNA were diluted to 1ng/nL and kept in 2uL aliquots at -80°C.

2.3 Temporal Expression of PAR-3

RT-PCR was used to determine the temporal expression of PAR-3. RNA was extracted from embryos at stage 2, 7, 8, 10.5, 12, 17, and 28, and cDNA generated by reverse transcription (gift from Bhanu Pilli) (63). A PCR reaction was carried out using the Δ PDZ1 forward and Δ PDZ3 reverse primers to amplify a 704bp fragment of PAR-3. The PCR reaction was prepared and run as described for Δ PDZ1-3 with the following alterations: 2uL cDNA was used as template, 1.25u Taq DNA polymerase was used along with 1xTaq buffer (supplied by manufacturer), the extension temperature was increased to 72°C, and the extension time

decreased to 45 seconds. A sample containing no cDNA was also amplified as a template negative control. The PCR was run for 18 cycles then 10 μ L of each sample was run on a 1% TAE agarose gel to determine the presence of PAR-3 RNA.

2.4 Tissue Culture

Xenopus A6 cells (ATCC# CCL-102) were maintained at room temperature in T70 flasks containing complete media (66% L-15 media (Sigma, Oakville, ON) supplemented with 10% fetal bovine serum (FBS, Wisent, St. Bruno, QC), 1% L-glutamine (Wisent, St. Bruno, QC), 1% Pennicillin/Streptomycin (Wisent, St. Bruno, QC), 1% sodium pyruvate (Wisent, St. Bruno, QC)). For transfection cells were plated on acid washed coverslips (64) in 60mm dishes and grown to 90-95% confluency. One microgram of purified plasmid diluted in 50 μ L 66% L-15 media was mixed with 1 μ L Lipofectamine 2000 (Invitrogen, Burlington, ON) diluted in 50 μ L of 66% L-15 media and left at room temperature for 20 minutes. The cells were transfected for 4-5 hours in 66% L-15 media supplemented with 2% FBS. The transfection media was then removed and fresh 2% serum media added. Cells were transferred back to complete media after 24 hours and cultured to confluent epithelial sheets.

2.4.1 Scratch Assay

Scratch assays (65) were used to estimate the sub-cellular compartmentalization of the GFP tagged PAR-3 constructs. Briefly a pipette tip was used to scratch the confluent A6 cell sheets (Section 2.4) creating grid pattern wounds in the epithelial sheet. The complete media was replaced to prevent resettling of the cells removed by scratching on the coverslips. The cells

were cultured until migration was observed in the wounded areas (~2 h), then the coverslips were removed and adherent cells fixed with 4% paraformaldehyde diluted in 1xPhosphate-buffered Saline (PBS; 10xPBS(-); 130mM NaCl, 3mM KCl, 10mM Na₂HPO₄, 2mM KH₂PO₄), supplemented with 1mM CaCl₂ and 1mM MgCl₂ (PBS) for 15 minutes. Coverslips were washed three times for 10 minutes with 1xPBS and stored in dishes containing 1xPBS at 4°C. Before imaging, the cells were stained with rhodamine phalloidin to visualize actin (1/8, 20 min, Biotium, Hayward CA) and nuclei stained with bisbenzamide (2µM, 5 min). Coverslips were mounted on slides with a drop of 30% glycerol and sealed with nailpolish. The cells were imaged using a Zeiss Axiovert 200 inverted microscope (Zeiss, Toronto, ON) equipped with a Qimaging retiga EXi digital camera (Qimaging, Burnaby, BC). The images were recorded using OpenLab software (PerkinElmer Inc, Waltham, MA).

2.4.2 Calcium Switch Assay

Calcium switch assays, adapted from Izumi *et al* 1998, were used to assess sub-cellular protein compartmentalization during cell polarization (66). Briefly, complete media was removed from confluent cell cultures (Section 2.4) and replaced with media containing 4mM EGTA. Cells were cultured in calcium depleted media until cells began to round (~2 h), then the media was replaced with complete media and the cells were cultured overnight. Cells were fixed as described in Section 2.4.1, at three time points: prior to addition of the EGTA media (confluent epithelial sheet), after cell rounding (non-polar), and after culturing overnight in complete media (re-polarization). Cells were stained and imaged as previously described (Section 2.4.1).

2.5 *Xenopus* embryos, microinjections and explants

2.5.1 Raising embryos

Xenopus laevis were purchased from Nasco (Fort Atkinson, Wisconsin) and housed in the Department of Biology Aquatic Facility at the University of Waterloo. Females were pre-primed with 20u HCG (Chorulon; Intervet, Kirkland, QC) 5-10 days before spawning. To induce spawning, females were injected subcutaneously with 600u of HCG. Eggs were obtained manually and fertilized *in vitro* using standard methods (67). The fertilized embryos were de-jellied in 2% cystein hydrochloride (BioShop, Burlington, Ontario) in 0.1x Modified Barth's Saline (MBS; 1X MBS; 88mM NaCl, 1mM KCl, 0.7mM MgSO₄, 1mM HEPES, 5mM NaHCO₃, 0.1mM CaCl₂), pH 8.3. Embryos were rinsed three times with deionized water to remove the cystein solution, rinsed in 0.1xMBS before being transferred to a 100mm petri dish. Embryos were raised in 0.1xMSB and staged according to Nieuwkoop and Faber (1967).

2.5.2 Microinjections

Injections were performed using a Narishige IM300 pressure injector (East Meadow, NY) with glass microinjection needles, made using a Narishige PC-10 puller (East Meadow, NY). For injection embryos were transferred to 0.5xMBS containing 4% Ficoll (BioShop, Burlington, ON) and arranged on mesh. The GFP-tagged mRNAs (described in Section 2.2) were injected into the marginal zone of the two dorsal blastomeres at the two or four cell stage. Injections were carried out on a 14°C chilled microscope stage. Following injection embryos were transferred to 0.1xMBS. Embryos were imaged on a Zeiss Lumar V12 dissecting microscope

(Zeiss, Toronto, ON) with a Qimaging MicroPublisher 5.0 RTV digital camera (Qimaging, Burnaby, BC) using Zeiss Axiovision 4 software.

2.5.3 Keller Explants

Keller explants were taken from Stage 10 embryos as described in Harland *et al.* (68). Briefly, embryos were transferred to plasticine coated petri dishes containing Danilchik's for Amy (69) (DFA; 49.5mM NaCl, 36.5mM gluconic acid sodium salt, 5mM Na₂CO₃, 4.5mM KCl, 1mM CaCl₂, 1mM MgSO₄, 0.1% BSA, 6mM HEPES, pH 8.1) and the vitelline envelopes removed. A dorsal section of the embryo was excised and mounted under a coverslip bridge in 60mm petri dishes coated with 50mg/mL BSA in 1xPBS (Figure 10). Explants were left to extend at 20°C then fixed for 2 hours in 3.7% formaldehyde in 1xMEMFA (10xMEMFA; 1M MOPS, 20mM EGTA, 1mM MgSO₄, pH to 7.4), with the fix being refreshed after 1 hour. Explants were then washed three times for 10 minutes in 1xPBS and stored in 1xPBS. Explants were mounted on slides and imaged using a Nikon Eclipse 90i confocal microscope fitted with a Nikon D-eclipse C1 scan head and recorded using Nikon EZ-C1 software (Nikon, Mississauga, ON).

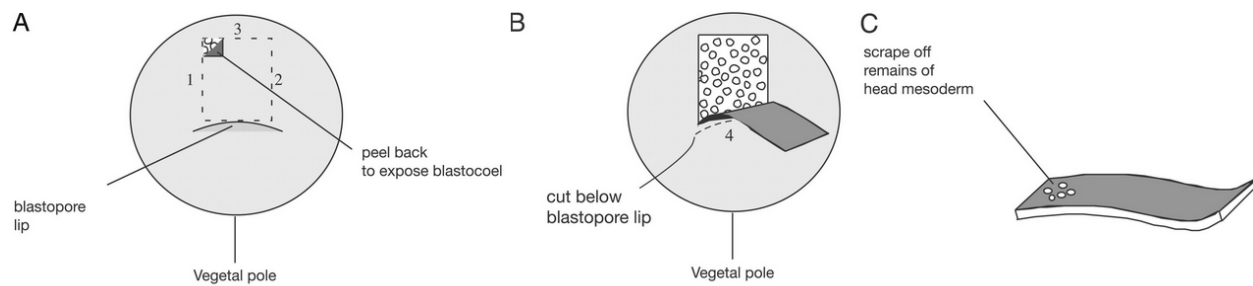


Figure 9. Keller Explants. Explants are cut from embryos at Stage 10+ (A). The cut section is then peeled back and removed by cutting below the blastopore lip (B). The explants is then trimmed and any remaining head mesoderm is removed (C). *Adapted from Sive et al, 2000*

2.6 Western Blot

Western Blots were conducted according to standard protocols (59). Five embryos injected with 1.5ng of mRNA were selected for each PAR-3 construct at Stage 12 and frozen in microfuge tubes at -80°C . Embryos were lysed in Embryo Solubilization Buffer (ESB: 100mM NaCl, 50mM Tris pH 7.5, 1% TritonX, 2mM PMSF, 1xProtease inhibitor, EDTA, 1mM Sodium orthovanadate), incubated on ice for 10 minutes, centrifuged at 14000rpm for 20 minutes at 4°C . The soluble protein layer was transferred to a new tube and 20% 5x Loading Buffer (5X; 312.5mM Tris-HCl pH 6.8, 1% SDS, 25% Glycerol, 0.015% Bromophenol Blue, 5% β -mercaptoethanol) added before heating to 95°C for 5 minutes. Approximately three embryo equivalents were loaded in each lane and separated by SDS-PAGE (59) gel using a Mini-Protean 3 system (Bio-Rad, Mississauga, ON). The protein was then transferred to a nitrocellulose membrane (GE Healthcare, Baie d'Urfe, QC) and the membrane was blocked overnight at 4°C in 1xTBS containing 5% skim milk and 0.1% Tween-20. The GFP-tagged PAR-3 constructs were detected using mouse anti-GFP primary (1/2000, Roche, Mississauga, ON, Cat. No. 11814460001) and horse radish peroxidase (HRP) conjugated anti-mouse secondary antibody (1/3000, Jackson ImmunoResearch, West Grove PA, Code# 115035146). Bands were visualized

using chemiluminescence (Solution 1: 2.5mM Luminol, 0.4mM p-cumaric acid, 100mM Tris-HCl pH 8.5; Solution 2: 0.02% H₂O₂, 100mM Tris-HCl pH 8.5). One milliliter each of Solutions 1 and 2 was mixed and left on the blot for one minute before exposure to RXB x-ray film (Labscientific; Livingston, NJ).

Chapter 3

Results

3.1 Cloning and Mutation of *Xenopus laevis* PAR-3

PAR-3 has not previously been described in *Xenopus laevis*. I obtained an EST clone of *Xenopus* PAR-3 from Image Consortium. The amino acid sequence encoded by the *Xenopus* PAR-3 EST coding sequence (subsequently referred to as PAR-3) was compared to known PAR-3 homologs and the percent identity (percent identical amino acids) and percent similarity (percent similar amino acids) were determined using the MacVector analysis suite (MacVector Inc., Cary, NC). PAR-3 shared 62.3% identity and 70.2% similarity with human, 59.4% identity and 68.2% similarity with mouse, a 59.2% and 70.9% similarity with zebrafish, a 17.7% identity and 30.7% similarity with fly, and a 14.5% identity and 25.3% similarity with worm PAR-3 proteins (Figure 10, A). The evolutionary relationships were displayed as a dendrogram (Figure 10, B) confirming that the vertebrate PAR-3s are more closely related than the invertebrate molecules. I then aligned the amino acid sequence of *Xenopus* PAR-3 to the PAR-3 homologs to identify conserved functional domains. *Xenopus* PAR-3 was found to contain a conserved N-terminal region (CR1), three PDZ domains, as well as conserved sequence representing an aPKC binding domain (Figure 11).

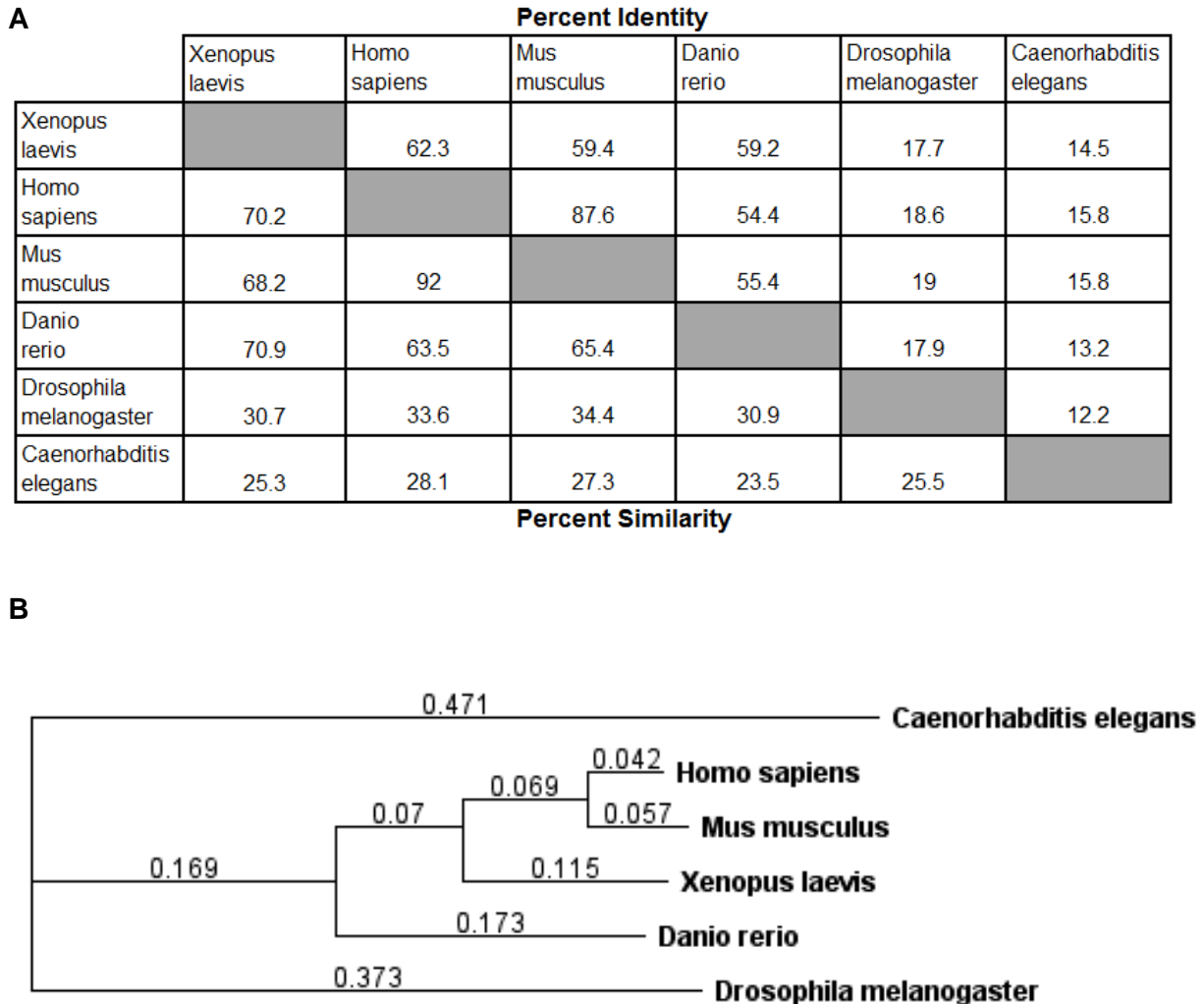


Figure 10. Comparison of *Xenopus* PAR-3 with known PAR-3 homologs. The percent identity and percent similarity between *Xenopus* PAR-3 and known PAR-3 homologs is shown in A. The evolutionary divergence of the *Xenopus* PAR-3 protein is shown in B. The values indicate the relative divergence between species. This data was generated by ClustalW alignment using MacVector software (MacVector Inc, Cary, NC).

10 20 30 40 50 60

Xenopus laevis
Homo sapiens
Mus musculus
Danio rerio
Drosophila melanogaster
Caenorhabditis elegans **MSASSTSSSSSTSCPEGGEPSSGSCSSDEGESTLKKRMQQYGIASGYANSSISTLDRSQYQ**

70 80 90 100 110 120

Xenopus laevis - - - - - **MKVTV[S]FGRTRVVVP CGDGNLKV[S]SLIQQAVT RYKKAIAKDPGYWIQVHRLEH**
Homo sapiens - - - - - **MKVTVCFGRTRVVVP CGDGHMKV[F]SLIQQAVT RYRKAIAKDPN YWIQVHRLEH**
Mus musculus - - - - - **MKVTVCFGRTRVVVP CGDGRMKV[F]SLIQQAVT RYRKAIAKDPN YWIQVHRLEH**
Danio rerio - - - - - **MKVTVCFGRTRVVVP CGDGNIKV[Q]SLVQQAA[MR]YRAIAK[GEE]YVWQV[Y]RLEH**
Drosophila melanogaster - - - - - **MKVTVCFGDV[R]ILVPCG[S]GELLV[R]DLVKEA[T]RRY[Y]KAAAGK-[P]DSWV[T]VTHL[Q]T**
Caenorhabditis elegans **[S]LPLNGT[R]RVTV[Q]FGRMKI[V]VPWK[E]SDQT[V]GQLADA[AL]LR YKKA[R]GMANEDR[I]HVRLE[C]**

130 140 150 160 170 180

Xenopus laevis - **GDGGI LDLDLDDI LCDVADDDKRLVAIYDEQDP** - - - - - **HHGGDGT[S]** - **ASSTGTQSPEIFGS**
Homo sapiens - **GDGGI LDLDLDDI LCDVADDDKRLVAVFDEQDP** - - - - - **HHGGDGT[S]** - **ASSTGTQSPEIFGS**
Mus musculus - **GDGGI LDLDLDDI LCDVADDDKRLVAVFDEQDP** - - - - - **HHGGDGT[S]** - **ASSTGTQSPEIFGS**
Danio rerio - **GDGGI LDLDLDDV LCDVADDDKRLVAVFDEQEP** - - - - - **H[V]GGDGT[S]** - **ASSTGTQSPELYCG**
Drosophila melanogaster - **Q[S]G[-]I LDP[DD]C[V]R[DV]ADDDRE[Q]I L[A]H[F]DDP[G]PDPGVP[Q]GGGGG[A]S[S]S[S]V[GT]G[S]PDI FRD**
Caenorhabditis elegans **[A]S[DG]GI LDMDDVLE[EV]FD[L]NYDQ[LA]ITDEAN** - - - - - **GGSTTPTYS[Q]IQKQOHHYAQP**

190 200 210 220 230 240

Xenopus laevis **ELGTN[S]-M[S]AFQPY[QAA]SEIEVTP[S]-VLRANMPLHVRR[S]-SDPALVGIT-TSVSDSNFT**
Homo sapiens **ELGTNN-V[S]AFQPY[QAT]SEIEVTP[S]-VLRANMPLHVRR[S]-SDPALIGLS-TSVSDSNFS**
Mus musculus **ELGTNN-V[S]AFQPY[QAT]SEIEVTP[S]-VLRANMPLHVRR[S]-SDPALTGLS-TSVSDNNSFS**
Danio rerio **EPSTSTP[L]SAFQPY[LPH]SEIEVTT[S]-TLR[T]NMP LHVRR[S]-SDPALLNLTAM[S]FSEP GSQ**
Drosophila melanogaster **PTN[T]EAP[T]CPRDLSTPHI[E]VTST[T]SGPMA[GL]GVGLM[V]RR[S]-SDPNLLASLKAE[GS]NKR[WS]**
Caenorhabditis elegans **LPYARKFDG[G]PSTPI[A]SAF[GS]VT[V]NHQ[A]HRA[AS]P[Y]N[V]GFAR[S]NSRD[F]APQ[PT]H[S]KERR[DS]**

250 260 270 280 290 300

Xenopus laevis **AEDP SRKNP SRWSTTAGFLTK[KN]S[S]AAK GANDITK[-]DEE[-]**
Homo sapiens **SEEP SRKNP TRWSTTAGFLKQ[NTA]GSPKTCDRK[-]KDENYRSLPRDT[S]NWSNQ[-]FQRDN**
Mus musculus **SEEP SRKNP TRWSTTAGFLKQ[NTA]GSPKTCDRK[-]KDENYRSLPRDP[S]SWSNQ[-]FQRDN**
Danio rerio **PEEP SRKNP TRWSTTAGFLKPR[F]ATGTNSLERKGR[GV]D[T]YRSLPRDAGQWSNQKEFQR[E]K**
Drosophila melanogaster **AAA[PH]YAGGD[-]S[PER]LFLDKAGGQLSPQWEE[-]**
Caenorhabditis elegans **VV[E]V[S]SFDQIP[QS]GLR[V]STPKP[S]RQSE[DV]I[D]GK[-]**

310 320 330 340 350 360

Xenopus laevis - - - - - **EAEENSRVEPVG-HADTSLERTSS[S]SLDDMVKLVE**
Homo sapiens **ARSSLASHPMV[GK]WLEK[QE]QDE[EG]TEEDNSRVEPVG-HADTGLEHINPFSLDDMVKLVE**
Mus musculus **ARSSLASHPMV[DR]WLEK[QE]QDE[EG]TEEDNSRVEPVG-HADTGLENMPNFSLDDMVKLVQ**
Danio rerio **ARSSLAS[AN]HPMV[DR]WLEK[QE]Q[-]DEEENGRIEPVG-RADT[C]LEHMGVRS[LDD]IVKLVE**
Drosophila melanogaster **DDP[SH]QLKEQLLH[Q]QOPHAANGGSSSGNHQP[FA]RS[GR]LSMQFLGDGN[G]YK[W]MEAAE**
Caenorhabditis elegans **PMNQP[IL]RSSLRTE[AS]GSRTEATPVKQS[R]VTLSP[E]VEKKLAEQDERK[SER]**

370 380 390 400 410 420

Xenopus laevis **V[S]NDGGPLGIHVVPYSARGGRTLGLLVKRLEKGGKAE[RE]NLFHEND--CIVRINNGDLR**
Homo sapiens **VPNDGGPLGIHVVPFSARGGRTLGLLVKRLEKGGKAE[HE]NLFREND--CIVRINDGDLR**
Mus musculus **VPNDGGPLGIHVVPFSARGGRTLGLLVKRLEKGGKAE[QE]NLFHEND--CIVRINDGDLR**
Danio rerio **V[S]NDGGPLGIHVVPFSGR[DR]RTLGLLVKRRLERGGKADVQGLFQEND--CIRIRINNGDLR**
Drosophila melanogaster **KLQ[N]QP[PA]QQTYYQGG[SH]HAGH[GQ]N[GAY]SSKSLPRESKRKEPLGQAY--ESI REKDGEML**
Caenorhabditis elegans **RKH YDKNP[GR]F[AR]GSDR[K]SRI[T]DALLDAR[DR]I[AD]OLE[S]ON[PA]E[ET]K[S]OM[IR]VKIDOGPMP**

	850	860	870	880	890	900
Xenopus laevis	MIQLIVARRV	KL S	-	-	-	ELLES
Homo sapiens	MIQLIVARRI	S	KCN	-	-	ELKSP
Mus musculus	MIQLIVARRI	S	R	CN	-	ELRSP
Danio rerio	MIQLIVARRI	N	KRL	-	-	EGESR
Drosophila melanogaster	TI	TLLVGRKI	L	R	S	A
Caenorhabditis elegans	MI	S	SNVRLTI	S	R	Y

	910	920	930	940	950	960
Xenopus laevis	VETML	DDRRERRI	SHSLYS	S	IEGF	DES
Homo sapiens	IETAL	DDRRERRI	SHSLYS	G	IEGL	DES
Mus musculus	IETEL	DDRRERRI	SHSLYS	G	IEGL	DES
Danio rerio	LSP	SPDDHERRI	SHSLYG	-	IEGL	DDN
Drosophila melanogaster	I	YLSPE	E	KRE	QR	C
Caenorhabditis elegans	L	S	R	I	T	V

	970	980	990	1000	1010	1020
Xenopus laevis	EDDRTP	VLP	S	QLSDH	S	S
Homo sapiens	EDDRLP	VLP	PHL	SDQ	S	S
Mus musculus	EDDRLP	VLP	PHL	SDQ	S	S
Danio rerio	EDDRPH	VLP	I	QLSDQ	S	S
Drosophila melanogaster	S	QQQQ	QRR	L	A	P
Caenorhabditis elegans	L	T	E	R	D	S

	1030	1040	1050	1060	1070	1080
Xenopus laevis	DP	S	L	A	F	Q
Homo sapiens	DP	V	L	A	F	Q
Mus musculus	DP	V	L	A	F	Q
Danio rerio	E	G	-	-	Q	F
Drosophila melanogaster	P	T	L	P	A	R
Caenorhabditis elegans	Q	H	I	K	L	F

	1090	1100	1110	1120	1130	1140
Xenopus laevis	QN	S	G	S	P	S
Homo sapiens	QK	A	G	S	P	S
Mus musculus	QK	A	G	S	P	S
Danio rerio	N	H	T	G	S	T
Drosophila melanogaster	S	G	V	E	H	F
Caenorhabditis elegans	N	L	D	D	S	D

	1150	1160	1170	1180	1190	1200
Xenopus laevis	IDK	S	Y	D	K	P
Homo sapiens	IDK	S	Y	D	K	P
Mus musculus	IDK	S	Y	D	K	P
Danio rerio	IDK	S	Y	D	R	P
Drosophila melanogaster	I	E	S	L	T	A
Caenorhabditis elegans	R	L	K	N	E	E

	1210	1220	1230	1240	1250	1260
Xenopus laevis	-	S	H	S	L	E
Homo sapiens	-	S	H	S	L	E
Mus musculus	-	S	Y	S	L	E
Danio rerio	L	P	V	T	E	Q
Drosophila melanogaster	S	L	E	S	L	Q
Caenorhabditis elegans	Q	L	R	S	V	E

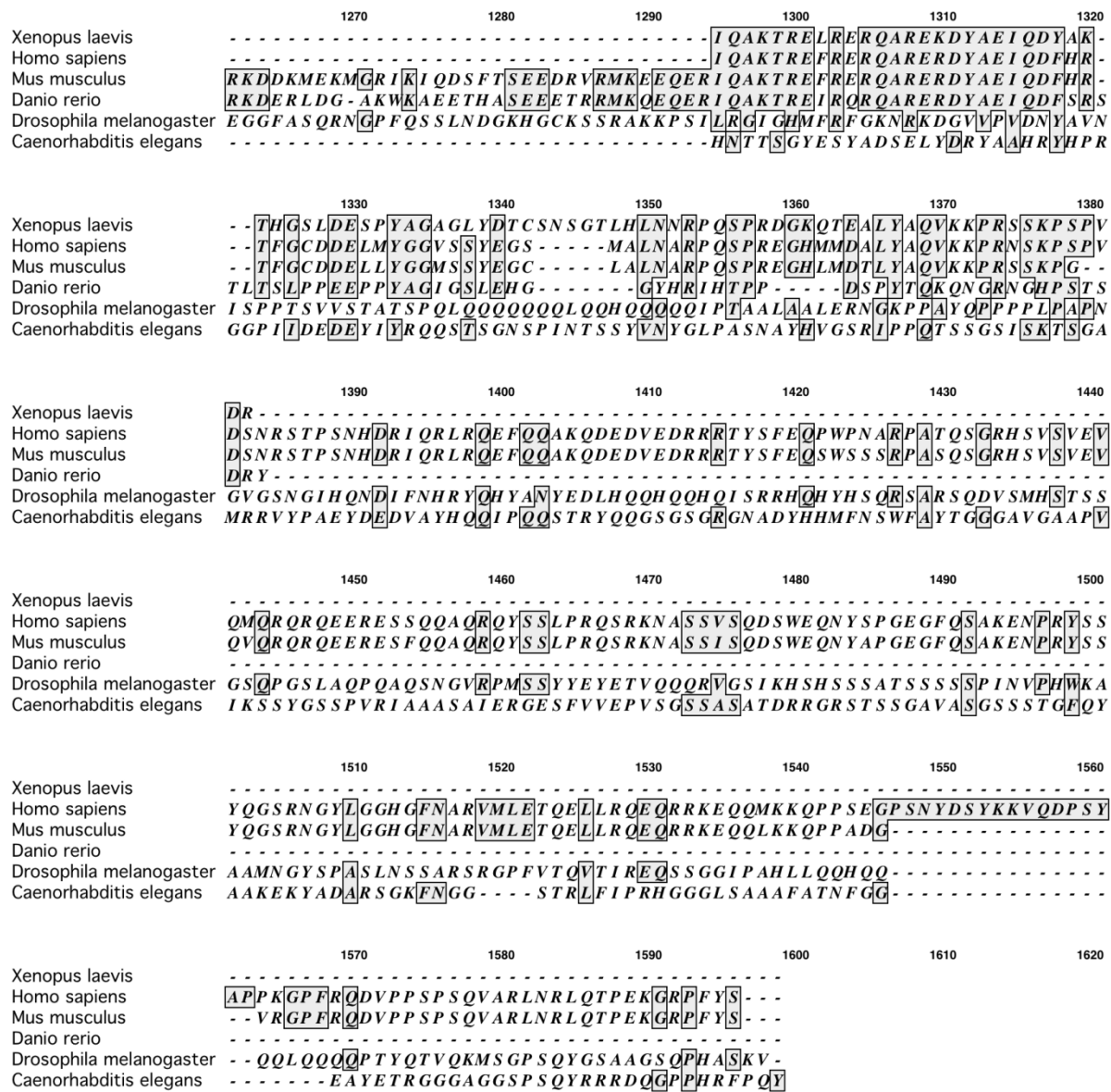


Figure 11. Alignment of *Xenopus* PAR-3 with known PAR-3 homologs. *Xenopus* PAR-3 was aligned with PAR-3 homologs from *H. sapiens*, *M. Musculus*, *D. rerio*, *D. melanogaster* and *C. elegans*. The N-terminal conserved CR1 domain is highlighted in Blue. The PDZ1 domain is highlighted in yellow, the PDZ2 domain is highlighted in red and the PDZ3 domain is highlighted in green. The aPKC binding region (orange) is also conserved. The aPKC phosphorylation site is indicated by ♦. This alignment was prepared using the ClustalW method with MacVector software.

3.2 PAR-3 is expressed throughout *Xenopus* gastrulation

It has previously been shown that PAR-3 is present in the *Xenopus* oocyte as a maternal protein (57), however further expression of PAR-3 during *Xenopus* embryonic development has not been characterized. I used RT-PCR to estimate the expression of PAR-3 during the early stages of *Xenopus laevis* embryogenesis. Template cDNA was made from RNA isolated from embryos at the following stages of development; Stage 2: cleavage, Stage 7: early blastula prior to initiation of zygotic transcription, Stage 8: mid-blastula after initiation of zygotic transcription, Stage 10.5: early gastrula, Stage 12: late gastrula, Stage 17: neurula, and Stage 28: early tadpole undergoing organogenesis. I used the Δ PDZ1 forward and Δ PDZ3 reverse primers (Table 1) to amplify a 704bp fragment encompassing bp 916-1620 of the PAR-3 coding sequence. The PAR-3 maternal transcripts persist until zygotic transcription begins at mid-blastula transition at Stage 7 (Figure 12, 2-7). PAR-3 then continues to be expressed by the zygote throughout gastrulation (Figure 12, 10.5-12), neurulation (Figure 12, 17) and at the start of organogenesis (Figure 12, 28). In summary, PAR-3 was expressed at all stages of development.

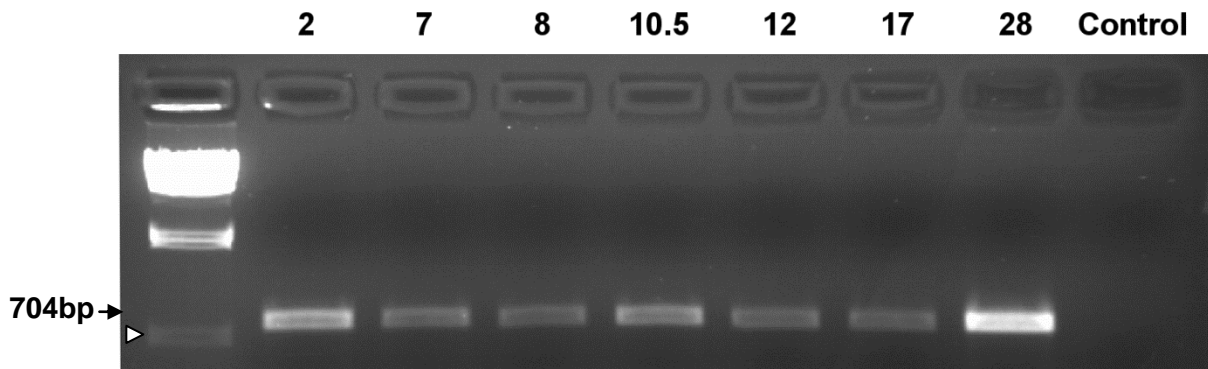


Figure 12. Temporal expression of PAR-3. PAR-3 is expressed throughout *Xenopus* development. RT-PCR was used to amplify a 704bp fragment of PAR-3 using cDNA obtained from key developmental stages (indicated along top of figure). PAR-3 is expressed as a maternal transcript in the early blastula (Stages 2-7) then expressed as a zygotic mRNA after mid-blastula transition (Stage 8). PAR-3 continues to be expressed during gastrulation (Stage 10.5-12) neurulation (Stage 17) and organogenesis (Stage 28). The first lane contains a λ /HindIII DNA ladder for size marker, with the bottom band corresponding to 564bp (arrowhead). A sample containing no template cDNA was included as a negative control.

3.3 Mutation of PAR-3

Deletion constructs were created to assist in defining the roles of conserved domains found in *Xenopus* PAR-3. Deletions were made using a PCR strategy. The conserved N-terminal region (CR1) has been identified as a self-oligomerization domain responsible for the formation of higher order PAR-3 scaffolds enhancing sub-cellular compartmentalization (36). The Δ CR1 construct (Figure 7) results in deletion of aa 1-50 completely removing this domain.

Individual PDZ domains were then removed using inverse PCR (61). The PDZ1 domain is responsible for interaction with PAR-6, JAMs 1-3, and nectins (27, 34, 43, 70, 71). The Δ PDZ1 construct contains a deletion of aa 212-305 removing most of this domain (Figure 7). The PDZ2 domain has been identified as a phosphoinositol lipid binding site and is responsible for recruitment of PAR-3 to the cell membrane (35). The Δ PDZ2 construct was created through

removal of aa 406-486 removing the majority of this domain (Figure 7). The PDZ3 domain interacts with PTEN and VE-cadherin is required for the maintenance of cell polarity (35, 37, 47). The Δ PDZ3 construct was generated through deletion of aa 541-627 removing the entire domain (Figure 7).

Interactions between PAR-3 and aPKC are essential for the proper function of PAR-3 and are modulated through phosphorylation of the first conserved serine residue in the aPKC consensus sequence (72). The S777A construct (Figure 7) was generated by altering serine 777 (AGC) to an alanine (GCC) through site directed mutagenesis. This inhibits aPKC phosphorylation of PAR-3 and is expected to form a stable PAR-3/PAR-6/aPKC complex preventing interaction with other PAR-3 binding partners. All constructs were tagged with an N-terminal GFP and the mutations confirmed by sequencing (Appendix A).

3.4 PAR-3 in *Xenopus* A6 cells

3.4.1 Polarized localization of PAR-3 in epithelial cells

Sub-cellular compartmentalization of PAR-3 has not been previously described in a *Xenopus* cell line. A6 cells are a highly polarized *Xenopus* kidney epithelial cell line (73) that should provide a good model for the sub-cellular compartmentalization of PAR-3. I therefore used A6 cells to test my PAR-3 construct ensuring that the N-terminal GFP tag did not alter PAR-3 localization as well as to characterize PAR-3 compartmentalization in a *Xenopus* system.

As an initial characterization I looked at the localization of the PAR-3 construct in A6 cells undergoing epithelial polarization. Calcium switch assays depolarize cells through removal of calcium. Without calcium epithelial adherens and tight junctions break down and cells detach

from their neighbors and become non-polar. Upon re-addition of calcium, polarization can be observed as the cells re-form the epithelial junctions. Using a Calcium switch assay the sub-cellular compartmentalization was observed in non-polar cells, polarizing cells initiating epithelial polarity, and confluent epithelial sheets. PAR-3 was not localized in the non-polar cells and was instead expressed uniformly throughout the cytoplasm (Figure 13, Non-polar). After re-addition of calcium to the culture media cells flattened and began to repolarize. In these cells PAR-3 was concentrated at points of cell-cell contact (Figure 13, Polarizing). This polarized compartmentalization of PAR-3 was then elaborated as a confluent epithelium formed and PAR-3 localized in a punctate pattern around the cell periphery at the maturing cell-cell junctions. PAR-3 over-expression did not appear to inhibit the initiation of epithelial polarization, and the PAR-3 transfected cells were observed to be fully integrated into the confluent epithelial sheet. These results demonstrate that the PAR-3 construct exhibits a polarized compartmentalization to sites of cell-cell adhesion in *Xenopus* A6 epithelia and this polarization is unaffected by the N-terminal GFP. Furthermore, PAR-3 over-expression does not act as appear to inhibit epithelial polarity in *Xenopus* A6 cells.

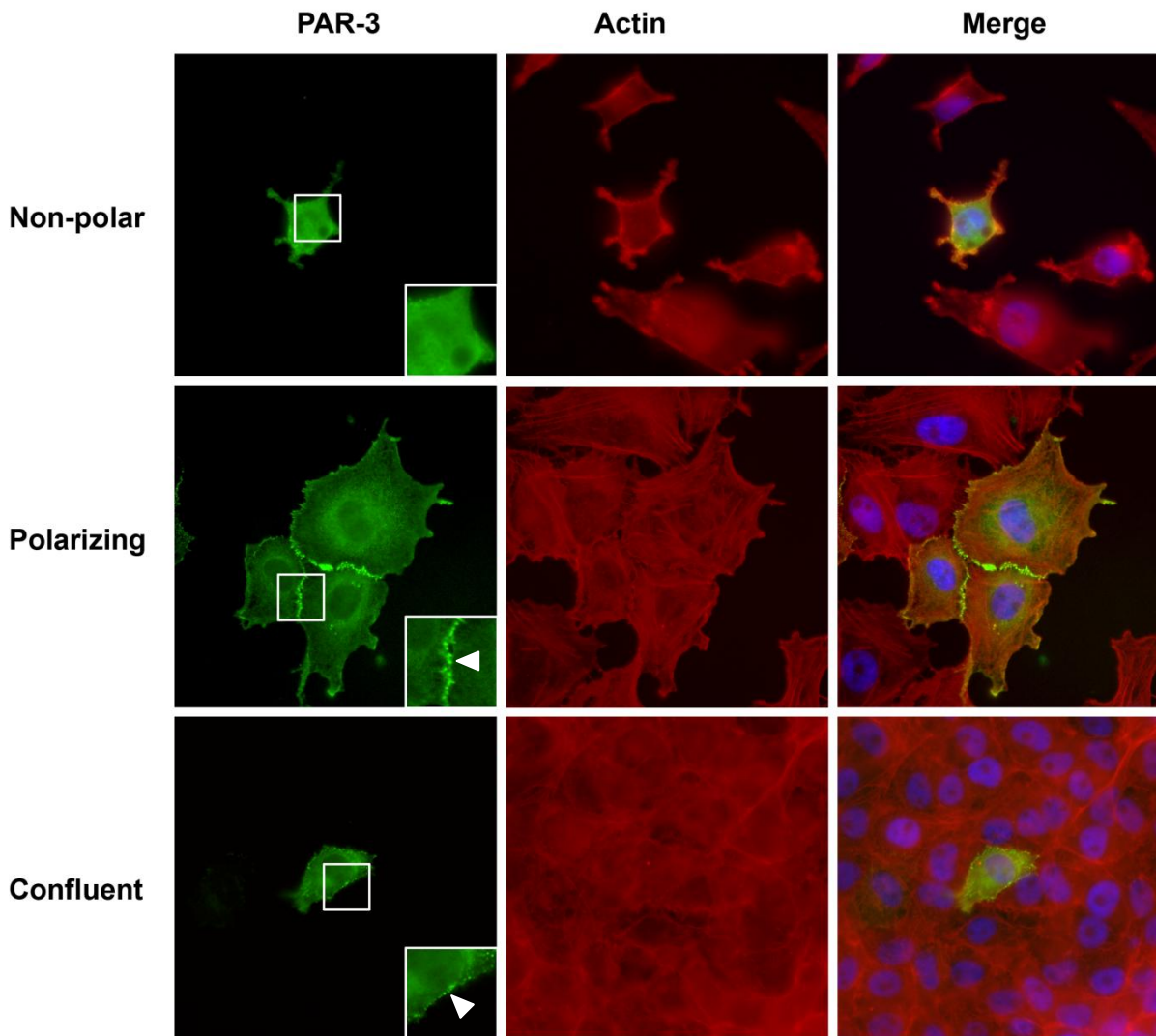


Figure 13. PAR-3 Localizes to cell-cell contacts in *Xenopus* A6 cells. GFP-PAR-3 transfected *Xenopus* A6 cells were subjected to calcium switch. Cells were fixed and stained with rhodamine phalloidin to visualize actin and nuclei stained with bisbenzamide. PAR-3 is uniformly distributed in calcium deprived unpolarized cells (Non-polar). Upon initiation of epithelial polarization PAR-3 was compartmentalized to sites on cell-cell contact (Polarizing). This polarized compartmentalization was elaborated in the confluent epithelium and PAR-3 is present in puncta around the entire cell periphery (Confluent). Arrowheads indicate sites of PAR-3 compartmentalization.

3.4.2 Polarized localization of PAR-3 in migrating cells

The sub-cellular localization of PAR-3 in migrating *Xenopus* A6 cells has not been previously described. When a confluent sheet of A6 cells is wounded in a scratch assay cells at the wound edges undergo an epithelial to mesenchymal transition and migrate into the free space where they proliferate to repair the epithelial sheet. In this situation epithelial cells have an apical/basal polarity while the migrating mesenchymal cells possess a front/rear polarity with a flattened and protrusive front edge, and a rounded rear end.

In the confluent epithelial sheets PAR-3 is localized in puncta around the cell periphery (Figure 14, Confluent). Upon wounding PAR-3 was released from cell-cell contacts and observed to re-localize to the leading front end of migrating cells (Figure 14, Wound). Cells within the epithelial sheet however, maintain PAR-3 compartmentalization at the cell periphery where other cells are attached (Figure 14, Arrows). Together these results indicate that the sub-cellular compartmentalization of PAR-3 in A6 cells is context dependant. Furthermore over-expression of PAR-3 does not inhibit migratory behaviour as cells were still observed to spread and migrate into wounded areas.

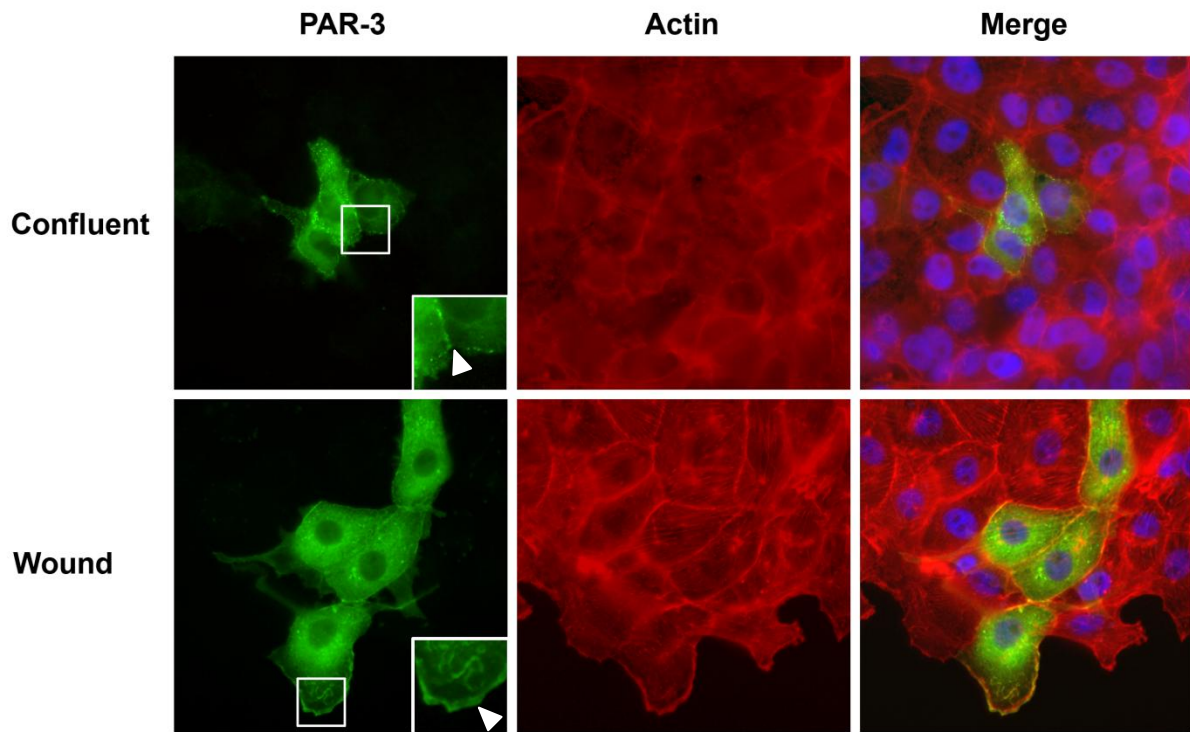


Figure 14. PAR-3 localizes to the leading edge of migrating A6 cells. GFP-PAR-3 transfected A6 cells were cultured until confluent then subjected to a scratch assay. Cells were fixed and stained for actin after migration was apparent at the wound edge. PAR-3 is compartmentalized to the periphery of cells contained in the epithelial sheet (Confluent). Cells at the wound edge exhibit enrichment of PAR-3 at the leading edge (Wound).

3.5 PAR-3 localization in A6 cells requires multiple functional domains

Cells transfected with the mutated PAR-3 constructs were used to define the roles of each domain in the polarized localization of PAR-3. The localization of the mutated constructs was observed in both a calcium switch assay and scratch assay. The polarized compartmentalization was compared to that seen with PAR-3 to determine domains required for localization. The effect of domain removal on generation of polarized behaviours was also observed.

3.5.1 The CR1 and PDZ1 domains of PAR-3 are required for membrane localization

When cells expressing the Δ CR1 construct were subjected to a calcium switch the Δ CR1 construct was found throughout the cytoplasm in non-polar cells (Figure 15, Non-polar). This expression was unchanged when cells were allowed to polarize and Δ CR1 remained cytoplasmic in both the polarizing (Figure 15, Polarizing) and confluent epithelial cells (Figure 15, Confluent). The cytoplasmic accumulation did not significantly alter cell behaviours and cells were still able to attach to neighboring cells and were fully integrated into a confluent sheet. Δ CR1 accumulated in the cytoplasm of migrating cells and was not enriched at the leading edge (Figure 16, Wound). Over-expression of Δ CR1 did not inhibit formation of protrusions or migratory behaviour. Similar results were observed for cells expressing the Δ PDZ1 construct. Δ PDZ1 was also unable to localize during the calcium switch assay and remained diffuse throughout the cytoplasm in non-polar (Figure 17, Non-polar), polarizing (Figure 17, Polarizing), and confluent (Figure 17, Confluent) cells. Behaviours were also unchanged as cells were able to repolarize, recognize neighboring cells, and form a confluent epithelium. The Δ PDZ1 construct also failed to localize in scratch assays with it remaining cytoplasmic in both confluent

(Figure 18, Confluent) and migrating cells (Figure 18, Wound) with no enrichment at either the cell periphery or leading edge. Migratory behaviour was similarly uninhibited by removal of the PDZ1 domain as protrusive activity was still observed at the leading edge. Together these results indicate that the Δ CR1 and Δ PDZ1 domains are required for recruitment of PAR-3 to cell-cell contacts and its subsequent compartmentalization to the cell periphery as well as for PAR-3 localization to the leading edge of migrating cells.

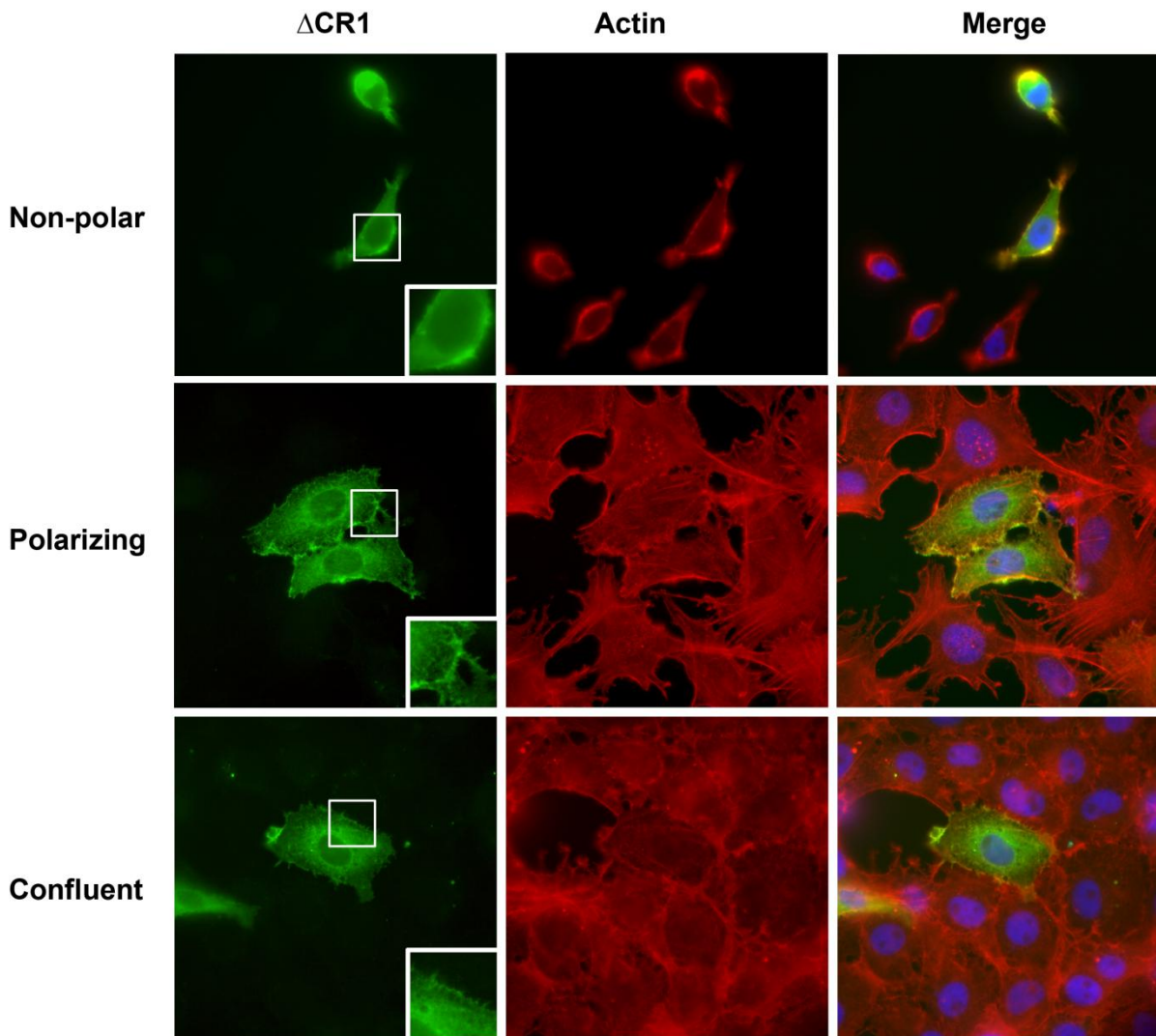


Figure 15. The CR1 domain is required for localization of PAR-3. *Xenopus* A6 cells were transfected with GFP- Δ CR1, lacking the PAR-3 self-oligomerization domain, and subjected to a calcium switch. Removal of the CR1 region resulted in a loss of PAR-3 compartmentalization and expression is cytoplasmic in both depolarized (Non-polar), polarized and confluent cells (Polarizing, Confluent). The ability of transfected cells to repolarize after calcium switch was unaltered.

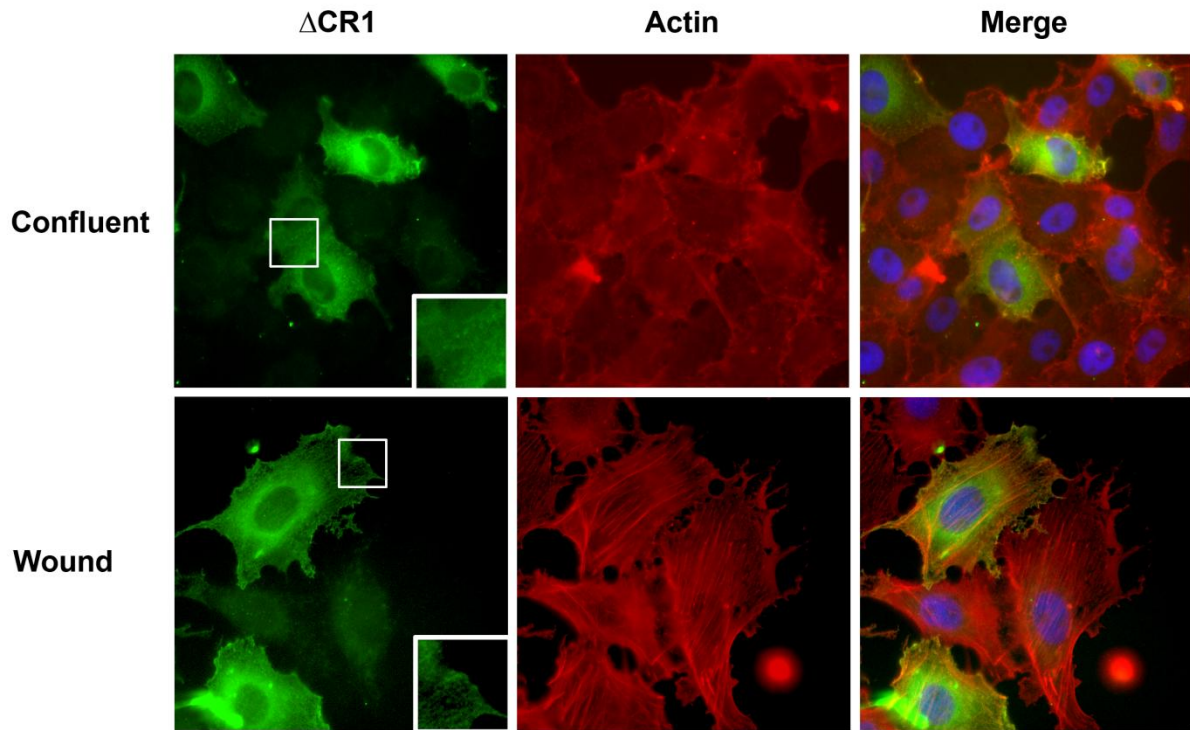


Figure 16. The CR1 domain is required for localization of PAR-3 in migrating cells. Cells transfected with the CR1 construct were subjected to a scratch assay. The CR1 construct was not compartmentalized in the epithelial sheet (Confluent) or in migrating wound edge cells (Wound). Over-expression of CR1 did not affect the transition from epithelial to migrating polarity.

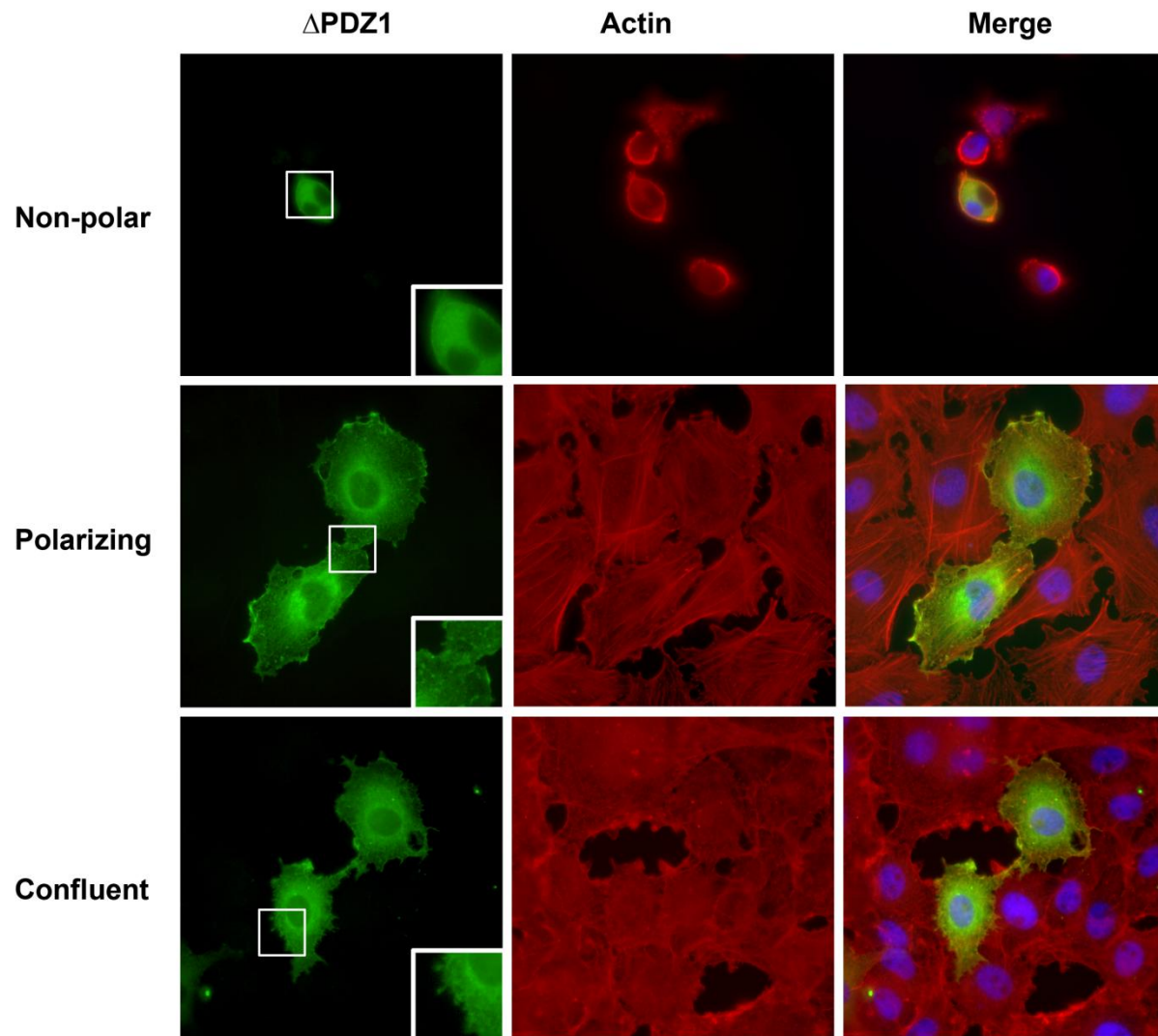


Figure 17. The PDZ1 domain is required for PAR-3 recruitment to cell-cell contacts. *Xenopus* A6 cells were transfected with GFP- Δ PDZ1, in which the first PDZ domain has been deleted. The PDZ1 construct is diffusely expressed in the cytoplasm of non-polar cells (Non-polar) is not compartmentalized to cell-cell contacts (Polarizing) or epithelial junctions (Confluent). Despite the failure in localization the cells were still able to form an epithelial sheet.

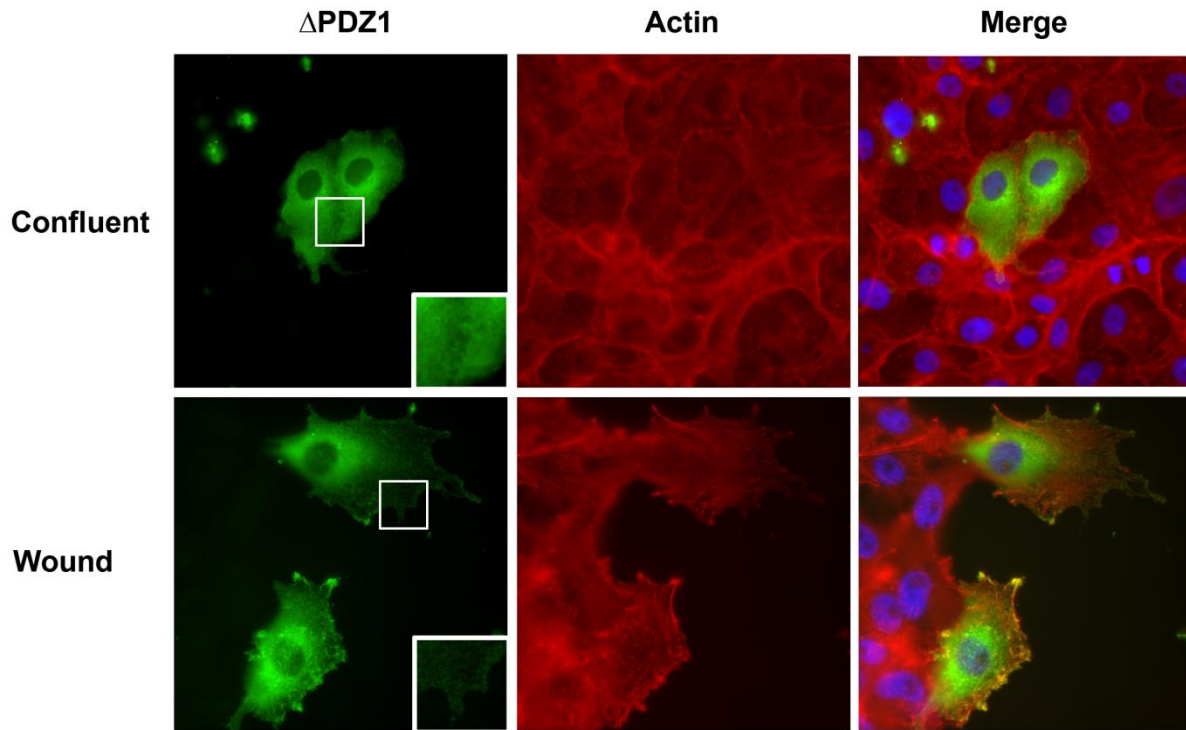


Figure 18. The PDZ1 domain is required for recruitment of PAR-3 to the leading edge. In scratch assays the PDZ1 construct was expressed throughout the cytoplasm in both epithelial (Confluent) and migrating cells (Wound). Over-expression of PDZ1 did not alter formation of epithelial junctions or protrusions.

3.5.2 The PDZ2 domain of PAR-3 is not required for membrane localization

Δ PDZ2 was able to localize in calcium switch assays. It displayed uniform cytoplasmic expression in non-polar cells (Figure 19, Non-polar) then was observed to compartmentalize to cell-cell contacts as cells repolarized (Figure 19, polarizing). The concentration of Δ PDZ2 at cell-cell contact sites appeared diminished when compared to the PAR-3 construct. Δ PDZ2 also had a reduced accumulation at the cell periphery in confluent cells as compared to the PAR-3 construct (Figure 19, Confluent). Apical puncta were only visible between two cells expressing the GFP construct suggesting that accumulation in opposing membranes was required to resolve the fluorescence. This suggests a lower efficiency of PAR-3 localization in the absence of the PDZ2 domain. Cell behaviours remained unaltered and cells were observed to repolarize and form contacts with neighboring cells as well as integrate into the confluent epithelial sheet. In scratch assays a diminished localization of Δ PDZ2 was also observed in the epithelial sheet, with localization only apparent in adjacent transfected cells. Migrating cells displayed enrichment of Δ PDZ2 at the leading edge also with a slightly diminished intensity (Figure 20, Wound). Protrusions were not inhibited by PDZ2 over-expression. These results suggest that the PDZ2 domain is not necessary for PAR-3 localization in either epithelial or migrating cells however, its presence may increase localization efficiency.

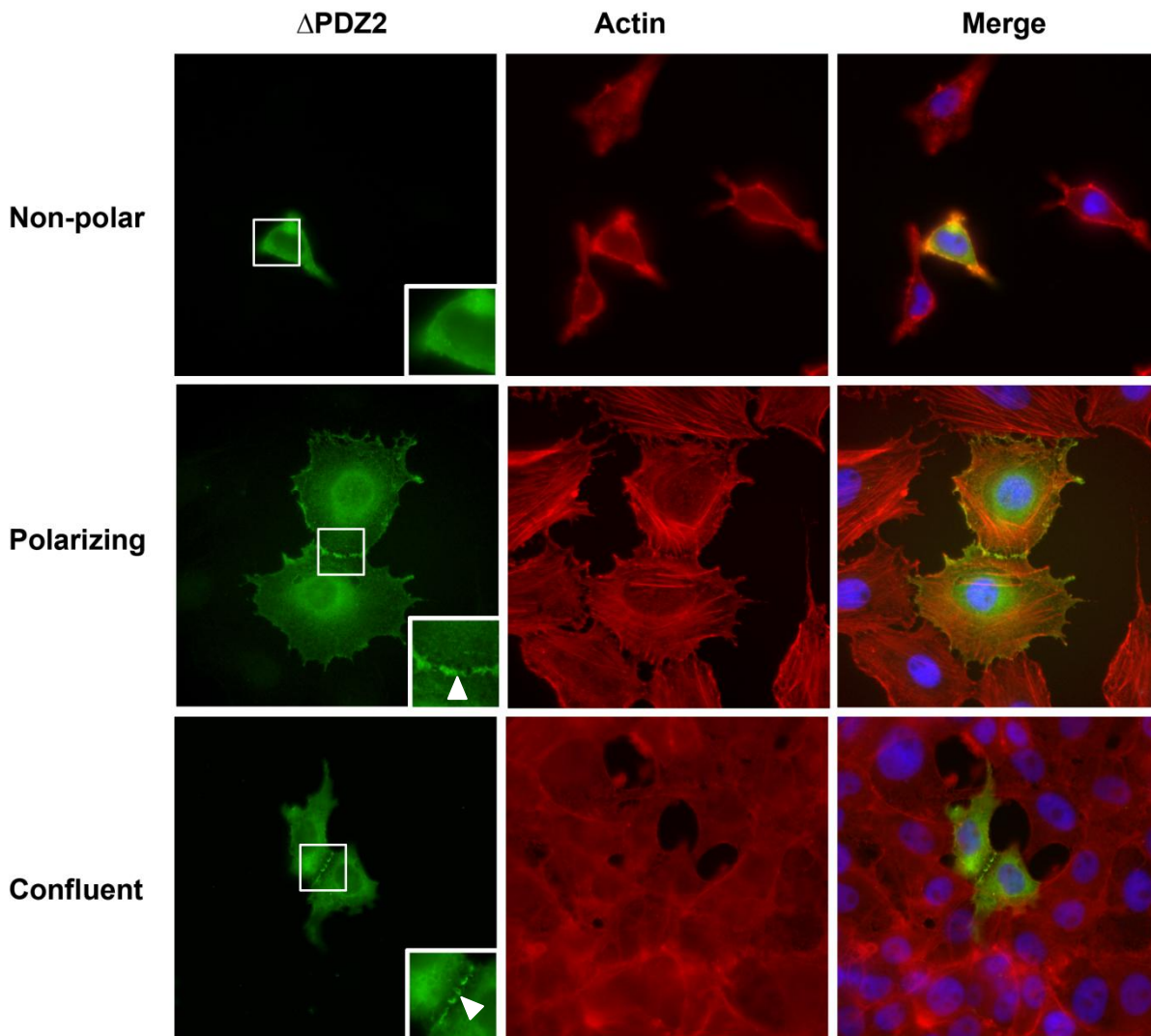


Figure 19. The PDZ2 domain is not necessary for PAR-3 localization in A6 cells. *Xenopus* A6 cells transfected with GFP- Δ PDZ2 compartmentalized the construct when subjected to a calcium switch. PDZ2 is cytoplasm in depolarized cells (non-polar) and is recruited to cell-cell contact upon repolarization (Polarizing). PDZ2 is compartmentalized in puncta at cell-cell contact regions between adjacent transfected cells in the epithelial sheet. No effect was observed on the ability of transfected cells to polarize. Sites of compartmentalization are indicated by arrowheads.

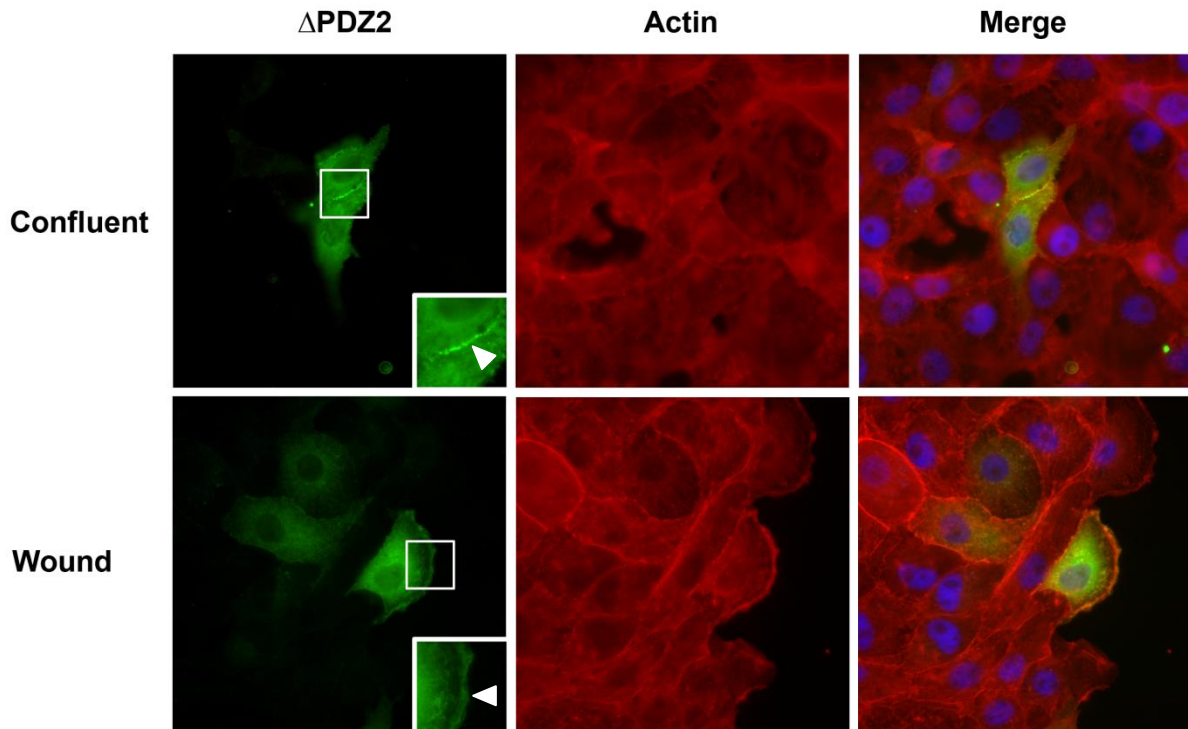


Figure 20. The PDZ2 domain is not necessary for localization of PAR-3 in wounded A6 cells. When subjected to a scratch assay Δ PDZ2 transfected cells were observed to migrate at the wound edge. The Δ PDZ2 construct was compartmentalized to regions of cell-cell contact in the epithelial sheet (Confluent), while it was enriched at the leading edge in migrating cells (Wound).

3.5.3 The PDZ3 domain of PAR-3 is required for contact inhibition

The Δ PDZ3 construct was unable to localize and was expressed throughout the cytoplasm of non-polar, polarizing and confluent sheets of A6 cells (Figure 21). Also, removal of the PDZ3 domain resulted in a loss of contact inhibition in A6 cells. When depolarized, cells were rounded and displayed a uniform distribution of Δ PDZ3 (Figure 21, Non-polar). Repolarizing cells were found to spread and failed to recognize neighboring cells resulting in cell overlap (Figure 21, Polarizing). Δ PDZ3 expressing cells in the epithelial sheet displayed similar loss of contact inhibition as they overlapped adjacent cells (Figure 21, Confluent). These cells also were unable to localize Δ PDZ3. When wounded, the lack of contact inhibition persisted and cells crawled over adjacent cells in the epithelial sheet instead of spreading into the empty wound area (Figure 22, Wound). Δ PDZ3 was also symmetrically expressed the wound edge cells. These results suggest that the PDZ3 domain is integral to the generation of both epithelial and migrating polarity with its removal resulting in a loss of contact inhibition and directional migration.

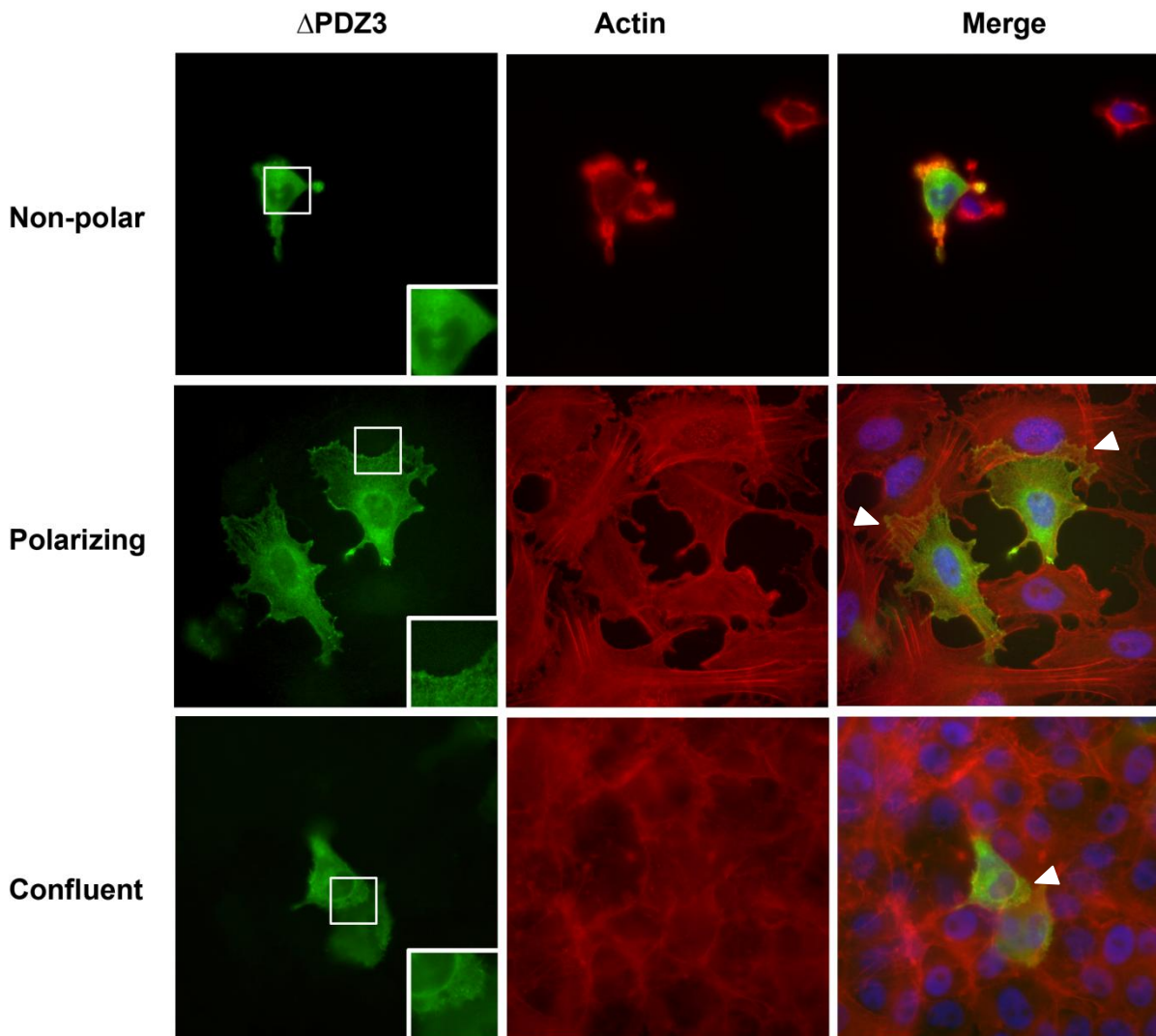


Figure 21. The PDZ3 domain of PAR-3 is required for epithelial polarity. *Xenopus* A6 cells were transfected with GFP- Δ PDZ3. The cells were depolarized (Non-polar) after transfection and the reformation of epithelial polarity observed. Removal of the PDZ3 domain resulted in a loss of contact inhibition in repolarizing cells (Polarizing). Transfected cells also overlapped in epithelial sheets (Confluent). Sites of overlap are indicated with arrowheads.

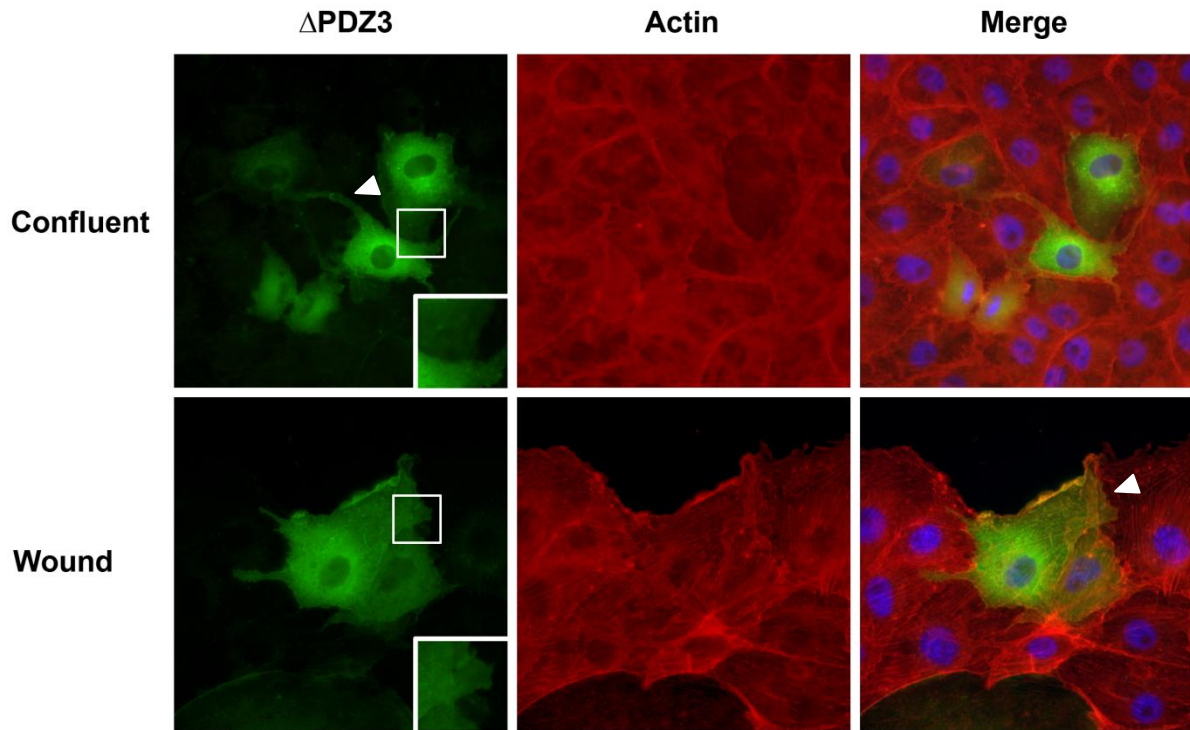


Figure 22. The PDZ3 domain of PAR-3 is required for wound healing. *Xenopus* A6 cells were transfected with GFP- Δ PDZ3 and cultured to confluent sheets. The cells were depolarized (Non-polar) after transfection and the reformation of epithelial polarity observed. Removal of the PDZ3 domain resulted in a loss of contact inhibition in repolarizing cells (Polarizing). Transfected cells also overlapped in epithelial sheets (Confluent). Overlapping areas are indicated by arrowheads.

3.5.4 Removal of the aPKC phosphorylation results in hyper-accumulation

The *S777A* construct exhibited a hyper-accumulation in the transfected cells. In calcium switch assays it displayed a similar pattern to PAR-3 being uniform in the cytoplasm of non-polar rounded cells (Figure 23, Non-polar), then collecting at cell-cell contacts in repolarizing cells (Figure 23, Polarizing), and compartmentalizing to the cell periphery in a punctate pattern in confluent epithelia (Figure 23, Confluent). *S777A* localization was more concentrated than PAR-3, being strongly localized to cell-cell contacts or the cell periphery and little protein present in the cytoplasm. *S777A* over-expression did not inhibit repolarization and cells formed adhesive contacts with adjacent cells, nor did it inhibit epithelial formation. The *S777A* construct was also observed to be hyper-accumulated in scratch assays with strong compartmentalization to the cell periphery in the epithelial sheet. When cells were wounded, *S777A* was observed throughout the cytoplasm with enrichment at the leading edge (Figure 24, Wound). The enrichment at the leading edge again appeared to be more intense than that observed with PAR-3. Cells were still able to migrate normally and spread into the wound as expected.

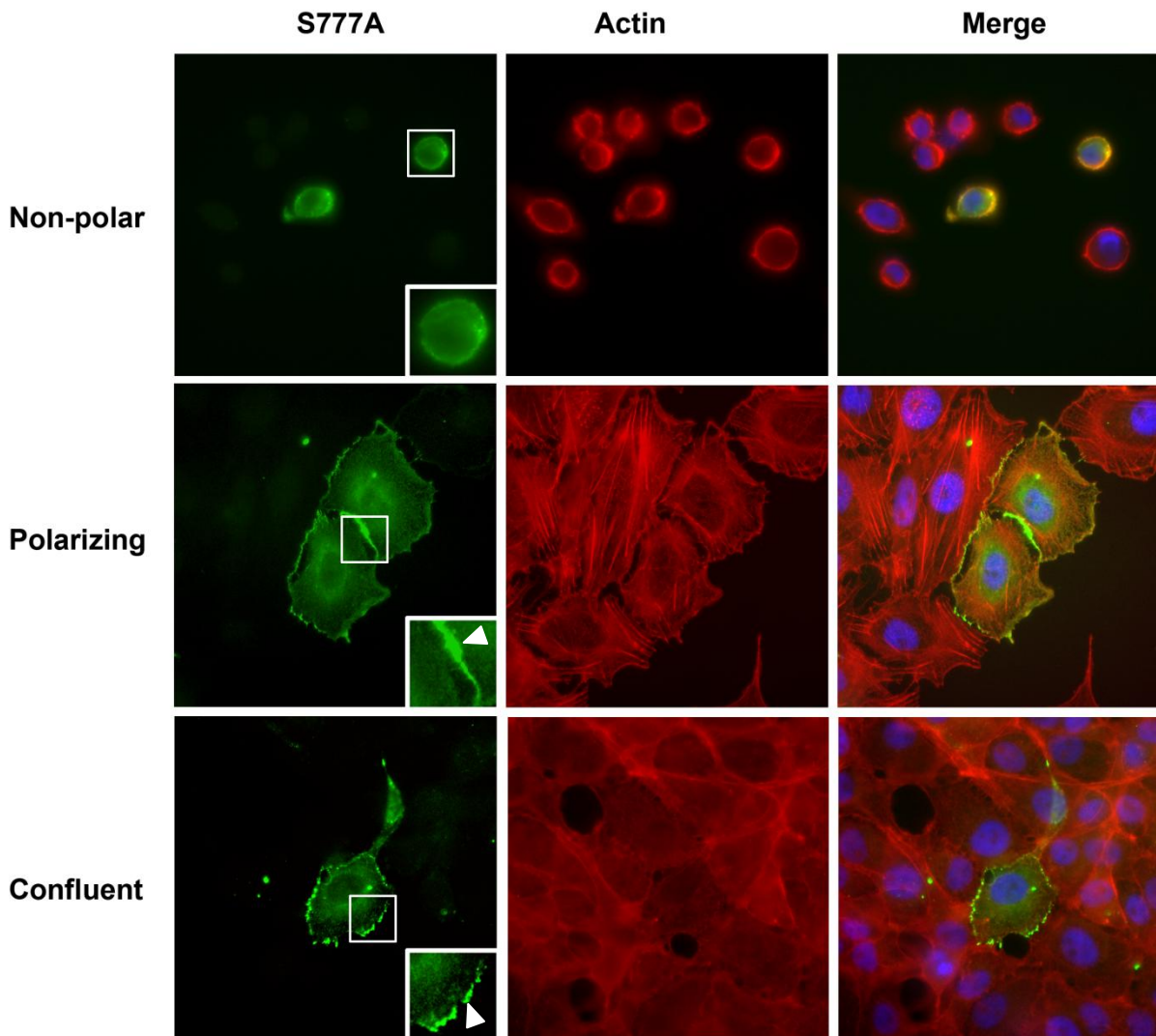


Figure 23. S777A is strongly localized to cell-cell contacts in *Xenopus* A6 Cells. GFP-S777A was hyper-accumulated in *Xenopus* A6 cells. Depolarized cells were observed to round and did not localize S777A (Non-polar). Upon repolarization S777A was strongly localized to points of cell-cell contact (Polarizing). It was then localized in puncta around the cell periphery in the confluent sheet (Confluent). Cell polarity was not inhibited and cells formed adhesive contacts and were integrated into the confluent sheet.

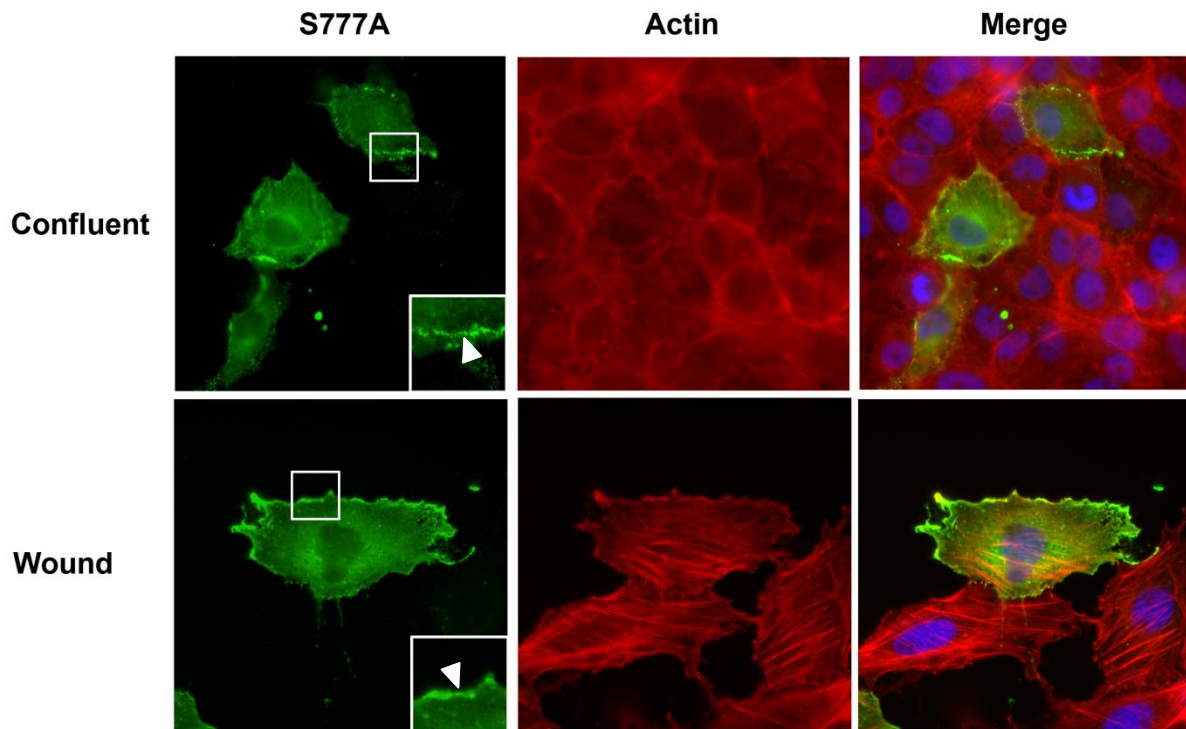


Figure 24. S777A localizes to the leading edge of wounded A6 cells. Epithelial sheets containing S777A transfected cells were wounded in scratch assays. S777A was hyper-accumulated in puncta at the cell periphery within the epithelial sheet (Confluent). S777A was also hyper-accumulated to the leading edge of migrating wound edge cells. Localization sites are indicated by arrowheads.

3.6 PAR-3 is required for convergent extension

PAR-3 has not been previously characterized during *Xenopus laevis* gastrulation. *Xenopus* embryos were injected with 1.5ng of PAR-3GFP mRNA into the dorsal marginal zone to determine the requirement of PAR-3 during gastrulation. Phenotypes were recorded at two time points: late gastrulation (Stage 12-12.5) and early tadpole (Stage 28) and classified into one of three categories at each stage, described below.

The progressive closing of the blastopore is an indicator of the progression of gastrulation. *Xenopus* gastrula viewed at Stage 12-12.5 have small blastopores either round or teardrop in shape. When gastrulation has been inhibited embryos are unable to internalize the yolk plug resulting in large open blastopores. Stage 12 embryos were classified as either normal (indistinguishable from controls), delayed (exhibited uneven or slowed blastopore closure), or inhibited (large open blastopore). Embryos over-expressing PAR-3 displayed delayed or inhibited blastopore closures (Figure 25a, C) when compared to uninjected embryos (Figure 25a, A). Furthermore, GFP injected embryos closed their blastopores normally (Figure 25a, B) demonstrating that this effect was specific to PAR-3 and not a result of injection or over-expression artifacts. Embryos were then examined using fluorescence microscopy to confirm expression and targeting. In GFP injected embryos expression was confined to the axial mesoderm, forming a distinct band along the dorsal side of the embryo (Figure 25a, D). The observed narrowing of the injected mesoderm suggests that the tissue has converged. PAR-3 fluorescence was also observed on the dorsal side of the blastopore however, it was clustered at the blastopore indicating a lack convergence in the injected tissue (Figure 25a, E).

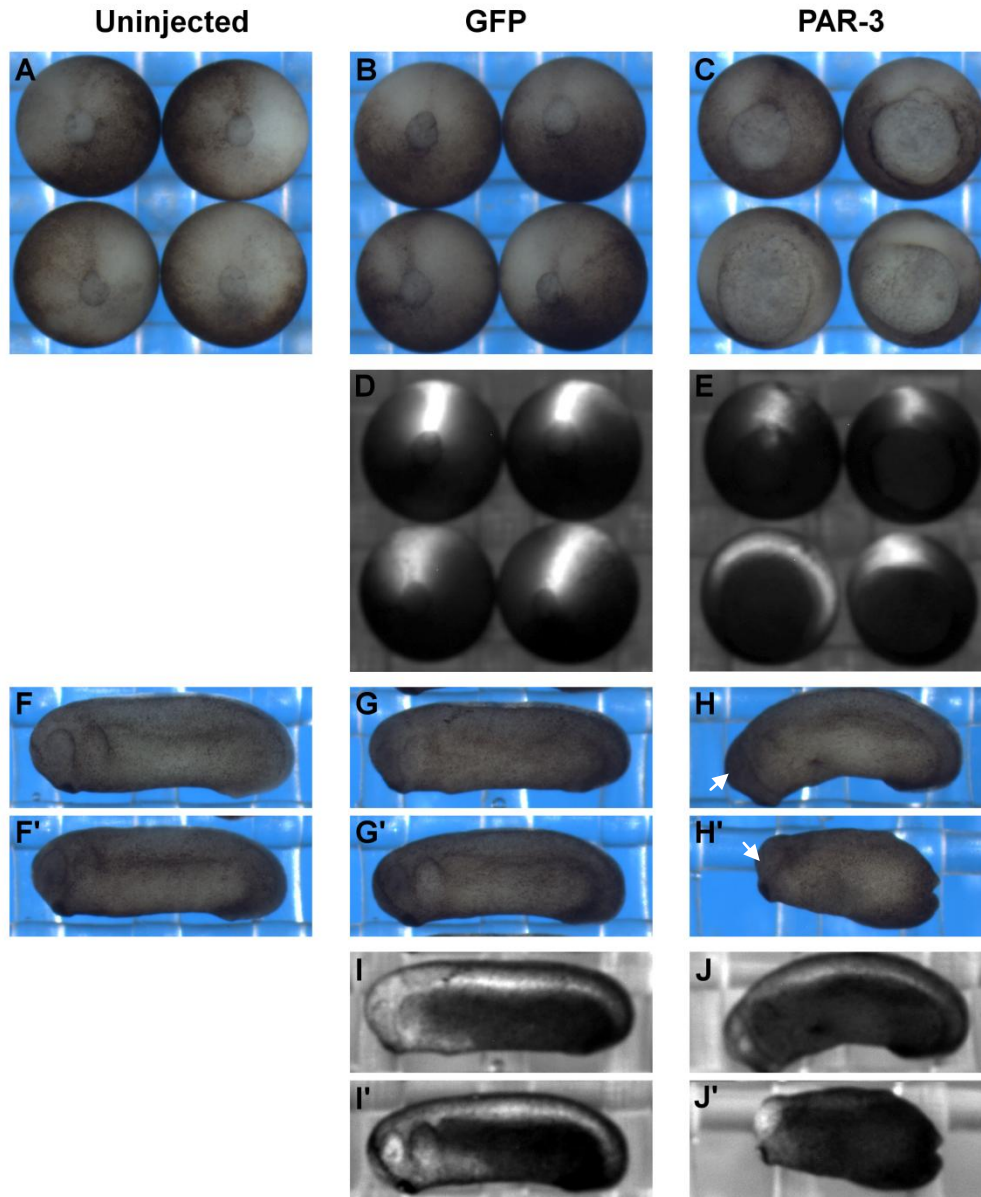


Figure 25a. PAR-3 is required for convergent extension. GFP-PAR-3 or GFP mRNA was injected into the dorsal marginal zone of early cleavage stage embryos. Uninjected embryos developed normally (A,F,F') as did GFP injected embryos at both late gastrula (B) and tadpole stages (G,G'). Embryos overexpressing PAR-3 failed to close their blastopores (C). PAR-3 injected tadpoles exhibited CE defects including no eyes (arrows), bent body axis (H) and exogastrulation (H'). Expression was confirmed by fluorescence microscopy (D-E, I-J').

Injected embryos were raised to early tadpoles (Stage 28) to confirm if convergent extension (CE) was inhibited. Several defects in tadpole development are associated with a failure in CE. The most common defect is a shortened and/or bent body axis. A lack of anterior features is also observed due to improper displacement of the mesendoderm responsible for inductive interactions in the anterior of the head. Lastly, complete failure of CE can result in exogastrulation, where embryos fail to close their blastopores and the mesoderm and endoderm are not internalized. Tadpole phenotypes were categorized as normal (indistinguishable from controls), moderate (lacking anterior structures, bent, or shortened), or severe (25% shorter than controls or exogastrula). The majority of PAR-3 injected tadpoles were observed to be shortened or bent (Figure 25a, H) and often did not develop anterior features, such as eyes (Figure 25a, arrow). PAR-3 injection also often resulted in exogastrulation (Figure 25a, H'). PAR-3 expression was confirmed through observation of fluorescence and was observed in the notochord and heads of affected tadpoles (Figure 25a, J,J'). The majority of GFP injected tadpoles developed normally (Figure 25a, G,G') with expression primarily present in the notochord and head (Figure 25a, I,I'). This demonstrates that inhibition of tadpole development is also not a result of over-expression artifacts. These results demonstrate that PAR-3 over-expression inhibits convergent extension.

3.7 The CR1 domain of PAR-3 is required for convergent extension

With the knowledge that PAR-3 is required for gastrulation I next wanted to identify the domains required for PAR-3 function. PAR-3 acts as a dominant negative, inhibiting gastrulation movements. I expected that constructs lacking functional domains key to this

process would rescue the defect and therefore exhibit normal phenotypes. Each of the mutated PAR-3 constructs were over-expressed in the dorsal mesoderm of embryos as described for PAR-3. Blastopore closure and tadpole phenotypes were then recorded as previously described. These results are summarized in Figures 26 and 27.

Over-expression of the Δ CR1 construct resulted in normal blastopore closure (Figure 25b, A). Moreover, GFP expression observed in the axial mesoderm indicated that convergence was occurring (Figure 25b, D). The intensity of fluorescence was also observed to be less than that observed for the other constructs. However, a Western blot confirmed equal expression of all injected constructs. The majority of tadpoles injected with Δ CR1 were also uninhibited and development normally (Figure 25b, G,G') with only a few tadpoles exhibiting minor anterior defects. The expression of Δ CR1 was observed to be more dispersed than PAR-3 displaying broad mesodermal expression instead of being confined to notochord (Figure 25b, J, J'). This is consistent with the expression seen in gastrula with both axial and lateral plate mesoderm being injected. The lack of inhibition seen with Δ CR1 over-expression suggests the CR1 domain is required for CE.

Embryos injected with the Δ PDZ1 construct exhibited either delayed or inhibited blastopore closure (Figure 25b, B). The expression in the embryos was observed at the dorsal surface with some clustering at the blastopore suggesting a lack of convergence at the dorsal lip (Figure 25b, E). The Δ PDZ1 injected tadpoles most commonly demonstrated severe convergent extension defects causing severely shorten body axes or exogastrulation (Figure 25b, H). Moderate phenotypes were also observed including bent backs and anterior defects (Figure 25b, H' arrows). Δ PDZ1 expression was again observed in the mesoderm often confined to head or

notochord (Figure 25b, K,K'). The S777A construct also disrupted gastrulation resulting in delayed or inhibited blastopore closure as well as exogastrulating embryos (Figure 25b, C). Disruption of CE was indicated by the clustered expression at the dorsal lip of the blastopore (Figure 25b, F). In tadpoles, S777A over-expression resulted mainly in exogastrulation (Figure 25b, I'). Shortened and bent tadpoles were also observed, as well as tadpoles without anterior structures (Figure 25b, I, arrows). S777A was also expressed in the head or notochord of affected embryos (Figure 25b, L, L'). Together, the phenotypes indicate that Δ PDZ1 and S777A both act as dominant negatives resulting in inhibition of CE. This suggests that neither PAR-3/PAR-6 binding nor aPKC phosphorylation of PAR-3 is required for CE.

The Δ PDZ2 and Δ PDZ3 constructs were also over-expressed in embryos. The blastopore closures in these embryos displayed significant variation between spawnings. Δ PDZ2 had no effect in some spawnings of embryos (Figure 28, Δ PDZ2 A) while causing exogastrulation in others (Figure 28, Δ PDZ2 B). The Δ PDZ3 construct on the other hand demonstrated a weaker phenotype with delays in blastopore closure (Figure 28, Δ PDZ3 B) or normal closure (Figure 28, Δ PDZ3 A). After repeated attempts I could not obtain consistent phenotypes with the Δ PDZ2 and Δ PDZ3 constructs. Due to this variability Δ PDZ2 and Δ PDZ3 were omitted from the summary graphs. The roles of the PDZ2 and PDZ3 domains in CE remain undetermined.

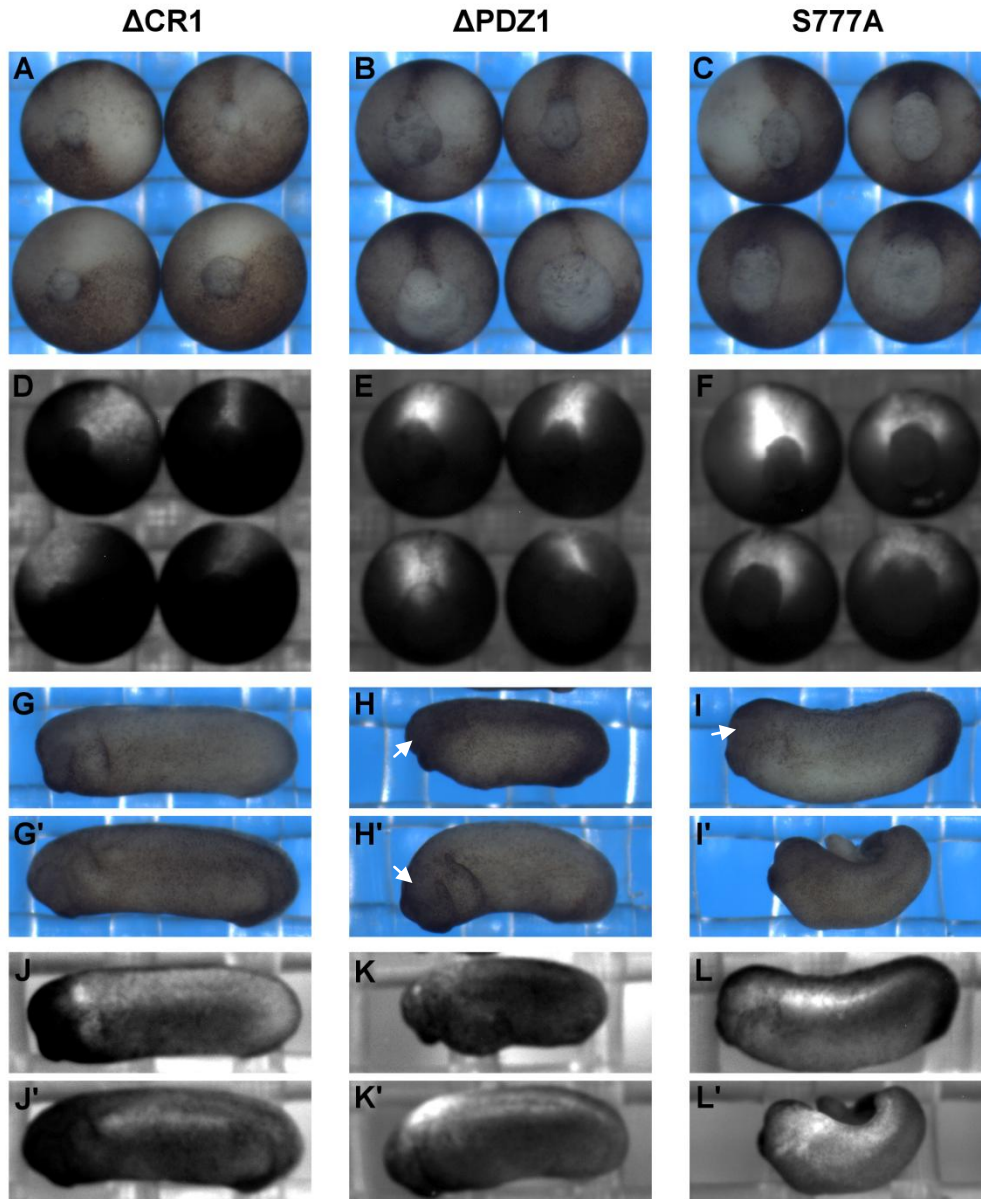


Figure 25b. The CR1 domain is required for convergent extension. *Xenopus* embryos were injected with N-terminal GFP-tagged Δ CR1, Δ PDZ1 and S777A mRNA. Δ CR1 over-expression did not inhibit gastrulation (A, G,G'). Δ PDZ1 injected embryos exhibited delayed blastopore closure (B), due to failure of convergent extension (CE) demonstrated by short (K) and bent (K') tadpoles lacking eyes (arrows). S777A over-expression also inhibited gastrulation resulting in open blastopores (C). Tadpole over-expressing S777A were shortened (I) or exogastrulated (I') indicating a failure of CE. Protein expression was observed through fluorescence (D-F, J-L')

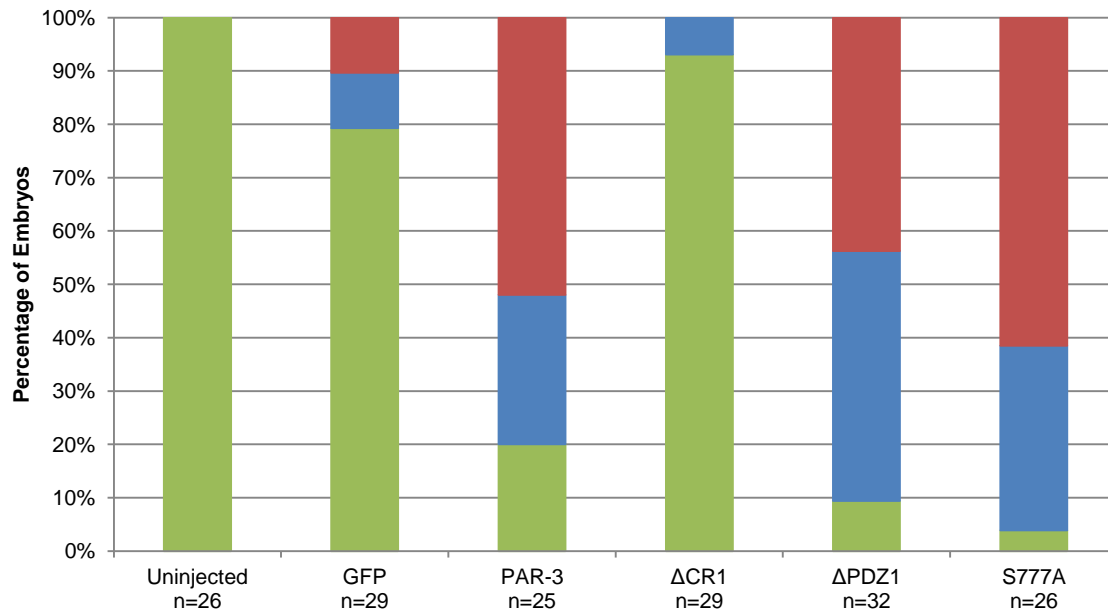
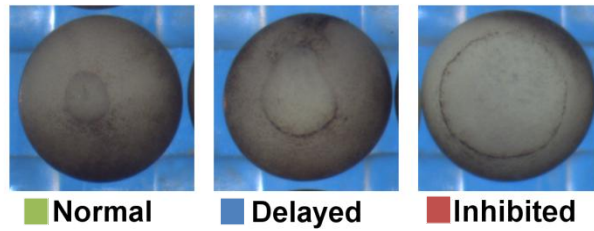


Figure 26. The CR1 domain of PAR-3 is required for *Xenopus* gastrulation. The degree of blastopore closure was grouped into three categories. Normal embryos were identical to controls. Delayed embryos had uneven or enlarged blastopores. Inhibited embryos had open blastopores. PAR-3 acted as a dominant negative, inhibiting or delaying blastopore closure. Δ PDZ1 and S777A phenotypes resembled PAR-3 while Δ CR1 phenotypes more closely resembled controls.

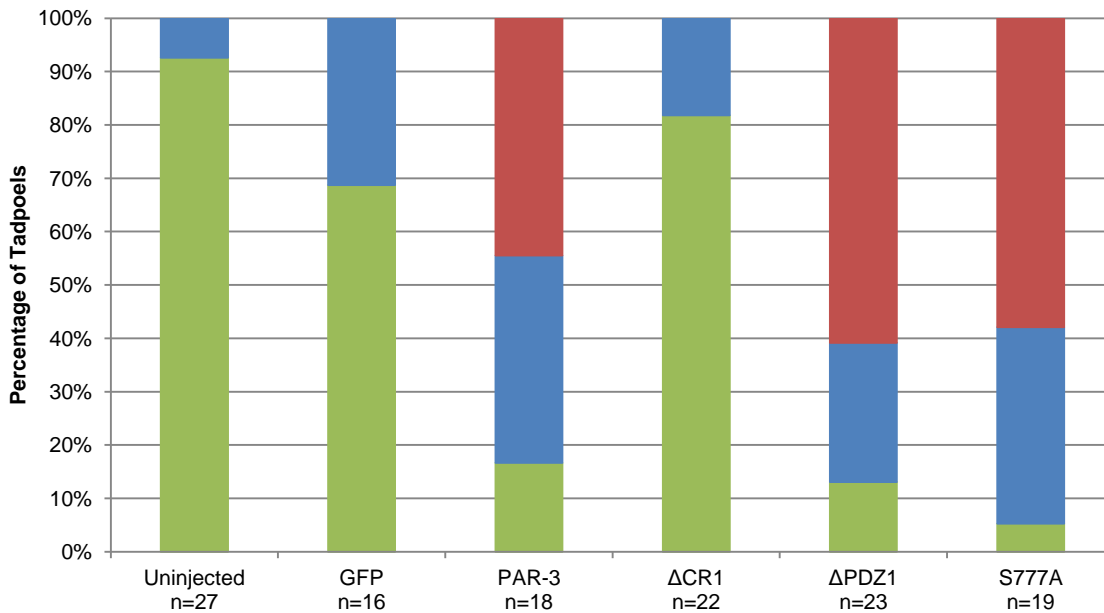


Figure 27. The CR1 domain of PAR-3 is required for *Xenopus* convergent extension (CE). Tadpole phenotypes were binned into three categories. Tadpoles identical to controls were considered normal. Bent or shortened body axes or no eyes were identified as moderate defects. Tadpoles more than 25% shorter than controls, or which had exogastrulated were considered severely defected. PAR-3 inhibited CE as did Δ PDZ1 and S777A. Δ CR1 tadpoles developed normally as did the uninjected and GFP controls.

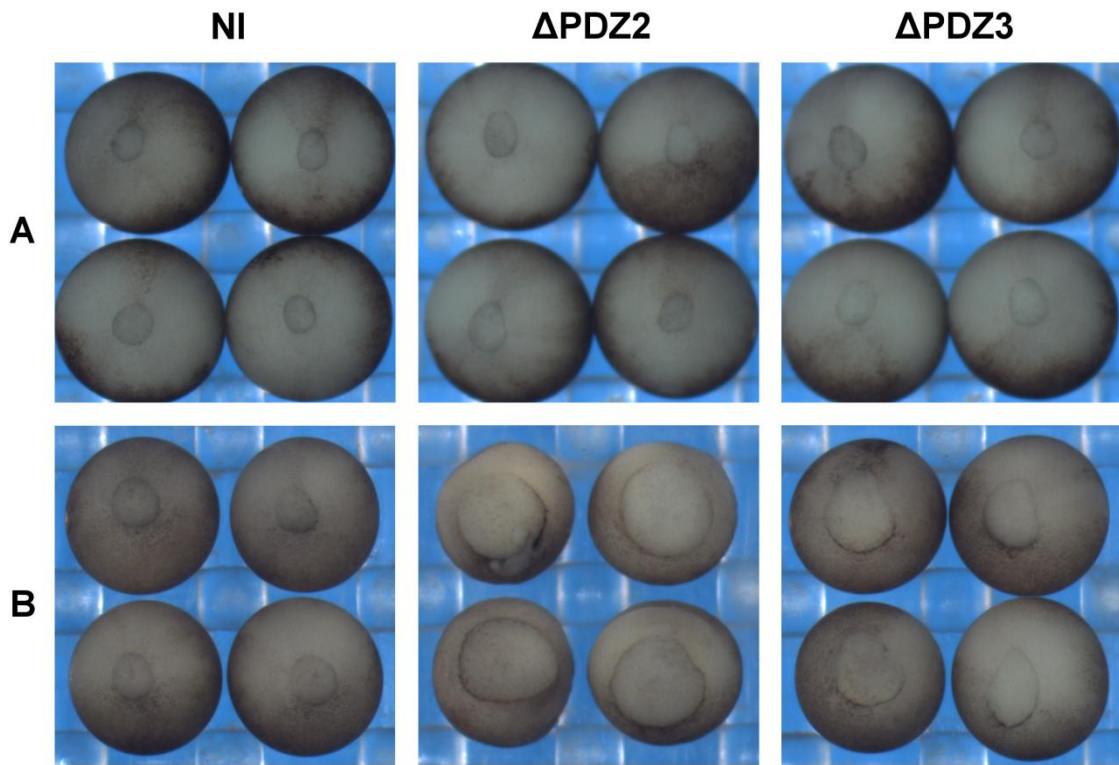


Figure 28. Δ PDZ2 and Δ PDZ3 phenotypes were inconsistent. Δ PDZ2 and Δ PDZ3 were injected into the dorsal marginal zone of *Xenopus* embryos. Over-expression effect was not determined as embryos were able to close their blastopore (A) or inhibited (B) depending on the spawning.

3.8 PAR-3 localizes to the cell membrane in *Xenopus* mesoderm cells

PAR-3 organizes polarity through localization to specific cellular compartments. I used Keller explants to determine if PAR-3 was localized in mesoderm undergoing convergent extension. PAR-3 was observed to localize to the cell membrane and is enriched at the periphery of mesoderm cells (Figure 29, PAR-3 arrowheads). Furthermore, there is no medial/lateral or anterior/posterior bias to this localization despite elongated cell shapes. This localization was confirmed to be specific to PAR-3 as GFP does not localize to the cell membrane and is seen either in the nucleus or cytoplasm of mesoderm cells (Figure 29, GFP). In summary, PAR-3 is localized to the cell membrane in the polarized mesoderm cells undergoing convergent extension in *Xenopus* embryos.

3.9 The CR1 domain is required for localization of PAR-3 in mesoderm cells

I then determined if there were specific domain requirements for the localization of PAR-3 in embryos. When expressed in the axial mesoderm the Δ CR1 construct did not localize to the membrane and was observed throughout the cell with a slight accumulation in the nucleus (Figure 30, Δ CR1). This suggests that the CR1 domain is required for localization of PAR-3 to the cell membrane in *Xenopus* embryos. The Δ PDZ1 and S777A constructs were both able to localize to the cell membrane in axial mesoderm cells are observed around the entire periphery of elongated mesoderm cells (Figure 30, Δ PDZ1 and S777A). The PDZ1 domain and aPKC phosphorylation site are hence not required for membrane localization of PAR-3. Together these results suggest that PAR-3 localization in mesoderm cells is dependent on oligomerization and independent of PAR-6 binding or aPKC interaction.

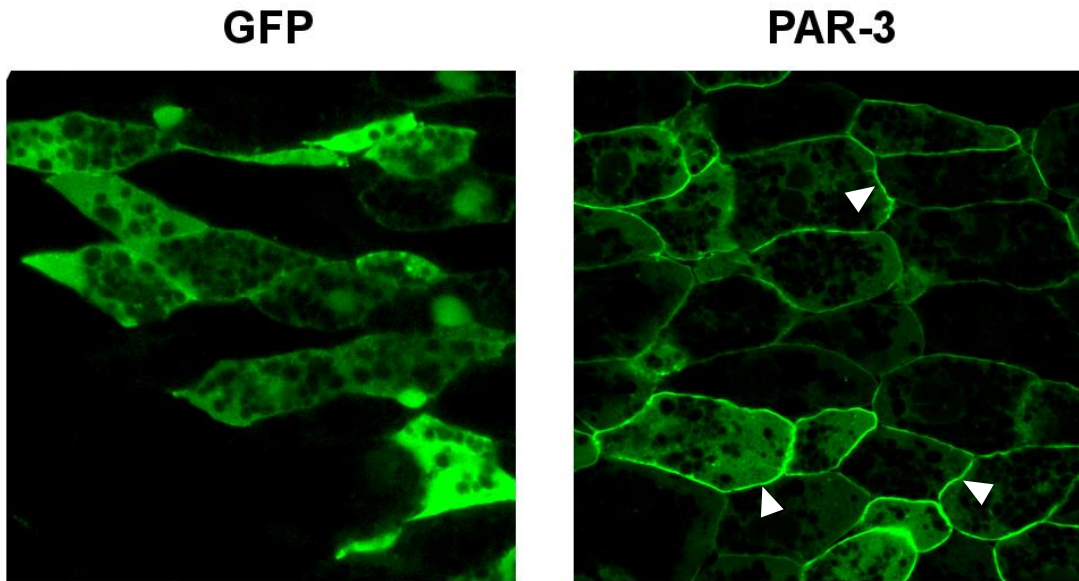


Figure 29. PAR-3 localizes to the cell membrane mesoderm cells. Keller explants were taken from embryo over-expressing GFP-PAR-3 or GFP. GFP did not localize in mesoderm cells and is present through the cytoplasm. PAR-3 was localized around the cell periphery in mesoderm cells (arrowheads).

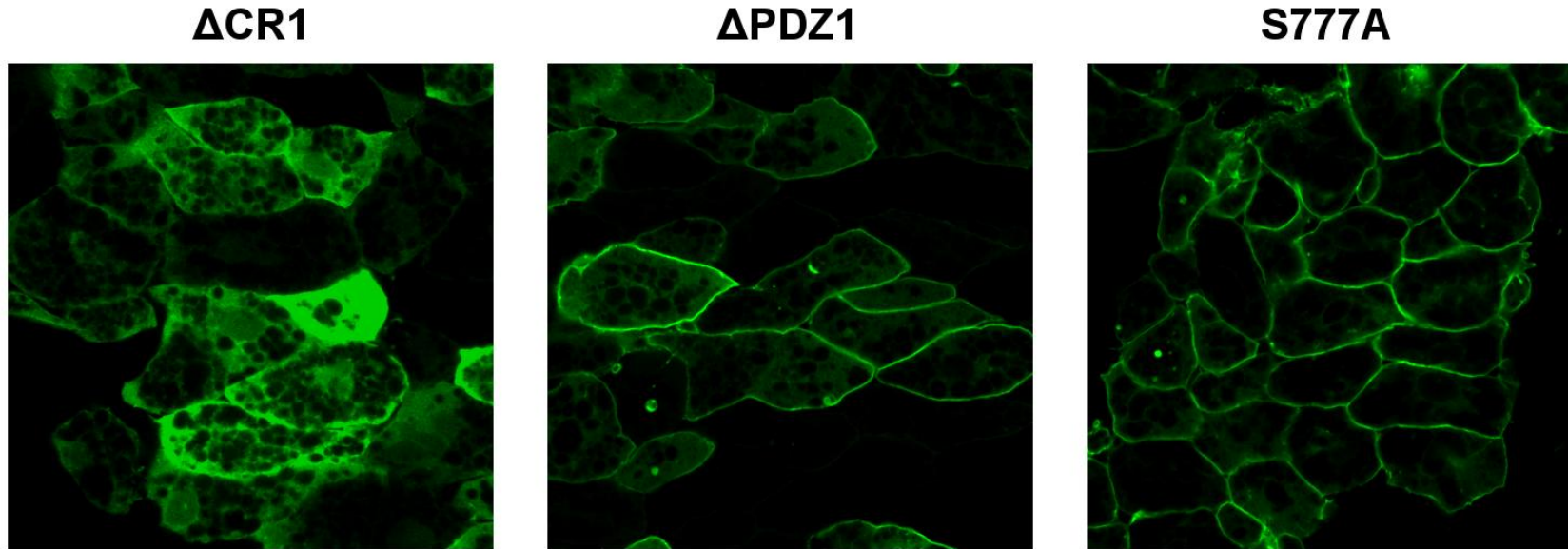


Figure 30. The CR1 domain is required for PAR-3 localization. Keller explants were taken from embryos injected with mRNA encoding the GFP tagged Δ CR1, Δ PDZ1, or S777A construct to determine functional domains responsible for localization. The Δ CR1 construct was unable to localize and is seen throughout the cell indicating the CR1 domain is required for localization. The Δ PDZ1 and S777A construct were localized to the cell membrane in mesoderm indicating the PDZ1 domain and aPKC phosphorylation site are not required for PAR-3 localization in mesoderm cells.

Chapter 4

Discussion

4.1 *Xenopus* PAR-3

A cDNA for *Xenopus* PAR-3 has not been previously described. Sequencing of the EST (Accession# NM_001092545) confirms a full-length cDNA that represents the *Xenopus laevis* homolog of previously described mammalian PAR-3. I will refer to the sequence and the corresponding protein as *Xenopus* PAR-3 in the discussion below. *Xenopus* PAR-3 shares the same domain structure as other known PAR-3 proteins. The N-terminal conserved region (CR1), three PDZ domains and an aPKC binding consensus sequence are present in the *Xenopus* sequence and the order and spacing of these domains is conserved. The overall amino acid similarity between *Xenopus* and mammalian homologs was 70%, but ranges from 93-100% within the conserved domains (CR1 96%, PDZ1 98%, PDZ2 96%, PDZ3 100%, aPKC consensus sequences 93%). This suggests that these functional domains are highly conserved but the intervening sequences are not. It is therefore likely that the described binding partners of these domains are also conserved in *Xenopus*. Deletion constructs were then created removing each of the conserved domains (Figure 7). The deletions were confirmed by sequencing and maintain the open reading frame (Appendix A).

4.2 PAR-3 is expressed throughout *Xenopus* development

Using RT-PCR I characterized the temporal expression of PAR-3 during early *Xenopus* development (Figure 13). Like most protein coding genes in *Xenopus*, PAR-3 is expressed as a maternal transcript in the cleavage and blastula stage embryo up to midblastula transition (74). Previously maternal expression of PAR-3 was described in the *Xenopus* oocyte where PAR-3 was found to be isolated to the animal pole (57). My results confirm this maternal expression of PAR-3. *Xenopus* PAR-3 is then continuously expressed through zygotic transcription throughout gastrulation, neurulation and organogenesis. These results are similar to the expression patterns previously described for PAR-3 in other organisms (75–78) where PAR-3 is expressed constitutively and ubiquitously throughout development. This broad temporal and spatial expression pattern suggests that *Xenopus* PAR-3 plays pleiotropic roles during embryogenesis.

4.3 PAR-3 in A6 cells

4.3.1 PAR-3 localization in epithelial cells

PAR-3 was initially discovered in *C. elegans* embryos where it regulates asymmetric cell divisions during cleavage (79). Subsequently PAR-3 homologs were identified in flies and mammals where they regulate apical/basal epithelial polarity (1, 31, 80). Extensive characterization of PAR-3 has since been undertaken in MDCK cells where PAR-3 localizes to the apical/basolateral boundary and aids in tight junction formation and generation apical/basal polarity (36, 37, 70, 81). *Xenopus* A6 cells are a *Xenopus* kidney tubule cell line similar to MDCK cells. As A6 cells polarize and behave in a similar fashion to MDCK cells they provide a model for the characterization of sub-cellular localization of *Xenopus* PAR-3.

Epithelial polarization was observed in MDCK cells through the use of calcium switch assays (37, 72). I similarly used calcium switch assays to characterize PAR-3 compartmentalization in the initiation of apical/basal polarity and to confirm that the GFP tag does not interfere with PAR-3 localization. In calcium switch assays, confluent sheets of polarized cells are cultured in calcium depleted media which causes disassembly of tight junctions resulting in depolarization of the epithelial cells (82). Upon re-addition of calcium the cells re-form their junctions and re-establish polarity. I found that PAR-3 is uniformly expressed in non-polar cells and then becomes compartmentalized as the cells polarize (Figure 13). In MDCK cells, epithelial polarity is initiated by cell-cell contact (83), and the subsequent formation of intercellular adhesions containing nectins and JAM is believed to recruit PAR-3 to these adhesion sites through interaction with its PDZ1 domain (29, 31, 46). In agreement with this model PAR-3 is localized to cell-cell contacts as MDCK cells repolarize (36). I also found that PAR-3 accumulated at points of cell-cell contact in polarizing A6 cells (Figure 13). PAR-3 may therefore be similarly recruited to intracellular adhesions in *Xenopus*. This demonstrates that localization of the PAR-3 construct is not altered by the GFP tag.

A6 cells form highly polarized confluent sheets of cells. In MDCK cells as the epithelium differentiates tight and adherens junctions are formed between the epithelial cells and PAR-3 is localized in an apical band at the mature tight junctions (37, 84). Similarly when A6 cells were stained with an antibody directed against rat PAR-3 it was found to localize at apical junctions, suggesting PAR-3 also localizes to tight junctions in A6 cells (57). I found GFP-tagged PAR-3 localized at the cell periphery of confluent A6 cells in a punctate pattern (Figure 13, Figure 14). The punctate pattern observed in my experiments may reflect the maturation state of the epithelium, indicating that the junctions have not completely formed. However, it is also

possible that a punctate pattern is seen in my experiments because the GFP-PAR-3 only represents a subpopulation of PAR-3 since the endogenous protein is still present. PAR-3 over-expression did not alter the ability of A6 cells to initiate polarity or form an epithelium. Previous studies have also found that over-expression of PAR-3 does not result in a loss of apical/basal polarity (37, 81, 85). In summary, this conserved localization at cell-cell contacts in A6 epithelia is consistent with that described in MDCK cells suggesting PAR-3 a similar mechanism is functioning in the recruitment and maintenance of PAR-3 localization in *Xenopus* A6 cells.

4.3.2 PAR-3 localization in migrating cells

Migrating cells exhibit polarized cell morphology with a flattened protrusive front end and a retracting back end. PAR-3 localization in migrating cells has been extensively characterized in mammalian cell lines through observation of individual migrating cells and with scratch assays. In this assay a confluent sheet of cells is wounded through scratching with a pipette tip and cells at the wound edge are observed as they undergo an epithelial to mesenchymal transition and migrate into the wound.

I used scratch assays to observe PAR-3 localization in migrating cells. I found that in *Xenopus* A6 cells, PAR-3 was localized to the cell periphery in the epithelial sheet while wound edge cells displayed PAR-3 enrichment at the front end (Figure 14). This suggests that sub-cellular localization of PAR-3 is re-compartmentalized to the front end in migrating cells. This front end localization differs from that seen in MDCK and NIH3T3 cell scratch assays where PAR-3 is only localized to cell-cell contacts displaying no front end enrichment(44). However, PAR-3 is observed at the protrusive end of individual migrating HeLa and Vero cells as well as

keratinocytes (38, 86). This is consistent with the behaviour of A6 cells as during wound healing they migrate out of the epithelial sheet, as opposed to MDCK cells which do not leave the epithelium and instead the confluent sheet expands to fill the wound. Therefore the localization of PAR-3 at the front end of migrating cells appears to be context dependant. It may be that PAR-3 can only move to front end lamellapodia when tight junctions are unstable and cells leave the epithelial sheet during wound healing. I also found that the sub-cellular localization of PAR-3 correlated with actin accumulation as well as membrane protrusive activity. Activated Rac has been implicated in lamellapodial formation through the regulation of actin dynamics(53). PAR-3 has been demonstrated to regulate Rac activity through Tiam1(37, 39) and it has previously been suggested that PAR-3 up regulation of Rac activity at the leading edge controls membrane protrusions (86). This mechanism may also be present in A6 cells but awaits confirmation of compartmentalized Rac activity as well as Tiam1 localization. In summary PAR-3 demonstrates a polarized localization to the leading edge of migrating A6 cells and likely functions in the generation of front/rear morphology in *Xenopus* A6 cells through control of the actin cytoskeleton.

4.3.3 Role of conserved domains in PAR-3 localization in *Xenopus* A6 cells

Knowing that PAR-3 becomes compartmentalized during A6 cell polarization, I then asked what role the conserved CR1 and PDZ domains as well as the aPKC phosphorylation site play. I generated N-terminal GFP-tagged constructs lacking each of the conserved functional domains (described in Section 2.1.2). I then transfected the mutated PAR-3 constructs into A6 cells and observed the localization in calcium switch and scratch assays. Through comparison to

wild type PAR-3 (Section 4.3.1, 4.3.2) I was able to correlate localization and cell behaviour with each functional domain in both apical/basal and front/rear polarity.

I found that Δ CR1 was not localized in either epithelial (Figures 15) or migrating (Figure 16) cells and was instead present throughout the cell cytoplasm. The CR1 domain has previously been implicated in oligomerization of PAR-3 allowing for the formation of higher order scaffolds resulting in enrichment at localization sites (85). In MDCK cells the CR1 domain has been shown to be essential for membrane localization as removal results in cytoplasmic accumulation (36, 85). My results indicate a similar role of CR1 in *Xenopus* suggesting PAR-3 oligomerization is required for localization of PAR-3 in *Xenopus* A6 cells. CR1 deletion is also associated with a delay of tight junction formation in MDCK cells however, over time the cells recover and are able to integrate fully into the epithelial sheet (36). My results correlate with MDCK cells observations as the Δ CR1 expressing cells also integrated into the confluent epithelial sheet in A6 cells.

The Δ PDZ1 construct also was not localized in apical/basal polarized A6 cells (Figure 17). The PDZ1 domain is believed responsible for recruitment of PAR-3 to tight junctions through binding of JAM and nectins (29, 31, 46). Support for this role comes from the observation that inhibition of PAR-3/JAM binding resulted in a loss of PAR-3 compartmentalization at cell-cell contacts in MDCK cell (41). It was therefore expected that Δ PDZ1 would result in a loss of compartmentalization in epithelial polarity. Over-expression of PDZ1 did not affect cell behaviour and cells were still fully integrated in the epithelial sheet consistent with results in MDCK cells where disruption of JAM/PDZ1 interaction delays but does not inhibit tight junction formation. These results confirm that localization of *Xenopus*

PAR-3 to the apical/lateral membrane in A6 epithelial cells requires the PDZ1 domain. Δ PDZ1 was also not localized in migrating cells A6 cells (Figure 18). The mechanism behind of PAR-3 recruitment to the front end of migrating cells remains uncharacterized and this is not a region of the cell that would be rich in JAM or nectins. However, the PDZ1 domain is also able to mediate interactions with PAR-6 in formation of the PAR complex (34). PAR-6 is observed at the leading edge of migrating cells in mammalian cell lines (29, 33). The loss of localization with removal of the PDZ1 domain may indicate that PAR complex formation is necessary for PAR-3 enrichment at the front end of migrating cells but awaits confirmation of compartmentalized PAR-6 in A6 cells. Furthermore, it suggests a novel role for the PDZ1 in recruitment of PAR-3 to the front end of migrating cells. The PDZ1 domain is however not sufficient for PAR-3 localization as the Δ CR1 construct failed to localize. This indicates that PAR-3 localization requires both recruitment by the PDZ1 domain and oligomerization.

Interestingly of the PDZ2 domain was not necessary for compartmentalization of PAR-3 as this construct was observed to compartmentalize to cell-cell contacts in epithelia (Figure 19) and was enriched at the leading edge of migrating cells (Figure 20). However, in my experiments Δ PDZ2 appeared to localize less efficiently than PAR-3 as it had a lower intensity of fluorescence and was often only seen between adjacent transfected cells in the epithelial sheet. Over-expression of Δ PDZ2 also did not inhibit cell polarization as Δ PDZ2 transfected cells were able to form epithelial junctions and exhibited protrusive behaviour when wounded. This was unexpected as the PDZ2 domain has been demonstrated to bind phosphoinositol lipid-containing membranes and is speculated to be responsible for localization of PAR-3 to the cell membrane (35). Previous studies in MDCK cells have provided contradicting results as removal the PDZ2 domain resulted is a loss of localization and tight junction formation in MDCK cells (35). The

localization I observed may be due to recruitment by endogenous proteins likely through the CR1 domain, or by PDZ1 recruitment to junction. Taken together this suggests that PDZ2 is not necessary for sub-cellular localization or function of PAR-3 in A6 cells but instead increases efficiency or maintains PAR-3 localization through association with the cell membrane.

Δ PDZ3 was also cytoplasmic in both epithelial (Figure 21) and migrating cells (Figure 22) however, this lack of compartmentalization may be due to an absence of polarity in these cells instead of a failure in PAR-3 localization machinery (discussed in Section 4.3.4).

The S777A construct appeared hyper-accumulated in both apical/basal (Figure 23) and front/rear (Figure 24) polarities. Phosphorylation of PAR-3 by aPKC has been shown to weaken interaction with the PAR complex in MDCK cells and results in dissociation of PAR-3 from the apical membrane (1, 72). My results may indicate that the aPKC consensus sequence is required for PAR-3 release from the membrane which is consistent with previous observations. I did not observe any inhibition in either epithelial or migrating polarity with over-expression of the S777A construct. Over-expression of an analogous point mutation has also been observed in MDCK cells, where it prevents tight junction formation demonstrated by the lack of junctional molecule ZO-1 between transfected cells. Currently we do not have reagents to unambiguously identify tight junctions in A6 cells hence this could not be observed in my assays. However, the transfected cells were still integrated fully into the epithelial sheet in MDCK experiments similar to A6 cells. This suggests that the aPKC consensus regulates maintenance of PAR-3 at the cell membrane but is not required for the generation of epithelial or migrating polarity.

4.3.4 The PDZ3 domain is required for the generation of polarity in A6 cells

While localization of PAR-3 required multiple domains the translation of this compartmentalization into apical/basal polarity required only the PDZ3 domain as only over-expression the Δ PDZ3 construct resulted in altered cell behaviour. Cells over-expressing the Δ PDZ3 construct were unable to recognize neighboring cells and were found to overlap adjacent cells instead of forming intercellular adhesions (Figure 21). This suggests a lack of contact inhibition which is essential in the establishment of epithelia. The Δ PDZ3 expressing cells were further unable to confer apical/basal polarity and were not integrated into the confluent epithelial sheet (Figure 21). This data coincides with the conclusions made in MDCK cells that generation of epithelial polarity is dependent on the PDZ3 domain (37, 87). This mediation of polarity is likely to be regulated by phosphoinositide signaling. The PDZ3 domain has been observed to interact with PTEN, a lipid phosphatase, providing a link between PAR-3 and phosphoinositide signaling (35). Furthermore, PTEN is required for the formation an apical/basal gradient of membrane phosphoinositol lipids with PI(4,5)P₂ (PIP₂) concentrated in the apical domain and PI(3,4,5)P₃ (PIP₃) in the basolateral domain (88, 89). Similar loss of contact inhibition was observed in migrating cells which crawled over adjacent cells rather than moving into the free wound space (Figure 22). This suggests a similar requirement for PDZ3 in the generation of migrating front end polarity. Phosphoinositide signaling has also been implicated in the regulation of cell migration with PTEN observed to localize to the leading edge of migrating cells (89, 90). Together this suggests phosphoinositide signaling is involved in translation of PAR-3 compartmentalization to apical/basal or front/rear polarity and that the PDZ3 domain of PAR-3 is required for regulation of cell polarity.

4.4 Localization of PAR-3 is required for convergent extension

Embryos over-expressing PAR-3 demonstrated significant delay or inhibition of blastopore closure, and when these embryos were raised to early tadpoles they exhibited defects consistent with inhibition of convergent extension including shortened or bent body axis, missing anterior structures, or exogastrulation (Figure 25a). I then over-expressed the deletion and point mutation constructs in embryos to determine which domains were required for CE. I found that deletion of either the PDZ1 domain or the aPKC phosphorylation site relieved the inhibition of gastrulation caused by full-length PAR-3 (Figure 25b). These results suggest that PAR-3 may not be functioning in the PAR complex in *Xenopus* as the Δ PDZ1 and S777A constructs both mediate PAR complex interaction. Δ CR1 was the only construct which consistently relieved PAR-3 dominant negative effects (Figure 25b) suggesting oligomerization is a critical step in PAR-3 signaling during convergent extension.

I then observed the localization of PAR-3 in mesoderm cells to determine if its function was dependant on localization. PAR-3 was localized to the cell membrane in mesoderm cells undergoing convergent extension (Figure 29). The Δ PDZ1 and S777A constructs were also observed to localize to the cell membrane in mesoderm cells (Figure 30). The localization of S777A is consistent with what was observed in A6 cells, but the PDZ1 localization differs suggesting an alternate method of PAR-3 membrane recruitment between A6 cells and embryos. Δ CR1 on the other hand did not localize and was expressed throughout the cytoplasm (Figure 30). Together these results indicate that PAR-3 must be localized to the cell membrane to regulate CE. The PAR-3 localization in mesoderm cells was observed to be unbiased to either the medial/lateral or anterior/posterior membrane. This result was unexpected as segregation of

PAR-3 to polarized domains is an essential part of PAR-3 function. This lack of localization may be due to over-expression of PAR-3 overloading the localization machinery. It also may indicate that these cells may not be molecularly polarized. Such a scenario is supported by the observation that the microtubule cytoskeleton of axial mesoderm cells is not polarized until these cells contact the notochord/somite boundary (91). The PCP protein Dishevelled is also observed around the entire periphery of axial mesoderm cells, further implying that these cells are not molecularly polarized (24). The only exception to this is the mediolateral localization of PAR-6 and aPKC that has been observed in axial mesoderm cells (92). However, these observations were made in explants which were plated on FN and exhibited over-elongated cell shapes therefore it is unclear if this represents the *in vivo* situation. In my experiments I could demonstrate mediolateral localization of several GFP tagged molecules as well as GFP alone when cells are plated on FN, suggesting this localization may be an artifact of cell adhesion rather than an *in vivo* phenomena.

My results suggest that PAR complex formation is not required for convergent extension, as the Δ PDZ1 and S777A constructs which should inhibit PAR complex interactions, did not relieve PAR-3 inhibition. It is therefore likely PAR-3 is interacting with a different signaling pathway during CE. It was expected that the PAR-3 inhibition of CE would be due to titrating of molecules that interact with PAR-3. This does not appear to be the case, as the Δ CR1 construct contains all three PDZ domains but still relieved PAR-3 inhibition of CE. As Δ CR1 was not compartmentalized to the membrane this suggests that PAR-3 signaling interactions at the cell membrane are required for CE. Localization of the PCP protein Dsh to the cell membrane is also required for CE (24). Furthermore, this localization is regulated by PAR-1 (26). This demonstrates a link between the PCP and PAR cassettes suggesting that PAR-3 may be

functioning alongside Dsh at the cell membrane. PAR-3 has also been shown to bind phospholipids through PDZ2 and mediates phosphoinositide signaling through interaction between PTEN and the PDZ3 domain (35, 87). I was unable to determine the requirement for these domains in embryos however, PDZ3 was essential to polarity in *Xenopus* A6 cells. Furthermore, inhibition of PI3K activity inhibits convergent extension (89, 93). PAR-3 may therefore regulate convergent extension through phosphoinositide signaling rather than the PAR complex.

4.5 Conclusions

I have provided an initial characterization of PAR-3 in the regulation of cell polarity in both *Xenopus laevis* tissue culture cells and embryos. I found that PAR-3 exhibits a compartmentalized localization during epithelial polarization of A6 cells. Initially PAR-3 is found at points of cell-cell contact then around the apical cell periphery as the epithelium matures. PAR-3 also was localized to the leading edge of migrating cells in wound assays. This localization was found to require both the CR1 and PDZ1 domains and to be increased with alteration of the aPKC phosphorylation site. Furthermore, I determined that the PDZ3 domain is essential to contact inhibition and the generation of both epithelial and migratory polarity in A6 cells. I also determined that PAR-3 is expressed throughout *Xenopus* development and is required for convergent extension. PAR-3 is compartmentalized to the cell membrane in mesoderm cells and this localization requires PAR-3 oligomerization and is essential to PAR-3 function. Moreover, my data suggests PAR-3 function in CE is independent of the PAR complex which raises the possibility that PAR-3 is functioning in an unknown alternate pathway.

4.6 Future Directions

My work has provided an initial characterization of PAR-3. While I was able to characterize the temporal expression of PAR-3, I was unable to determine the spatial regulation of PAR-3 expression. This knowledge would provide further insight into what other morphogenetic movements may be regulated by PAR-3. I also determined that PAR-3 is required for *Xenopus* convergent extension. Further investigation is required to determine how PAR-3 is regulating cell polarity in CE. I used over-expression to determine PAR-3 regulation of CE. PAR-3 expression in *Xenopus* embryos can conversely be knocked-down through the use of morpholino oligonucleotides. Elimination of endogenous PAR-3 then rescue with the deletion constructs I have generated would clarify domain specific functions. Also the roles of the PDZ2 and PDZ3 domains remain uncharacterized. The use of knockdown experiments may be able to clarify the effects of these domains. The results of this study suggest the possibility that the PAR complex is not formed in *Xenopus*. A double deletion construct removing both the PDZ1 and aPKC binding region would clarify the interaction as it eliminates potential rescue by the complementary domain.

Appendix A

Δ CR1	ATG	CGT	TTG	GAA	CAT	GGT	GAC	GGG	GGC	ATT	TTG	GAT	CTT	GAC
aa1-50	M	R	L	E	H	G	D	G	G	I	L	D	L	D
Δ PDZ1	GTG	GAA	CCT	GTC	GGC	CAT	GCT	CCC	GTG	ATC	TGG	TTC	CAC	GTG
aa212-305	V	E	P	V	G	H	A	P	V	I	W	F	H	V
Δ PDZ2	GTC	AAC	TCC	CCC	ACC	AAC	AGT	CGA	AGC	ACC	AAG	ATG	GAC	GGA
aa212-305	V	N	S	P	T	N	S	R	S	T	K	M	D	G
Δ PDZ3	ACT	CCA	GAT	GGA	ACA	CGG	GAG	AGA	GGG	ATG	ATC	CAG	CTA	ATT
aa212-305	T	P	D	G	T	R	E	R	G	M	I	Q	L	I
S777A	TTC	CAG	AGG	GAA	GGG	TTT	GCC	CGC	CAA	GCC	ATG	TCC	GAA	AAA
	F	Q	R	E	G	F	A	R	Q	A	M	S	E	K

Figure A1. Sequencing of deletions and point mutation constructs. The generated constructs were sequenced to confirm mutations. The start of the deletion is shown in green and the end of the deletion is shown in red. The point mutation of serine 777 is indicated in yellow.

References

1. B. Goldstein, I. G. Macara, The PAR proteins: fundamental players in animal cell polarization., *Developmental cell* **13**, 609–22 (2007).
2. M. Simons, M. Mlodzik, Planar cell polarity signaling: from fly development to human disease., *Annual review of genetics* **42**, 517–40 (2008).
3. C. Jones, P. Chen, Planar cell polarity signaling in vertebrates., *BioEssays : news and reviews in molecular, cellular and developmental biology* **29**, 120–32 (2007).
4. F. L. Marlow, Maternal Control of Development in Vertebrates, *Colloquium Series on Developmental Biology* **1**, 1–196 (2010).
5. S. F. Gilbert, *Developmental Biology 8th Edition* (Sinauer, 2006).
6. L. Solnica-Krezel, Conserved patterns of cell movements during vertebrate gastrulation., *Current biology : CB* **15**, R213–28 (2005).
7. R. Keller, Cell migration during gastrulation., *Current opinion in cell biology* **17**, 533–41 (2005).
8. R. Keller, Shaping the vertebrate body plan by polarized embryonic cell movements., *Science (New York, N.Y.)* **298**, 1950–4 (2002).
9. R. Keller, M. Danilchik, R. Gimlich, J. Shih, The function and mechanism of convergent extension during gastrulation of *Xenopus laevis*., *Journal of embryology and experimental morphology* **89 Suppl**, 185–209 (1985).
10. R. Winklbauer, M. Schürfeld, Vegetal rotation, a new gastrulation movement involved in the internalization of the mesoderm and endoderm in *Xenopus*., *Development (Cambridge, England)* **126**, 3703–13 (1999).
11. S. Evren, EphA4 Receptor Tyrosine Kinase and PAK1 Signaling : Novel Regulators of *Xenopus laevis* Brachyury Expression and Involution Movements During Gastrulation, *MSc. Thesis* (2010).
12. J. Hardin, R. Keller, The behaviour and function of bottle cells during gastrulation of *Xenopus laevis*., *Development (Cambridge, England)* **103**, 211–30 (1988).
13. G. Lee, R. Hynes, M. Kirschner, Temporal and Spatial Regulation in Early *Xenopus* Development of Fibronectin, *Cell* **36**, 729–740 (1984).
14. R. Winklbauer, Mesodermal cell migration during *Xenopus* gastrulation., *Developmental biology* **142**, 155–68 (1990).
15. M. Nagel, R. Winklbauer, Establishment of substratum polarity in the blastocoel roof of the *Xenopus* embryo., *Development (Cambridge, England)* **126**, 1975–84 (1999).

16. R. Keller *et al.*, Mechanisms of convergence and extension by cell intercalation., *Philosophical transactions of the Royal Society of London. Series B, Biological sciences* **355**, 897–922 (2000).
17. L. a Davidson, Integrating morphogenesis with underlying mechanics and cell biology., *Current topics in developmental biology* **81**, 113–33 (2008).
18. P. . Nieuwkoop, J. Faber, *Normal Table of Xenopus laevis (Daudin)*. (1967).
19. J. B. Wallingford, S. E. Fraser, R. M. Harland, Convergent extension: the molecular control of polarized cell movement during embryonic development., *Developmental cell* **2**, 695–706 (2002).
20. M. Marsden, D. W. Desimone, Regulation of cell polarity, radial intercalation and epiboly in *Xenopus*: novel roles for integrin and fibronectin., *Development (Cambridge, England)* **128**, 3635–47 (2001).
21. P. a Wilson, R. Keller, Cell rearrangement during gastrulation of *Xenopus*: direct observation of cultured explants., *Development (Cambridge, England)* **112**, 289–300 (1991).
22. P. N. Adler, Planar Signaling and Morphogenesis in *Drosophila*, *Developmental Cell* **2**, 525–535 (2002).
23. T. Goto, L. Davidson, M. Asashima, R. Keller, Planar cell polarity genes regulate polarized extracellular matrix deposition during frog gastrulation., *Current biology : CB* **15**, 787–93 (2005).
24. J. B. Wallingford *et al.*, Dishevelled controls cell polarity during *Xenopus* gastrulation., *Nature* **405**, 81–5 (2000).
25. S.-W. Cha, E. Tadjuidje, C. Wylie, J. Heasman, The roles of maternal Vangl2 and aPKC in *Xenopus* oocyte and embryo patterning., *Development (Cambridge, England)* **4000**, 3989–4000 (2011).
26. O. Ossipova, S. Dhawan, S. Y. Sokol, J. B. a Green, Distinct PAR-1 proteins function in different branches of Wnt signaling during vertebrate development., *Developmental cell* **8**, 829–41 (2005).
27. E. Assémat, E. Bazellères, E. Pallesi-Pocachard, A. Le Bivic, D. Massey-Harroche, Polarity complex proteins., *Biochimica et biophysica acta* **1778**, 614–30 (2008).
28. R. Moore, L. Boyd, Analysis of RING finger genes required for embryogenesis in *C. elegans*., *Genesis (New York, N.Y. : 2000)* **38**, 1–12 (2004).
29. A. Suzuki, S. Ohno, The PAR-aPKC system: lessons in polarity., *Journal of cell science* **119**, 979–87 (2006).
30. I. G. Macara, Parsing the polarity code., *Nature reviews. Molecular cell biology* **5**, 220–31 (2004).
31. D. St Johnston, J. Ahringer, Cell polarity in eggs and epithelia: parallels and diversity., *Cell* **141**, 757–74 (2010).

32. D. Michel, L. Lane-guermontprez, J. Arsanto, CRB3 Binds Directly to Par6 and Regulates the Morphogenesis of the Tight Junctions in Mammalian `ne Delgrossi , Emmanuelle Me, **15**, 1324–1333 (2004).
33. P. O. Humbert, L. E. Dow, S. M. Russell, The Scribble and Par complexes in polarity and migration: friends or foes?, *Trends in cell biology* **16**, 622–30 (2006).
34. D. Lin *et al.*, A mammalian PAR-3-PAR-6 complex implicated in Cdc42/Rac1 and aPKC signalling and cell polarity., *Nature cell biology* **2**, 540–7 (2000).
35. H. Wu *et al.*, PDZ domains of Par-3 as potential phosphoinositide signaling integrators., *Molecular cell* **28**, 886–98 (2007).
36. K. Mizuno *et al.*, Self-association of PAR-3-mediated by the conserved N-terminal domain contributes to the development of epithelial tight junctions., *The Journal of biological chemistry* **278**, 31240–50 (2003).
37. X. Chen, I. G. Macara, Par-3 controls tight junction assembly through the Rac exchange factor Tiam1., *Nature cell biology* **7**, 262–9 (2005).
38. D. M. Pegtel *et al.*, The Par-Tiam1 complex controls persistent migration by stabilizing microtubule-dependent front-rear polarity., *Current biology : CB* **17**, 1623–34 (2007).
39. T. Nishimura *et al.*, PAR-6-PAR-3 mediates Cdc42-induced Rac activation through the Rac GEFs STEF/Tiam1., *Nature cell biology* **7**, 270–7 (2005).
40. T. Nishimura, K. Kaibuchi, Numb controls integrin endocytosis for directional cell migration with aPKC and PAR-3., *Developmental cell* **13**, 15–28 (2007).
41. K. Ebnet *et al.*, The cell polarity protein ASIP/PAR-3 directly associates with junctional adhesion molecule (JAM)., *The EMBO journal* **20**, 3738–48 (2001).
42. G. Joberty, C. Petersen, L. Gao, I. G. Macara, The cell-polarity protein Par6 links Par3 and atypical protein kinase C to Cdc42., *Nature cell biology* **2**, 531–9 (2000).
43. K. Takekuni *et al.*, Direct binding of cell polarity protein PAR-3 to cell-cell adhesion molecule nectin at neuroepithelial cells of developing mouse., *The Journal of biological chemistry* **278**, 5497–500 (2003).
44. J. Schmoranzer *et al.*, Par3 and dynein associate to regulate local microtubule dynamics and centrosome orientation during migration., *Current biology : CB* **19**, 1065–74 (2009).
45. L. M. McCaffrey, I. G. Macara, Widely conserved signaling pathways in the establishment of cell polarity., *Cold Spring Harbor perspectives in biology* **1**, a001370 (2009).
46. D. St Johnston, B. Sanson, Epithelial polarity and morphogenesis., *Current opinion in cell biology* **23**, 540–6 (2011).

47. S. Iden *et al.*, A distinct PAR complex associates physically with VE-cadherin in vertebrate endothelial cells., *EMBO reports* **7**, 1239–46 (2006).
48. J. Nance, J. Zallen, Elaborating polarity: PAR proteins and the cytoskeleton, *Development* **138**, 799–809 (2011).
49. S. Etienne-Manneville, Cdc42--the centre of polarity., *Journal of cell science* **117**, 1291–300 (2004).
50. T. Yamanaka *et al.*, Lgl mediates apical domain disassembly by suppressing the PAR-3-aPKC-PAR-6 complex to orient apical membrane polarity., *Journal of cell science* **119**, 2107–18 (2006).
51. R. Benton, D. St Johnston, Drosophila PAR-1 and 14-3-3 inhibit Bazooka/PAR-3 to establish complementary cortical domains in polarized cells., *Cell* **115**, 691–704 (2003).
52. H.-R. Wang *et al.*, Regulation of cell polarity and protrusion formation by targeting RhoA for degradation., *Science (New York, N.Y.)* **302**, 1775–9 (2003).
53. K. Wennerberg, C. J. Der, Rho-family GTPases: it's not only Rac and Rho (and I like it)., *Journal of cell science* **117**, 1301–12 (2004).
54. R. Bose, J. L. Wrana, Regulation of Par6 by extracellular signals., *Current opinion in cell biology* **18**, 206–12 (2006).
55. O. Ossipova, X. He, J. Green, Molecular cloning and developmental expression of Par-1/MARK homologues XPar-1A and XPar-1B from *Xenopus laevis*., *Mechanisms of development* **119 Suppl** , S143–8 (2002).
56. S. Choi, J. Kim, J. Han, Identification and developmental expression of par-6 gene in *Xenopus laevis*, *Mechanisms of Development* **91**, 347–350 (2000).
57. M. Nakaya *et al.*, Meiotic maturation induces animal-vegetal asymmetric distribution of aPKC and ASIP/PAR-3 in *Xenopus* oocytes., *Development (Cambridge, England)* **127**, 5021–31 (2000).
58. M. Kusakabe, E. Nishida, The polarity-inducing kinase Par-1 controls *Xenopus* gastrulation in cooperation with 14-3-3 and aPKC., *The EMBO journal* **23**, 4190–201 (2004).
59. J. Sambrook, D. W. Russell, *Molecular Cloning: A Laboratory Manual 3rd Edition* (2001).
60. D. Hanahan, in *DNA Cloning*, D. Glover, Ed. (ORL Press, Ltd, London, 1985), pp. 109–135.
61. J. Sambrook, D. W. Russell, Inverse PCR., *Cold Spring Harbor Protocols* (2006).
62. P. Carter, Site-directed mutagenesis., *The Biochemical journal* **237**, 1–7 (1986).
63. B. Pilli, Role of PINCH during early *Xenopus* embryogenesis, *Msc. Thesis* (2012).
64. A. H. Fischer, K. A. Jacobson, J. Rose, R. Zeller, Preparation of Slides and Coverslips for Microscopy, *Cold Spring Harbor Protocols* (2008).

65. M. G. Lampugnani, Cell migration into a wounded area in vitro., *Methods in molecular biology* (Clifton, N.J.) **96**, 177–82 (1999).
66. Y. Izumi *et al.*, An Atypical PKC Directly Associates and Colocalizes at the Epithelial Tight Junction with ASIP, a Mammalian Homologue of *Caenorhabditis elegans* Polarity Protein PAR-3, *The Journal of cell biology* **143**, 95–106 (1998).
67. H. L. Sive, R. M. Grainger, R. M. Harland, *Early development of Xenopus laevis: A laboratory manual* Cold Spring Harbor Laboratory Press (Cold Spring Harbor, NY), 2000).
68. H. L. Sive, R. M. Grainger, R. M. Harland, *Xenopus laevis Keller Explants*, *Cold Spring Harbor Protocols* (2007).
69. L. A. Davidson, B. G. Hoffstrom, R. Keller, D. W. DeSimone, Mesendoderm extension and mantle closure in *Xenopus laevis* gastrulation: combined roles for integrin alpha(5)beta(1), fibronectin, and tissue geometry., *Developmental biology* **242**, 109–29 (2002).
70. M. Itoh *et al.*, Junctional adhesion molecule (JAM) binds to PAR-3: a possible mechanism for the recruitment of PAR-3 to tight junctions., *The Journal of cell biology* **154**, 491–7 (2001).
71. K. Ebnet *et al.*, The junctional adhesion molecule (JAM) family members JAM-2 and JAM-3 associate with the cell polarity protein PAR-3: a possible role for JAMs in endothelial cell polarity., *Journal of cell science* **116**, 3879–91 (2003).
72. Y. Nagai-Tamai, K. Mizuno, T. Hirose, A. Suzuki, S. Ohno, Regulated protein-protein interaction between aPKC and PAR-3 plays an essential role in the polarization of epithelial cells., *Genes to cells : devoted to molecular & cellular mechanisms* **7**, 1161–71 (2002).
73. K. A. Rafferty, Mass culture of amphibian cells: methods and observations concerning stability of cell type, *Biology of amphibian tumors* , 52–81 (1969).
74. I. B. Dawid *et al.*, Gene expression in *Xenopus* embryogenesis., *Journal of embryology and experimental morphology* **89 Suppl**, 113–24 (1985).
75. J. Nance, J. R. Priess, Cell polarity and gastrulation in *C. elegans*., *Development (Cambridge, England)* **129**, 387–97 (2002).
76. L. Gao, I. G. Macara, G. Joberty, Multiple splice variants of Par3 and of a novel related gene, Par3L, produce proteins with different binding properties., *Gene* **294**, 99–107 (2002).
77. X. Wei *et al.*, The zebrafish Pard3 ortholog is required for separation of the eye fields and retinal lamination., *Developmental biology* **269**, 286–301 (2004).
78. S. D. M. Simões *et al.*, Rho-kinase directs Bazooka/Par-3 planar polarity during *Drosophila* axis elongation., *Developmental cell* **19**, 377–88 (2010).
79. J. Nance, PAR proteins and the establishment of cell polarity during *C. elegans* development., *BioEssays : news and reviews in molecular, cellular and developmental biology* **27**, 126–35 (2005).

80. S. Ohno, Intercellular junctions and cellular polarity: the PAR-aPKC complex, a conserved core cassette playing fundamental roles in cell polarity., *Current opinion in cell biology* **13**, 641–8 (2001).
81. T. Hirose *et al.*, Involvement of ASIP/PAR-3 in the promotion of epithelial tight junction formation., *Journal of cell science* **115**, 2485–95 (2002).
82. M. Cerejido, A. Studies, Role of calcium in tight junction between epithelial cells formation, *Current* (1990).
83. A. Suzuki *et al.*, aPKC kinase activity is required for the asymmetric differentiation of the premature junctional complex during epithelial cell polarization, *Journal of Cell Science* **115**, 3565–3573 (2002).
84. T. Yoshii *et al.*, sPAR-3, a splicing variant of PAR-3, shows cellular localization and an expression pattern different from that of PAR-3 during enterocyte polarization., *American journal of physiology. Gastrointestinal and liver physiology* **288**, G564–70 (2005).
85. W. Feng, H. Wu, L.-N. Chan, M. Zhang, The Par-3 NTD adopts a PB1-like structure required for Par-3 oligomerization and membrane localization., *The EMBO journal* **26**, 2786–96 (2007).
86. M. Nakayama *et al.*, Rho-kinase phosphorylates PAR-3 and disrupts PAR complex formation., *Developmental cell* **14**, 205–15 (2008).
87. W. Feng, H. Wu, L.-N. Chan, M. Zhang, Par-3-mediated junctional localization of the lipid phosphatase PTEN is required for cell polarity establishment., *The Journal of biological chemistry* **283**, 23440–9 (2008).
88. F. Martin-Belmonte *et al.*, PTEN-mediated apical segregation of phosphoinositides controls epithelial morphogenesis through Cdc42., *Cell* **128**, 383–97 (2007).
89. L. C. Skwarek, G. L. Boulianne, Great expectations for PIP: phosphoinositides as regulators of signaling during development and disease., *Developmental cell* **16**, 12–20 (2009).
90. S. Funamoto, R. Meili, S. Lee, L. Parry, R. A. Firtel, Spatial and Temporal Regulation of 3-Phosphoinositides by PI 3-Kinase and PTEN Mediates Chemotaxis, *Cell* **109**, 611–623 (2002).
91. A. Shindo, T. S. Yamamoto, N. Ueno, Coordination of cell polarity during *Xenopus* gastrulation., *PloS one* **3**, e1600 (2008).
92. J. Hyodo-Miura *et al.*, XGAP, an ArfGAP, is required for polarized localization of PAR proteins and cell polarity in *Xenopus* gastrulation., *Developmental cell* **11**, 69–79 (2006).
93. S. Nie, C. Chang, PI3K and Erk MAPK mediate ErbB signaling in *Xenopus* gastrulation., *Mechanisms of development* **124**, 657–67 (2007).